Study of Photovoltaic System

Technical Report

By

Falinirina F. Rakotomananandro

Advisor:

Professor Ali Keyhani

Mechatronics Green Energy Laboratory

The Ohio State University

2011

Abstract

The human activities contribute to the global warming of the planet. As a result, every country strives to reduce carbon emissions. The world is facing not only the depletion of fossil fuels, but also its rising prices which causes the worldwide economic instability. Numbers of efforts are being undertaken by the Governments around the world to explore alternative energy sources .and to achieve pollution reduction. Solar electric or photovoltaic technology is one of the biggest renewable energy resources to generate electrical power and the fastest growing power generation in the world. The main aim of this work is to analyze the interface of photovoltaic system to the load, the power electronics and the method to track the maximum power point (MPP) of the solar panel.

The first chapter consists of an overview of the PV market and cost. It describes the application of the PV system, the energy storage and the different standard requirement when having grid-connected PV system.

Then main emphasis is to be placed on the photovoltaic system, the modeling and simulation photovoltaic array, the MPP control and the DC/DC converter will be analyzed and evaluated. The step of modeling with MATLAB and Simulink of the photovoltaic system is shown respectively and simulation results are provided.

The Simulink model of the PV could be used in the future for extended study with different DC/DC converter topology. Optimization of MPPT algorithm can be implemented with the existing Photovoltaic and DC/DC converter.

Table of contents

List of Figures

List of Tables

Chapter 1: Introduction

1.1 Background and Overall Trends

Governments around the world are facing a steadily rising demand on global electric power. To face this challenge, they are striving to put in place regulatory guidelines to aid the adoption of best practices by utilities in terms of the Smart Grid and renewable energy applications. Smart Grid organization provides the consumers with the ability to monitor and control energy consumption. This is crucial because as the world population grows the electricity demand will also increase, but at the same time, we will need to reduce our electricity consumption to fight global warming.

By using the Smart Grid, energy consumers will have an incentive to create power on their own with the use of wind turbines or solar paneling, and subsequently sell any power that is generated in excess to electrical companies. Several researches are being made to improve the system and reduce its cost and size. As a result, the photovoltaic (PV) system is becoming much easier to install but the efficiency of solar module is still low (about 13%). Furthermore, it is desirable to operate the module at the peak power point.

This technical report will discuss about the photovoltaic system, the power electronics interface and the method to track the maximum power point (MPPT) of the solar panel. Before getting into detail, this first chapter will describe the PV market and its future, the application of energy storage with photovoltaic system and the different standard requirement when having a grid connected PV system.

1.1.1Photovoltaic Market

The energy prices keep rising as well as the consumer demand but thanks to the monetaryadvantages that the states or government channels are offering, the market for solar power equipment is on the rise within the United States.

Photovoltaic (PV) installation's capacity was completed during 2010 and has increased by over 55 per cent in comparison to 2009, along with that the typical size of the PV system is also expanding Significant incentives program are being offered by many states and as a result, the PV market is expanding to those different states. Long-term situation of the solar market looks bright. [54]

Overall Trends in Installations and Capacity

During 2010, the annual US installation capacity in terms of the PV more than doubled at an estimated 820 MWDC, which included not only the off-grid but also the grid markets. Even though the growth in terms of said installations has seen a more typically stable trend for the past few years, it has doubled in the last few years. [55]

According to recent studies by the Solar Energy Industries Association (SEIA), the U.S market for solar photovoltaic (PV) grew 20% per year until 2006 when growth jumped to 36% due to the new incentives. [54]

1.1.2 Photovoltaic cost

A steady decline of the solar PV costs is expected, presumably as much as 50% within the next 4 to 7 years. The primary aim is to reduce the expenses related to the installation and the PV panel. In 2015, the target is to decrease the price for residential use to 8- 10 cents Kwh. At this price, the solar PV will be affordable for the masses.

Several ways were attempted in order to bring down the expenses of the PV. Bringing down the costs of manufacturing, augmenting performance along with expanding upon the reliability of the technologies that are being used was few. Another important avenue where costs could be brought down was the local interaction and learning by means of an expanded capacity of manufacturing. A forecast suggests that electricity will be stable and consistent through 2025; elements such as tax legislation for carbon, fuel prices on a global level, facility/importation constructions, costs of labor, inflation and exchange rates could act as contributor to the achievement parity of solar energy with electricity prices even faster than presently projected. The solar market cost goal will be achieved with “5-10 GW of PV fitted by 2015 within the country and over 70-100 GW by the year 2030.”[55]

Table 1.1 shows that the projection cost of Kwh will be half of the actual price in the next five years (2015 cost 5-7 cents /Kwh for utility company and for residential will be 8-10 cents/kwh)

		Cost of energy(cent/kwh		
Market sector	Current US market price range for conventional electricity(cent/kwh)	2005	2010	2015
Utility	4.0-7.6	13-22	13-18	5-7
Commercial	5.4-15.0	16-22	9-12	6-8
Residential	5.8-16.7	23-32	13-18	8-10

Table 1.1:Projection cost Kwh of PV [55]

1.2 Typical application of the PV system

Photovoltaic systems have become an energy generator for a wide range of applications. The applications could be standalone PV systems or grid connected PV systems. A standalone PV system is used in isolated applications where PV is connected directly to the load and storage system. With a standalone photovoltaic, when the PV source of energy is very large, having energy storage is beneficial. Whereas a PV system that is connected through a grid is used when a PV system injects the current directly into the grid itself. The advantage of the grid-connected system is the ability to sell excess of energy.

Figure 1.1 shows a block diagram of typical hybrid renewables sources of energy. The integrated system has wind turbine and PV array as sources of energy. They are

connected to the DC bus that could be connected to a different energy storage system, or inject the current directly with a DC/AC inverter. Therefore, the characteristic of energy storage for a PV system will be explained as well as some specification and standards for a grid connected PV system.

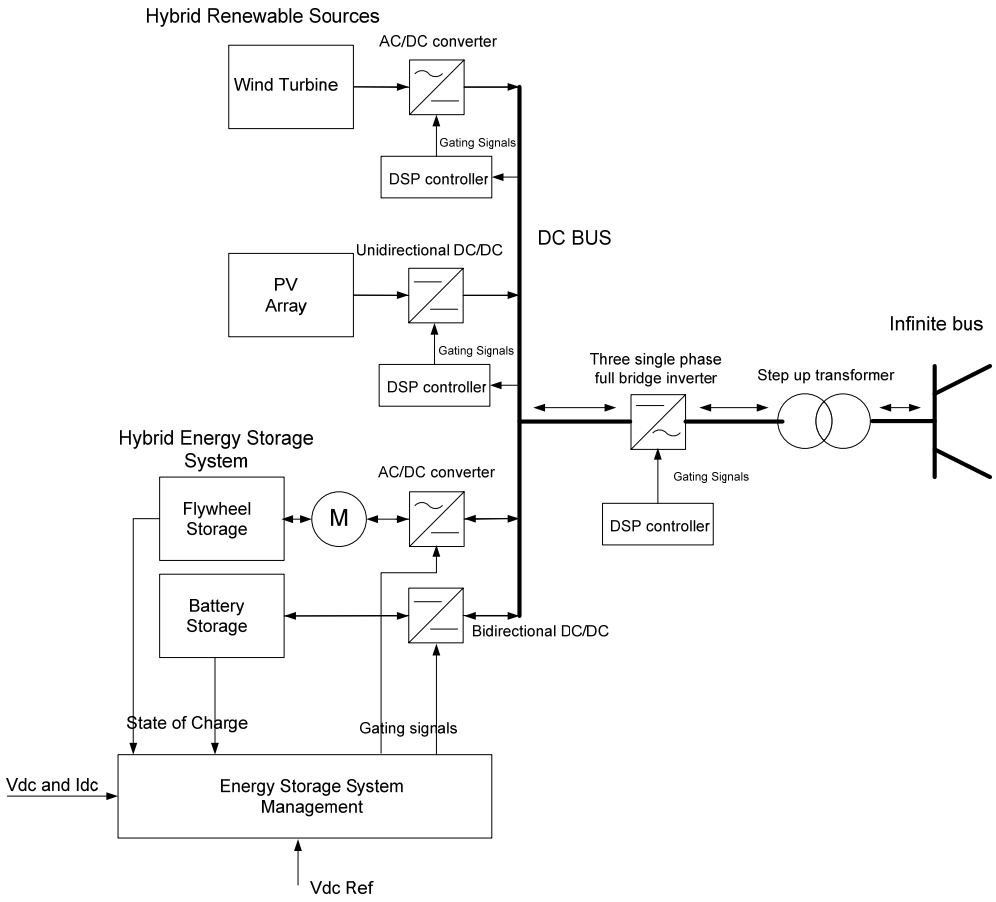

Figure 1.1: Block diagram ofrenewable energy system

1.2.1 Photovoltaic system and energy storage

The main benefit of integrating storage with renewable energy is the capability of shifting the peak demands using charging/discharging (charging when the excess

electricity is stored, discharging when there is a peak demand). The storage can be charged from the renewable sources or from the grid. The demand on the grid can be met with the renewable sources (wind, solar) or energy storage or both.

The other benefits are:

- "Mitigation of short-term solar power intermittency and wind gust effects and minimizing its impacts on voltage, frequency, and power fluctuations in power system" [56]
- "Lowering the transmission and distribution costs by increasing the confidence in renewable distributed generation".[56]
- Improving power system stability, reduction of harmonics,

Characteristics of Energy Storage System

Energy storage plays a crucial role not only in maintaining system reliability but also in insuring energy efficiency and power quality. The functions of an energy storage system vary from its applications. The role of storage in power system determines the size and type of storage used. The problem is to analyze the domain of application of the storage system. With an appropriate choice of storage parameters, the storage unit may be used as multifunctional device, able to solve a wide number of problems. The combination of storage with grid connected PV system is beneficial.

There are different applications that an energy storage system can fulfill:

- Spinning reserve

- Generation capacity deferral
- Frequency control
- Integration with renewable generation
- Load leveling
- Transmission line stability
- Distribution facility deferral
- Transit system peak
- Reliability, power Quality, uninterruptible power supply

1.2.2 Specifications and standards for grid connected PV systems

Power electronics inverters are necessary to transform into AC current then inject to the grid the energy delivered by the PV systems. Therefore, there are special standards and requirements concerning the connection of the PV to the grid. The rules and regulations set by the utility companies must be obeyed. These standards are to maintain the power quality produced by the photovoltaic distribution system.

The grid-connected standards covered the topics about voltage, DC current injection, flicker, frequency, harmonics current, maximum current, total harmonics distortion (THD) and power factor.

Some definitions used in grid connected PV are:

Islanding:

Acondition in which the photovoltaic system and its load remain energized while disconnected from the grid.

Distributed resource islanding:

An islanding condition is when the photovoltaic sources of energy supply the loads not from the utility system.

Non-islanding inverter:

An inverter ceases to energize the utility line

Grounding

NEC 690 standard requires the system and interface equipment should be grounded and monitored. It gives more safety and protection in case of ground faults inside the PV system.

Voltage disturbances

The utility company set the voltage of grid network (in U.S 120 V). The PV system cannot control the voltage of the grid so the output voltage of the PV has to be within the operating range defined by the standards. The inverters should detect abnormal voltages and prevent islanding of the system. The table 1.2 gives boundaries limits of the voltage and the maximum trip time allowed for ceasing to energize the grid. The PV systems remain connected to the grid and should reconnect when the

voltage was restored. The voltage operating range is detailed in IEEE standard 929 [29].

Voltage	Maximum trip time
V<60(V<50%)	6 cycles
60≤V<106 (50%≤V<88%)	120 cycles
106≤V≤132 (88%≤V≤110%)	Normal operation
132<V<165 (110 %< V<137%)	120 cycles
165≤V(137%≤V)	2 cycles

Table 1.2: Response to abnormal voltage [29]

DC component injection

According to [30] IEC 61727, the DC current injected should be less than "0.5% of rated inverter output current into the utility AC interface." The DC current could produce inundation of the delivery converters within the grid.

Total distortion harmonics

The topology has to be chosen along with the modulation scheme of the inverters should give an AC current with low level of harmonic distortion. High current harmonics can cause adverse effects on the diverse equipment connected to the grid. Table 1.3 gives the maximum limit of acceptable distortion current according by [29]. The table shows the output harmonics current for six pulse inverters.

- "Total harmonic current distortion shall be less than 5% of the fundamental frequency current at rated inverter output."[29]

- Even harmonics shall be < 25% of the odd harmonics limits

Odd harmonics	Distortion limit
3rd-9th	<4.0%
11th-15th	<2.0%
17th-21st	<1.5%
23rd-33rd	<0.6%
Above 33rd	<0.3%

Table 1.3: Harmonics current limits for six-pulse converters [29]

Voltage flicker

The voltage flicker should not exceed the maximum limits in IEC 61727 [30].

Islanding protection

The inverters must have a feature that can identify a situation of islanding and respond accordingly to safeguard the people and equipment involved. For instance, the standard stated that the inverter should disconnect from the utility line when there is disturbance from the system.

In islanding, the inverters continue to supply local loads even in the case that the grid is no longer connected to the inverter.

Inverters that are tied to the grid overlook the utility line and can turn themselves off with great speed if required (in 2 seconds or less) in the event that abnormalities occur on the utility system

The principal concern is that a utility line worker could be exposed to a line that is unexpectedly energized

Power factor

The IEEE standard929 [29] specifies that the power factor of the PV system should be > 0.85 (lagging or leading) when output is >10%. The grid connected PV inverter is designed to have a control current with a power factor unity. Sometimes the inverter is used for reactive power compensation; therefore, the inverter should be capable to control the output power factor.

Reconnect after disturbance

The PV system should not be reconnected until continuous normal voltage and frequency are maintained by the utility for a minimum of five minutes, at which time the inverter can automatically reconnect.

Frequency

According to [29], the PV systems should have a fixed frequency between 59.3 – 60 Hz. The PV systems should stay synchronized with the grid. For small PV systems, the frequency trip should be 59.2 Hz and 60.6 Hz. When there is variation of

frequency outside the range specified above, the inverter has to stop energizing the line of utility within a span of over six cycles. The time delay is set to avoid the PV to trip for short time disturbance

Chapter 2: Literature Review

The photovoltaic (PV) generation system has been reviewed as listed below:

1- The system topology
2- The model of photovoltaic
3- The Maximum power point tracking (MPPT) controller and algorithm
4- The power electronic interface
5- Voltage and current control
6- The modulation techniques

2.1 The system topology

Soeren Baekhoej *et al.* [9] did a classification of Inverter Topologies for photovoltaic system. The inverter could be a single stage inverter, dual stage inverter. Each topology has their advantages and disadvantages. An optimization is necessary for the choice of topology. The topology should guarantee that the output current is a high quality sine wave and in phase with voltage if grid connected, also with low distortion harmonic.

In In figure 2.1, the different topology of the photovoltaic is shown. In figure 2.1a, the PV array is connected in series and parallel then linked by a singular inverter. A PV string is for PV array connected in series then connected into single inverter in figure 2.1b, and a multistring PV is when multiple PV string are connected to a single DC bus then connected to a DC/AC inverter.

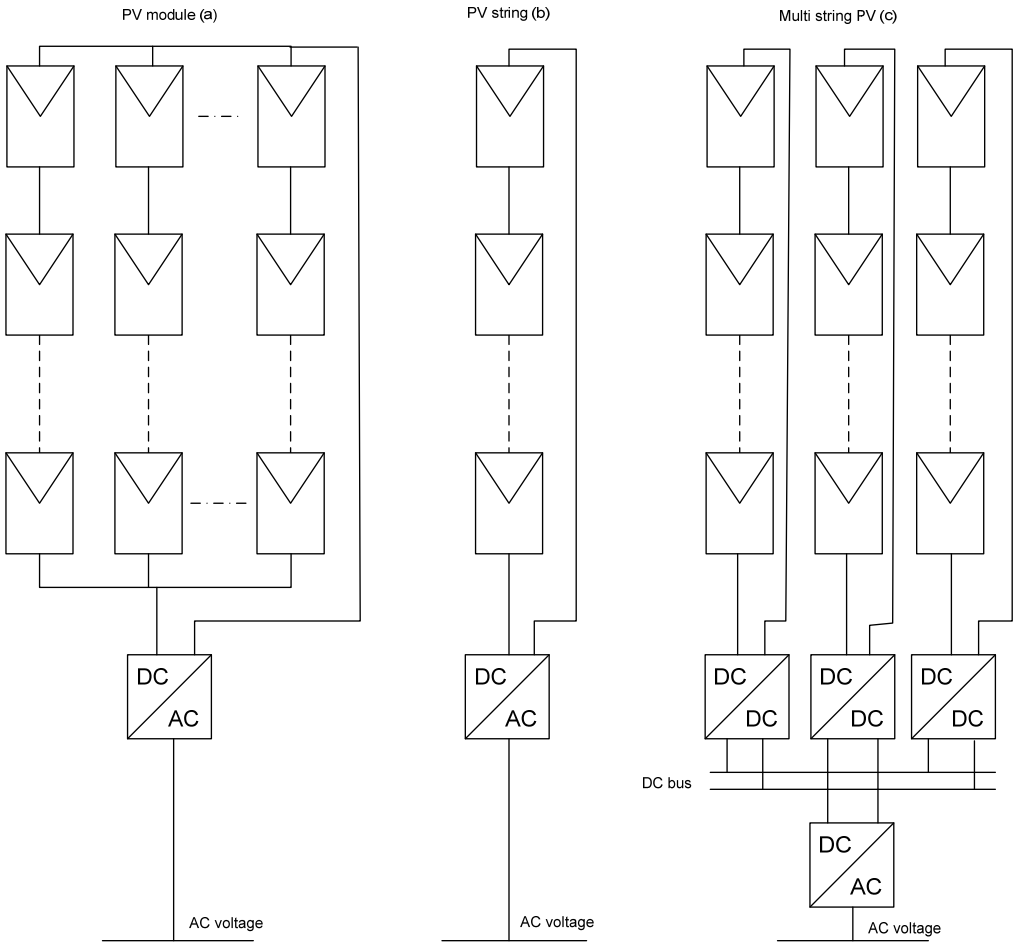

Figure 2.1: Topology of PV module, PV string and multi string PV [9]

Central inverters or single stage photovoltaic system

Central inverter topology can be called also single stage photovoltaic. In this topology, the photovoltaic system includes a series-parallel connection arrangement, which is connected to a single inverter DC/AC for the transferal of the higher amount of power possible to the grid or the load. Single stage photovoltaic is shown in figure 2.2. It has one inverter DC/AC that must handle the MPPT, control the current on the grid along with the amplification of the voltage, which makes the single stage more complex to control. Sachin Jain *et al.* proposed, "Using conventional H-bridge inverter followed by step up transformer or using a PV array with sufficiently large PV voltage." [10] Thus, the boost converter is no longer necessary. However, the extra transformer adds up to the cost and the size of the PV system. In addition, the large PV array has the disadvantage of "reduced safety and increased probability of leakage current through the parasitic capacitance between the panel and the system ground." [10]. In single stage PV system, the dc/ac inverter must ensure all the functions: MPPT, boosting and inversion as shown in figure 2.2.

In [14] Martina Calais *et al*. defined the central inverter topology as cheap, robust and highly efficient. The major disadvantage is the low power factor 0.6 and 0.7. The actual PWM full bridge inverter, switched at great frequencies improves the efficiency of the system.

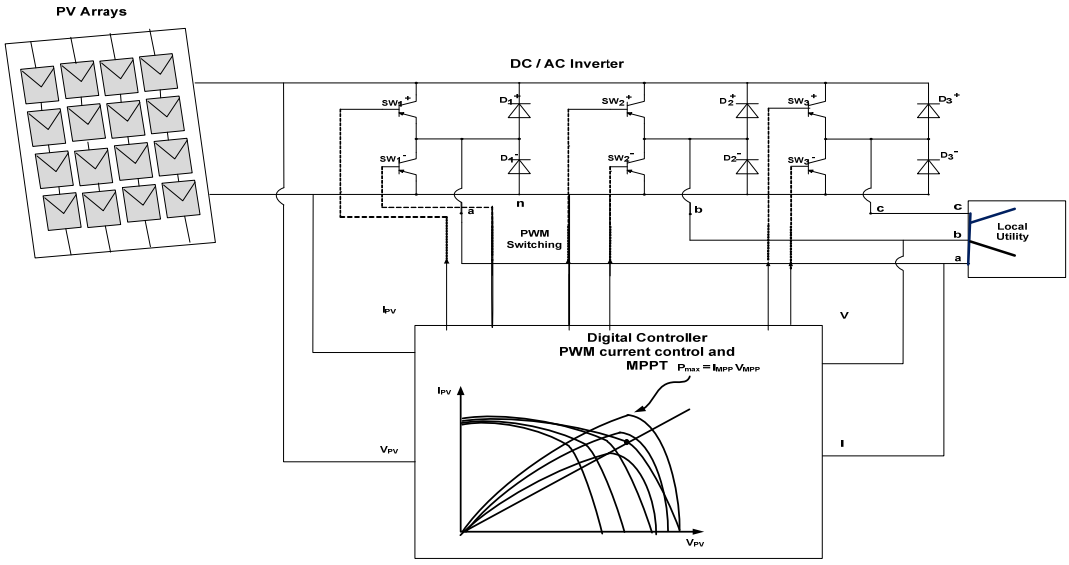

Figure 2.2: Circuit diagram of DC/AC grid-connected PV system

String inverter ortwo stages photovoltaic system

The photovoltaic modules in the given topology are linked in a structure whereby they end up forming a string; the voltage from the PV array ranges between 150-450 V [13]. The DC/DC converter realizes the MPPT along with the amplification of the voltage. The DC/AC inverter controls the grid current with a pulse width modulation (PWM) control scheme. The initial stage is utilized as a means to boost the voltage for the PV array and track MPP of solar power; subsequent to this, the second phase coverts the dc power into ac power. The two stages have the following drawbacks of lower effectiveness, higher count for parts, lower level of reliability, bigger size and higher cost. This topology is mostly used due to its simplicity. The two-stage PV system is shown in figure 2.3.

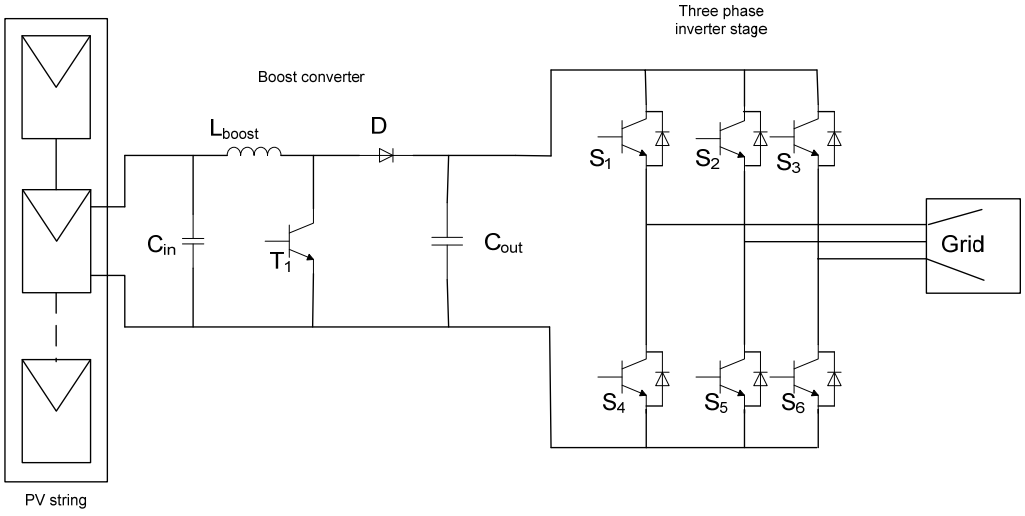

Figure 2.3: Two stage PV system with boost converter and three-phase inverter [13]

Multi string inverter

In this topology, "multiple PV module or string is connected to a dedicated dc-dc converter that is connected to a common dc-ac inverter."[14]. Each PV string has its own boost converter and MPPT. Each PV operates at MPP. Figure 2.4 represents the multi string inverter and can be noted that each dc-dc converters typically link with each other by means of DC bus via an inverter. The advantage with multistring inverter is its ability to add an extra PV module to the bus if more power is needed in the future. In case of failure of one PV string, the PV system still able to operate with the remaining PV.

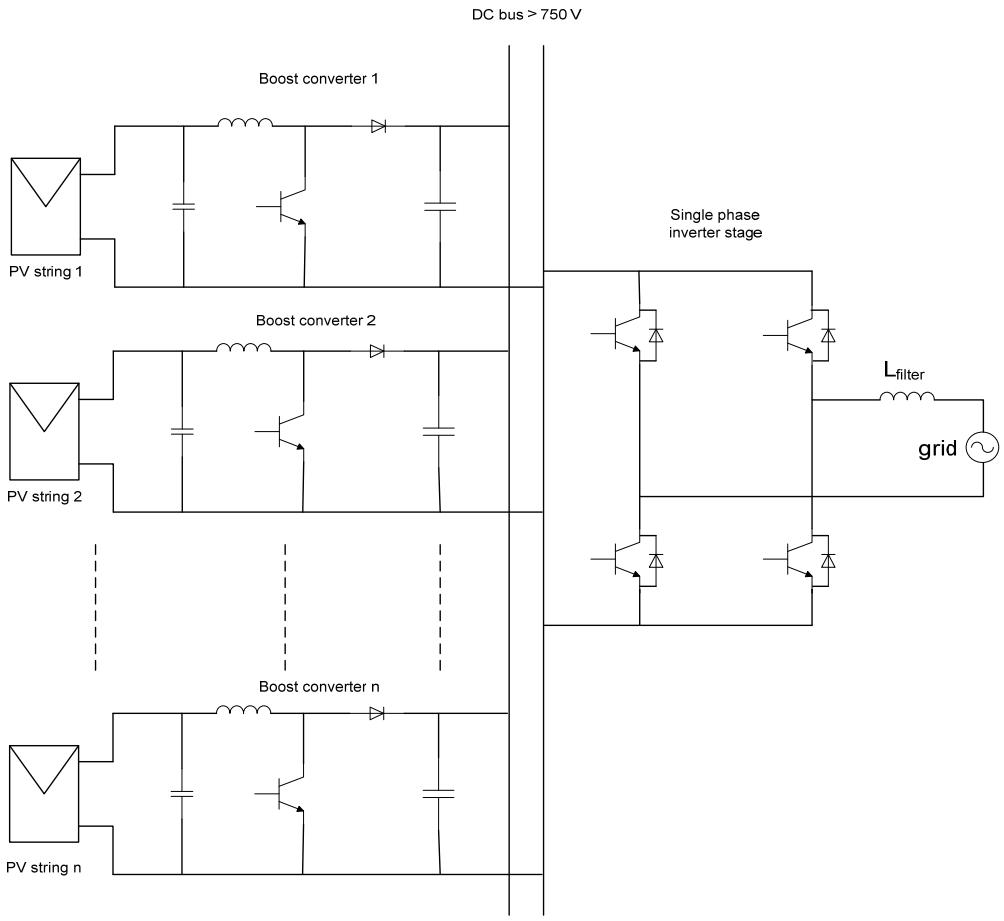

Figure 2.4: Multistring PV system [14]

2.2 Modeling the photovoltaic array

In order to study the photovoltaic system in distributed generation network, a modeling and circuit model of the PV array is necessary. A photovoltaic device is a nonlinear device and the parameters depend essentially on sunlight and temperature. The photovoltaic cell converts the sunlight into electricity. The photovoltaic array consists of parallel and series of photovoltaic modules. The cell is grouped together to form the panels or modules. The voltage and current produced at the terminals of a PV

can feed a DC load or connect to an inverter to produce AC current. The model of photovoltaic array is obtained from the photovoltaic cells and depends on how the cells are connected.

Marcello Gradella *et al.* [3] use the basic equation from the theory of semiconductor to describe mathematically the I-V characteristic of the ideal photovoltaic cell. It is a semiconductors diode with p-n junction. The material used is monocrystalline and polycrystalline silicon cells. Figure 2.5 is the model of photovoltaic cell with the internal resistance and diode. A real photovoltaic device must include the effects of series and parallel resistance of the PV.

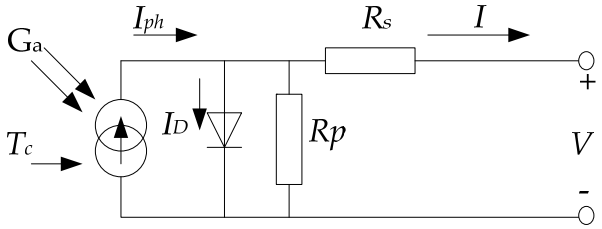

Figure 2.5: Single diode equivalent circuit of a solar cell

The equations that give the behavior of the PV are:

$$I = I_{pv} - I_0 \left[exp\left(\frac{qV}{akT}\right) - 1 \right]$$

$$I = I_{pv} - I_0 \left[exp\left(\frac{V + R_s}{V_t a}\right) \right] - \frac{V + R_s I}{R_p}$$

where

I_{pv}: current generated by the incident light

I_0:reverse saturation

q: electron charge (1,602 10-19 C)

k :Boltzmann constant

T: the temperature of the p-n junction

V_t: the thermal voltage of the array

R_s:the resistance series

R_p: the resistance parallel.

The problem of modeling a PV array is to calculate the resistance series R_s and resistance parallel R_p.R_s and R_p are determined iteratively, based on the manufacture datasheet in [3].

The model is obtained with the parameters of the I-V equation given by manufacturer datasheet such as open-circuit voltage V_{oc}; short-circuit current I_{sc}, maximum output power P_{max}, voltage and current at the maximum power point (V_{mpp}, I_{mpp}). The method used "the mathematical model of I-V curve without need to guess or estimate any other parameters except the diode constant a" [3]. The relation between I_{pv} and I_{sc} replaces the assumption that I_{pv} is equal to I_{sc}. The model in [3] gives a good correlation of PV characteristic and I-V curve.

Dezso Sera *et al*. in [15] have proposed a model for PV panels, which stems from values from the datasheet. The model uses a single-diode and determines five-parameters framework constructed from the parameters defined in the datasheet. The goal is to establish a structure for the PV panels that exudes the given particular details in the datasheet. The five parameters are:

I_{ph} the photo generated current in STC

I_0 dark saturation current in STC

R_s: series resistance

R_{sh}: parallel (shunt) resistance

A: diode quality (ideality) factor

The equations are detailed in [15], which allow calculating the five parameters. The equations are based from the equal circuit of the single-diode for PV cells. The other equations are derived from open circuit point, maximum power point and the short circuit point of the PV. The model obtained represents the stipulations put forth through the datasheet for the product. The method proposed a new method depends on the temperature of the dark saturation current.

H. Atlas *et al*. [16] develop other method of modeling the PV cell. The voltage serves as one of the main functions of the photocurrent, which is identified or measured by solar irradiation. The voltage equation is given by

$$V_c = \frac{AkT_c}{e} ln\left(\frac{I_{ph} + I_0 - I_c}{I_0}\right) - R_s I_c$$

where

I_c: cell output current,

I_{ph}: photocurrent, function of irradiation

I_0: reverse saturation current,

R_s: series resistance of cell

T_c: reference cell operating temperature

V_c: cell output voltage

For the purpose of calculating the voltage array, the equation has been to become the product of the cells that are linked within the set. The operating temperature changes during the irradiation and ambient temperature change. This method introduces new temperature coefficients C_{tv} for cell output voltage and C_{ti} for cell photocurrent. In addition, two constants correction factors C_{sv} and C_{si} are introduced which expressed the variation in the operational temperature, along with the photocurrent because of the deviances within the solar irradiation. The coefficients are expressed in [16] by the following

$$C_{TV} = 1 + \beta_T(T_a - T_x)$$

$$C_{TI} = 1 + \frac{\gamma_T}{S_C}(T_x - T_a)$$

β_T and γ_T are constant for the cell temperature at 20ºC. The other relations are detailed in [16]. The results of simulation shows the loads begin to draw current from the photovoltaic array and current and voltage begin moving to the operating values. The framework includes the impact of solar irradiation and temperature.

J.A Gow *etal.* [38] used a dual exponential framework. The equivalent circuit is shown in figure 2.6. The model has one extra diode. The double exponential models are obtained from PV cells constructed with polycrystalline silicon.

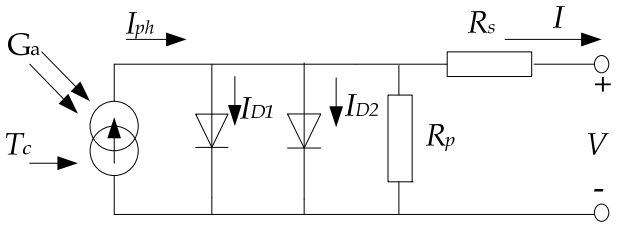

Figure 2.6: Equivalent circuit of PV cell with two diodes [38]

The equation of the double exponential model is given by

$$I = I_{ph} - I_{s1}\left[e^{\frac{e(V+IR_S}{kT}} - 1\right] - I_{s2}\left[e^{\frac{e(V+IR_S)}{Akt}} - 1\right] - \frac{V + IR_s}{R_p}$$

I_{s1}: saturation current of diode 1

I_{s2}: saturation current of diode 2

R_s: cell series resistance

R_p: cell shunt resistance

k: boltzmann's constant, 1.38x 10-23 J/K

e: electronic charge, 1.6x 10-19 C

The model is nonlinear and implicit. To obtain an analytical solution of its five parameters, [38] proposed a set of data at specific temperature and used a numerical solution using curve fitting method and Newton Raphson iteration. The first double exponential model does not take variation irradiance but only depends on variation temperature. The model is unstable. Later on, a new model is developed and the variation of irradiance will be taken into account .The equations are developed in [38] and applicable to any PV cells with the double exponential model. The equations have thirteen constants, which are specific to the cells.

2.3 Maximum power point controller and algorithm

Since the Photovoltaic has a non-linearity characteristic, maximum power point controller allows operating the photovoltaic array at MPP.The MPPT adjust the pulse width of the DC/DC converter or DC/AC of the inverter. Cited below are different strategies to obtain the MPP for the PV system.

Perturb and Observe (P&O)

G. M. S. Azevedo *etal.* use this method in [8]. It tries to measure the prior value's power in terms of the new value and then makes the decision of whether the voltage for the PV array can be increased or decreased. The reference voltage value is adjusted until the maximum power point is reached. In [8], two parameters control the MPP: the sample rate and the reference voltage. With this method, the DC link voltage wavers over the supreme point of power. The voltage is increased or decreased with constant value ΔV. The choice of ΔV determines how fast the MPP controller tracks the voltage. It is important to note that the reference voltage and MPP never coincide in steady state. The output voltage of the PV oscillates and causes loss of energy.

A P&O algorithm is used in [41] to interface the PV module to the grid. In figure 2.7, a boost converter is used to step up the voltage from the PV system and a single-phase inverter DC/AC is used for the connection to the grid. According to Fangrui Lui *etal*[41], in the event that the solar irradiation goes through a change, the voltage that is being output is prone to faster stabilization, 4 to 5 cycles with P&O method, instead of 12 cycles with Hill climbing.

Although the P&O algorithm is typically seen as more appropriate in comparison to Hill climbing, , P&O method tends to oscillate about the MPP. In [41], with larger step size, PV voltage and output power result in ripples of a considerable size, and the dc capacitor, which is paralleled with the PV arrays, undergoes tremendous over and under voltages that can lead to the deterioration of the PV converter's performance.

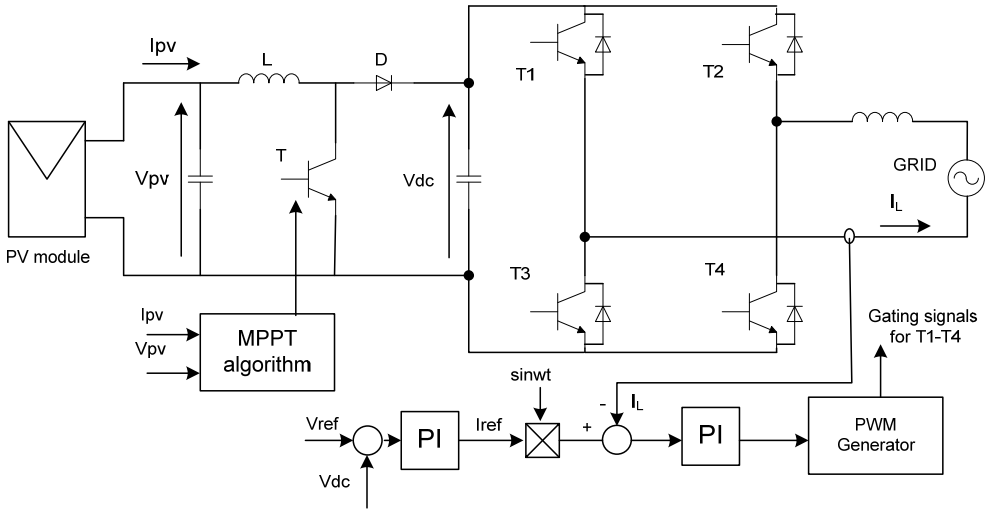

Figure 2.7: Two-stagegrid connected PV system with boost converter [41]

Incremental conductance INC

MPPT INC method is used to feed a DC motor pump in [42]. In figure 2.8, the DC/DC boost converter is the power electronic interface. The duty ratio for the converter is obtained from the MPPT controller. INC method is used for better result. An incremental algorithm principle associates the prompt conductance of the PV module (I/V) to its augmenting conductance (*dI/dV*) and choses between decreasing and increasing the control variable appropriately [42].

By Elgendy*etal* [42], INC has higher tracking performance compared to P&O. The transient of the motor is better with INC MPPT when the irradiance and cell temperature are constant. The tracking efficiency result is 99.73% with step size 0.02% when a step change of irradiance and temperature are applied. The motor current and torque waveforms have low frequency ripple content depending on the

rate of the dc link capacitance alone with the size of the step that is utilized in altering the duty cycle converter.

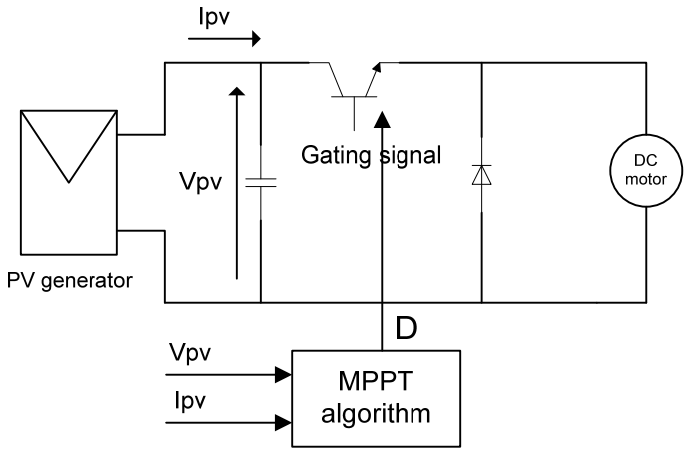

Figure 2.8: PV system with boost converter [42]

Therefore, in [43] a variable size of step INC MPPT is suggested to improve the performance of the conventional fixed step size INC algorithm. The variable step size INC adjusts automatically the size of the step to the MPP of the PV array It can improve the MPPT speed and its accuracy simultaneously.

This method calculates the slope of power versus voltage characteristic to determine the direction of the perturbation as described in [8].

2.4 The power electronic interface

2.4.1 DC/DC converter stage

Boost

The boost converter is widely used to pinpoint the ultimate point of power of the PV array. It is a simple circuit with good response speed. Any algorithm of maximum power point is flexible to implement with software and hardware. The boost converter circuit is shown in figure 2.9.

It is explained in [18] that the boost converter can operate in continuous conduction mode along with discontinuous conduction mode. The mode of conduction depends of the capacity for storage of energy along with the relative timeframe of the switching. The output voltage is dependent of the duty cycle; it is adjusted by the maximum power controller. The relation of the output voltage with the input voltage as function of duty cycle is given by

$$\frac{V_0}{V_i} = \frac{T_s}{t_{off}} = \frac{1}{1-D}$$

V_0= average output voltage

V_i: the input voltage, PV voltage

T_s: switching period

D: duty cycle

T_{off}: switching off of the IGBT

The boost converter in [18] is designed for all possible duty cycles and for all irradiations of the PV array.

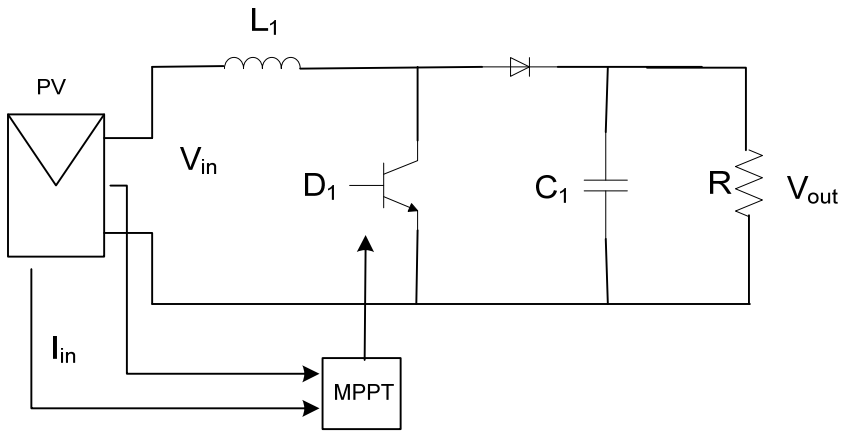

Figure 2.9: Boost converter for PV

Buck

The buck converter can be used in the same method as the boost converter. The main difference is the link in terms of the output and input voltage. The buck is utilized in reducing the voltage for output, since the voltage, power and current of the PV array change continuously with temperature and irradiation, the converter conduction mode changes too. The duty cycle still changes continuously to track the highest possible point of power of the PV. An example of design of Buck converter is given in [19]. The buck converter is used with the PV array to charge a battery. The

inductor current can be continuous or discontinuous. The size of the inductor and switching frequency depends on the efficiency, power and weight requirements. Eftchios K. *et al.* [19] show the buck converter has higher efficacy, lesser costs and can adjust to bear a higher amount of energy. Figure 2.10 shows the buck converter with PV, MPPT with battery load.

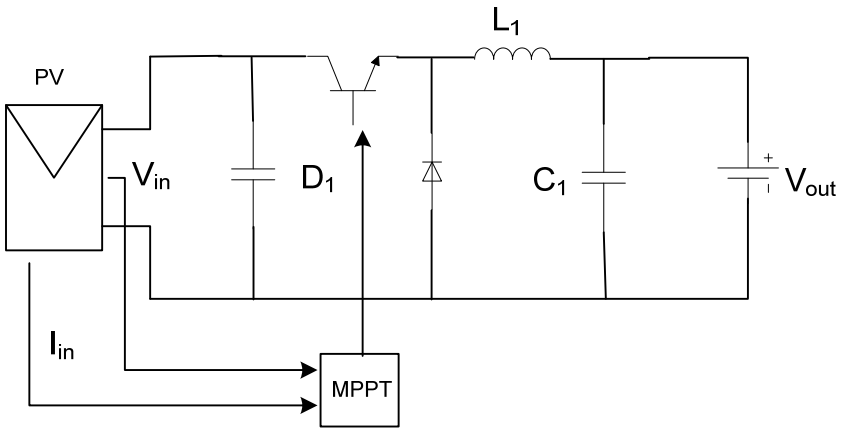

Figure 2.10: Buck converter charging battery [19]

Buck-boost

Weiping Luo *et al*. use Buck boost converter in [11] to obtain the MPPT of the grid-connected PV generation system. The buck boost is a simple converter with good response speed and the controlling method is flexible. The overall efficacy of the photovoltaic with buck boost is improved. The output voltage function of the duty cycle is given by

$$V_{out} = -V_{in}\frac{D}{1-D}$$

In buck boost converter, the duty cycle is less than one to allow the converter operating both boost and buck modes.

Dual stage boost buck-boost converter

Sairaj V. *etal* proposed in [17] a boost buck-boost converter to find the MPP of the photovoltaic array. The buck-boost stage tracks the maximum power by matching the output load to the optimal photovoltaic impedance. The two power stages shown in figure 2.11 worked independently, solving the problem of ineffectiveness, and transfer efficiency. The buck-boost tracks the maximum power in continuous conduction mode and the boost minimizes the PV current ripple. The duty cycle of the boost can be set to control the dc bus voltage. The dual stage has a better efficiency but increase the cost by introducing additional stage to the converter.

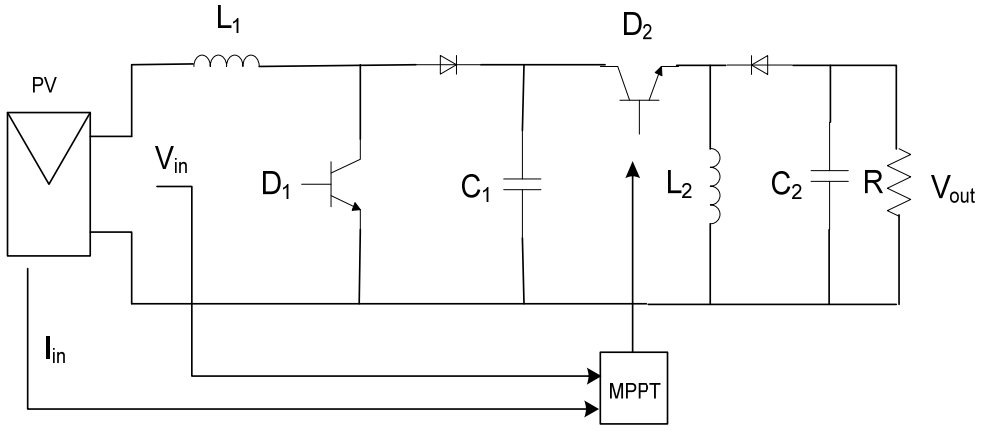

Figure 2.11: Dual stage boost buck boost converter [17]

2.4.2 DC/AC inverter

The function of the DC/AC inverter is presented in [9]. It should mold the current into a waveform i.e. sinusoidal, and subsequently transform the current to ac current with low harmonics content. The PV array is used to inject a sinusoidal current to the grid.The topology adopted depends on the application whether it is a standalone PV system or grid connected. Other criteria such as the power output of the PV, the total current harmonics and the cost could influence the choice of inverter design. In grid connected PV system, the inverters should have island detection, power quality within the standards, grounding, etc.

The typical DC/AC inverter could be a line frequency-commutated current source inverter (CSI), a full-bridge three-level, half-bridge diode clamped three-level VSI, etc. In [9], line commutated inverters are qualified robust, efficient and cheap but have a power factor between 0.6 and 0.7. Self-commutated inverters are used quite often; they are capable switching at high frequency, which introduce more losses in semiconductor. The self-commutated inverter is robust and cheap technology.

As described in [9], line frequency-commutated inverter uses a signal sinusoidal to generate the AC output. The drawbacks with this configuration are the power quality of the harmonics and unnecessary fault situation. The harmonics can cause series resonance with the capacitors installed around the system.

The full-bridge inverter is the most used in PV system. Figure 2.12 shows the single-phase full bridge inverter. The inverter could be unipolar or bipolar depending

on the shape of the output voltage waveform. The drawbacks with bipolar is “two IGBT and two diodes switching at the switching frequency with whole input voltage, therefore doubling the switching losses” [21].

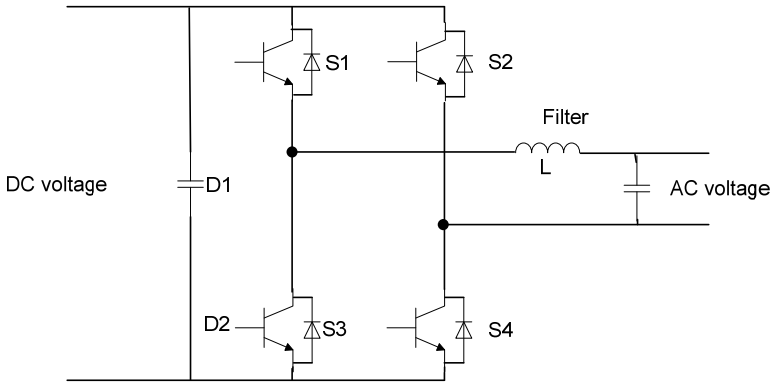

Figure 2.12: Single-phase full bridge inverter [9]

Figure 2.13 is the three-phase full bridge inverter. The command of the switch depends on the modulation schemes to obtain the sinusoidal output.

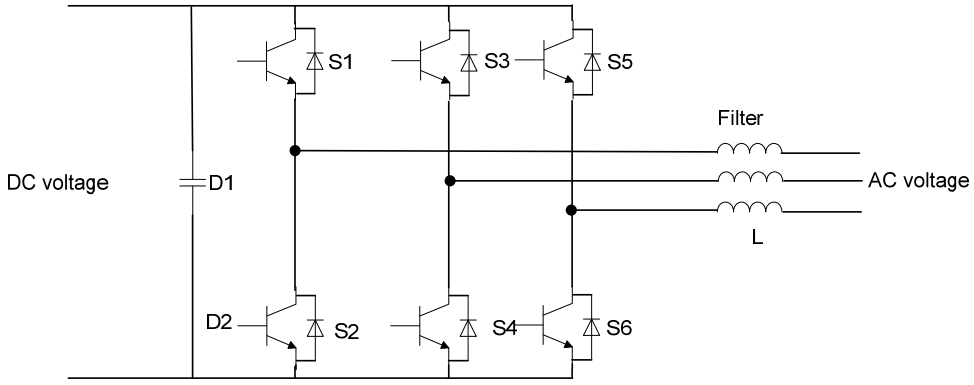

Figure 2.13: Three-phase full bridge inverter

2.5 Voltage and current control

In order to control the current delivered by photovoltaic array, it is essential to transform the three-phase ac signals into d-q reference frame. The voltage control and current control are processed in DC equivalents instead of the three-phase originally sinusoidal signals. In [7], the current control is realized by extracting the reactive and active power from the PV array. After, the regulation is realized by decoupling the d and q axis current. The voltage control is to make the dc-link voltage constant. In current control, it is imperative that the current be within the phase in terms of the voltage of the grid and the system has to be robust with respect to system disturbances.

- PI controller with feed forward compensation (figure 2.14):

Zhou Dejia *etal*. [4] design a three-phase current controlled space vector PWM inverter in rotating synchronous coordinate d-q to connect the photovoltaic array to the grid. The control scheme is a PI current regulator that regulates the d and q current components. A voltage regulator PI that regulates the PV DC bus voltage generates the command id. This type of regulation allows operating the system close to unity power factor by setting the i_q command equal to zero. The gain parameter of the regulator is obtained by trial and error. The result gives a unity power factor with low total harmonic distortion (THD). With the MPPT controller, the MPP of the PV array is reached quickly and smoothly. A feed forward compensation is added to the current loop, which gives a good dynamic and better performance in steady state. The advantage of this type of control is that the design and assessment of the loop of the

current control is practical and simple. Liang ma *et al.* [6] adopted a Synchronous PI current control for the grid-connected photovoltaic inverter. The principle is to convert the abc reference frame of the current in d-q two-phase rotating frame to achieve the rotating frame control structure. By changing the reference frame the three-phase symmetric grid voltage and grid current become DC variables. The current loop can obtain no steady state error. The results obtained with this method show that the output current and voltage were of the same phase with power factor unity. The harmonic contents are very low.

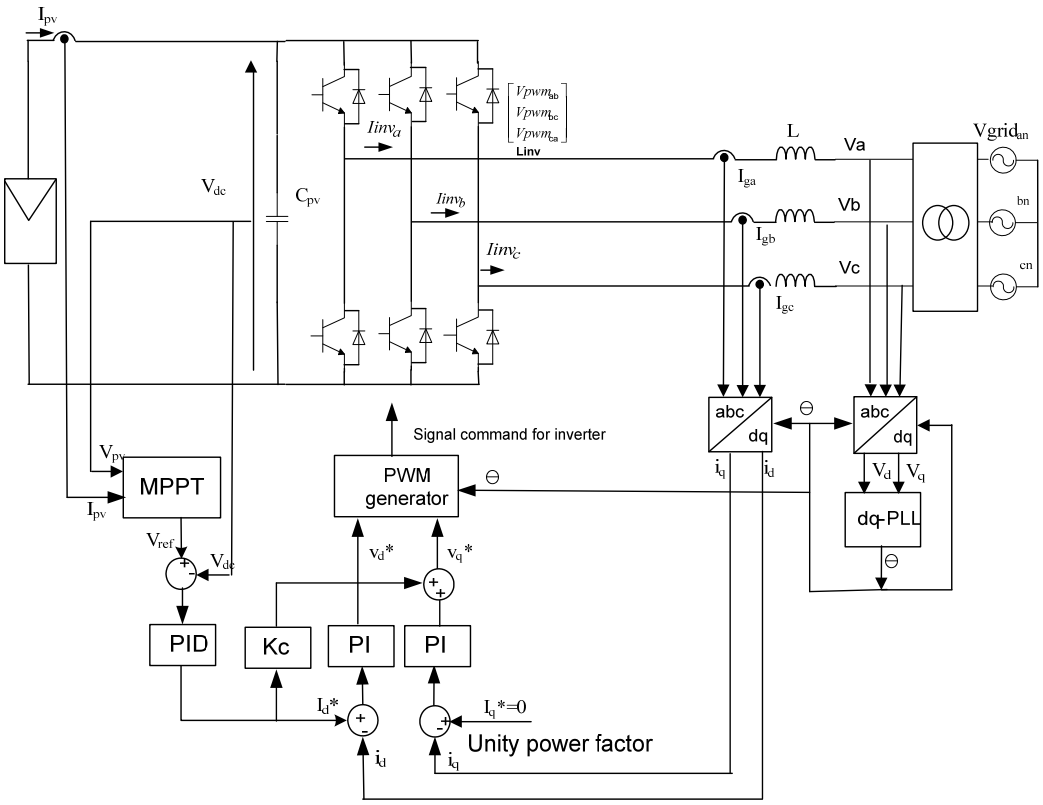

Figure 2.14: PI controller with feed forward [6]

2.6 Modulation techniques

The modulation used to command the three-phase inverter is space vector Pulse width modulation (SVPWM). This technique is largely used in power electronics nowadays and is easier to implement digitally. The basic techniques are the same for three-phase inverter. Jiyong Li *etal*. [1] have proposed a Space vector PWM control scheme for three-phase PWM inverter in PV generation system. Each state voltage is calculated from the V_{dc}input voltage of the inverter. The reference voltage vector is calculated within the appropriateregion for the purpose of minimizing the time for switching along with current harmonics [1]. At first, the voltage in αβ reference frame is determined, then the duration period T_1 and T_2 time duration for each vector in each PWM cycle. The advantages with SVPWM modulation techniques are "low total harmonic distortion (THD), constant switching frequency, well-defined output harmonic spectrum, optimum switching pattern and excellent dc-link voltage utilization" [1]. However, the drawbacks of SVPWM are explained in [2] by Q. Zeng *etal*. In their research, they find that the regulator of current is sensitive to variation of the current due to the non-linearity of the system, time delay and sampling time. The SVPWM is a problem when connected to the grid because of the "lacks of inherent over current protection of the SVPWM" [2].

2.7 Problem Statement

The above literature review shows the existing research resulting for photovoltaic system. Thus, the following problem topics still need further investigation: maximum power point tracker of the PV, the topology of the photovoltaic system, the power electronics interface, the voltage control and current control in island mode and grid connected mode. The single stage photovoltaic system is a cheap topology because it uses fewer components; costs less and weighs less. The DC/AC inverter handles the maximum power point and inverts the DC current into AC current. The goal is to operate the PV system at the maximum power point and at the same time to produce current with less harmonic distortion.

The Perturb and Observe algorithm is widely used in maximum power point algorithm. However, this method oscillates around the MPP. The incremental conductance is more stable, but It is not efficient with a boost converter. Having a maximum power point control stable, efficient and fast tracking is the goal.

Since the different area of the photovoltaic system required more investigation, a simulation model is required study and analyzes the different converter topology, current harmonics, stability and control of the photovoltaic system.

Therefore, this technical report will develop a study of the photovoltaic system. It will analyze and develop the modeling and simulation of the photovoltaic array, the maximum power point control and the DC/DC converter. The step of modeling with MATLAB and Simulink of the photovoltaic system are shown respectively and

simulation results are provided. The Simulink model of the PV could be used in the future for extended study with different DC/DC converter topology. Optimization of MPPT algorithm can be implemented with the existing Photovoltaic and DC/DC converter

After this literature review, the report is organized with the following structure:

Chapter 3 will address the theory and modeling of the PV system,

Chapter 4 will describe the Simulink block used to model the PV system,

Chapter 5 will give an example of PV system and analyze the results,

Chapter 6 will conclude the report and future research.

Chapter 3:System Description and Modeling ofthe Photovoltaic System

3.1 General topology of photovoltaic system

As discussed in the previous chapter, there are several methods to connect the solar panel. The grid can be directly linked to it or the load itself. The topology of the PV system determines the type of converter interface that should be used. It depends on the configuration, the cost and the efficacy objective. In the single stage configuration, as shown in figure 3.1, the interface of the PV array to the grid is realized with the DC/AC inverter. The DC/AC inverter functions are to boost the PV voltage, track the MPP of the PV array and control the current injected to the grid.

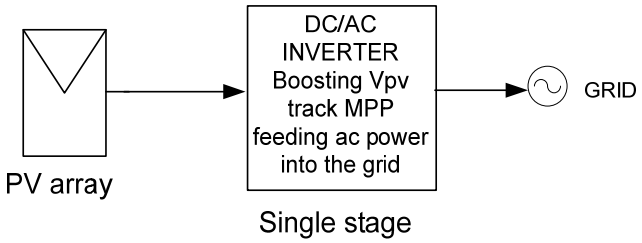

Figure 3.1**:** Structure of Single stage DC/AC Photovoltaic system

In the other side, the dual stage configuration represented in figure 3.2 is composed of the DC/DC and DC/AC inverter to connect the PV array to the grid.

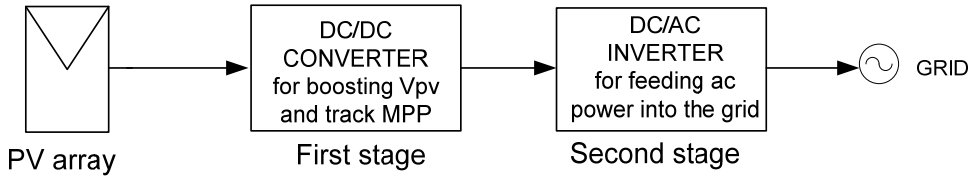

Figure 3.2:Structure of dual stageDC/DC and DC/AC Photovoltaic system

The topology study in this technical report will be a photovoltaic linked with a converter focusing on the boost along with a resistive load. A boost converter with a controller for the maximum power point, which is used to track the MPP of the PV. This topology is shown in figure 3.3. It allows studying the efficiency of the maximum power point control method and the performance of the PV to achieve the maximum power at different temperature, irradiance and load.

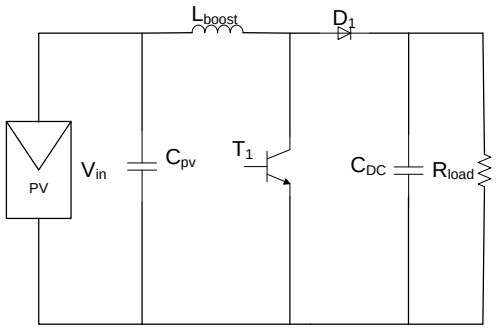

Figure 3.3: Topology of PV with boost converter and resistive load.

Figure 3.4 is a three-phase photovoltaic system with resistive load. In this topology, the photovoltaic array is the source of energy, the DC/DC boost converter isto adjust the DC-link voltage, tracks the maximum power and boost the PV voltage; the DC/AC inverter injects the AC currents to the load.

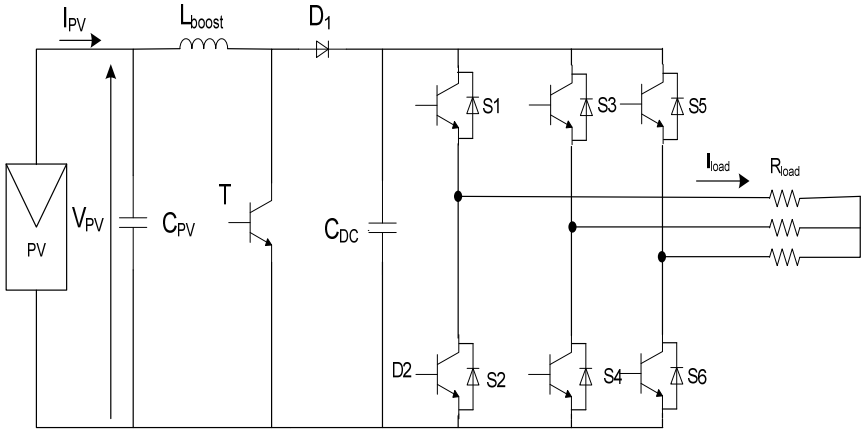

Figure 3.4: Topology dual stage three-phase photovoltaic system with resistive load

3.2 Photovoltaic array modeling

3.2.1Curves I-V Characteristics of the PV array

Figure 3.5 and 3.6 show the current voltage (I-V) characteristics of PV panel. This curve is nonlinear and crucially relies on the temperature along with the solar irradiation. In figure 3.5, when the irradiation increases, the current increases more than the voltage and the power maximum power point P_{mpp} increases as well.

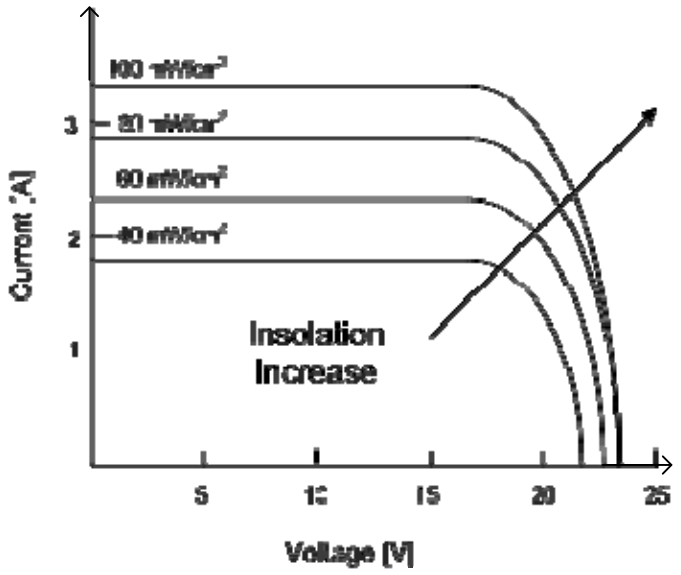

Figure 3.5: I-V Characteristics of the PV as function of irradiance

Figure 3.6 shows the variation of the current with the temperature, the current changes less than the voltage.

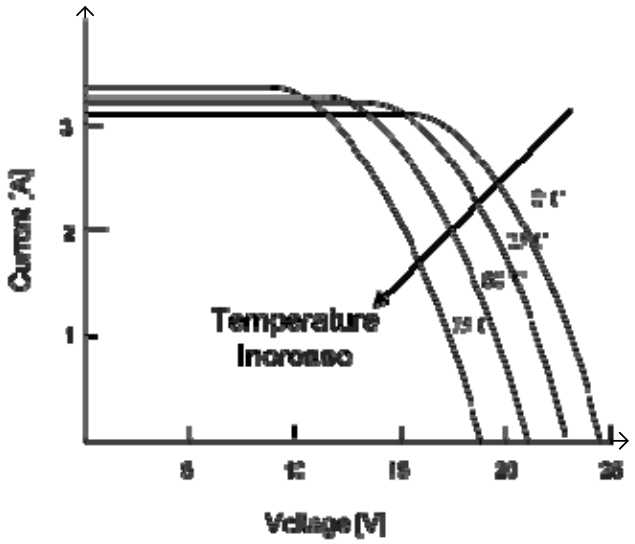

Figure 3.6: I-V Characteristics of the PV as function of Temperature

Thus, a dynamic point exists on the I-V curve called the Maximum power point MPP. The entire PV system has to execute at its maximum output power as shown in figure 3.7. The location of the power point maximal is unknown, for that reason we use calculation models and search algorithms methods to sustain the PV array functioning mark at the MPP.

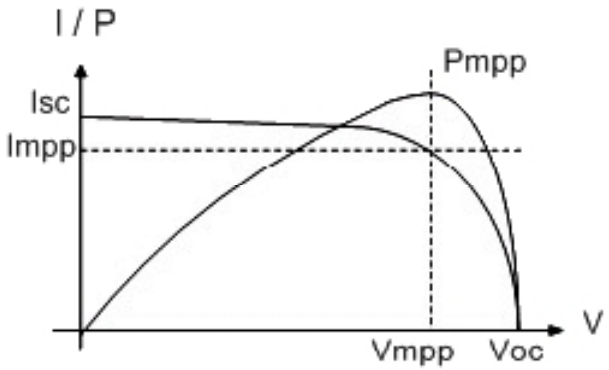

Figure 3.7: I-Vcurve, P-V curve with the MPP

3.2.2 Model of the PV cell

PV cell is a semiconductor p-n intersection that transforms sunlight to electrical power. To model a solar cell, it is imperative that we asses the effect of different factors on the solar panels and to consider the characteristics given by the manufacturers in the datasheet. It is to be noted that to form a PV module, a set of cells are connected in series or in parallel. To form a PV array, a set of PV modules are connected in series and in parallel. Thus, the mathematical models for PV array are attained while utilizing the basic description equivalent circuit of the PV cells.

A PV cell is usually embodied by an electrical equivalent of one-diode, resistance series $R_s$and resistance parallel $R_p$as shown in Figure 3.8.

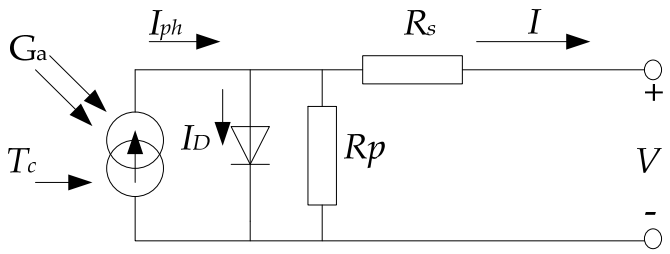

Figure 3.8: Equivalent circuit of solar cell with one diode

From the figure 3.8, the different parameters characteristics of the PV cells are:

I_{ph}: currents generated by the solar cells (A)

R_s: resistance series (Ω)

R_p: resistance parallel (Ω)

G_a: irradiance from the sunlight(W/m2)

T: cell temperature (K)

I_d: diode current (A)

I: output current of the PV (A)

V: output voltage of the PV (V)

Manufacturer of the solar module gives the another parameters needed to model the solar cells. The datasheet which gives the electrical characteristics is calculated under standard test condition STC when the temperature T is 25°C and the irradiance G is 1000 W/m2. The parameters that can be found inside the datasheet are:

V_{oc}: open circuit voltage (V)

I_{sc}: short-circuit current(A)

P_{mp}: power at maximum power point,

V_{mp}: voltage at maximum power point

I_{mp}: current at maximum power point

The solar cell is model first, then extendsthe model to a PV module, and finally models the PV array. From figure 3.5, the output current of the PV cell is

$$I = I_{ph} - I_d$$

where

I_{ph}: photon produced by the cell,

I_d:diode current

By Shockley equation, the diode current I_d is given by

$$I_d = I_0\left(e^{qV_d/kT} - 1\right)$$

where

I_0: reverse saturation current of diode,

q: elementaryelectron charge (1.602×10^{-19}C),

V_d: diode voltage,

k: Boltzmann constant 1.381×10^{-23} (J/K)

T: temperature in kelvin (K)

The relation between voltage and current result by replacing the diode current

$$I = I_{ph} - I_0\left(e^{qV_d/kT} - 1\right)$$

where V_d is the output voltage of the PV cell.

The reverse saturation $I_0$is found by using the above equation. By setting the current I equal to zero and calculating at temperature T_1[39]

$$I_0(T_1) = \frac{I_{ph}(T_1)}{(e^{qV_{oc}/kT} - 1)}$$

The current generated by the solar cells I_{ph} can be approximated with the short circuit current I_{sc} in [40]. The current generated can be calculated for other irradiance. The standard current, temperature and irradiance from the datasheet are used to determine the current at different condition.

$$I_{sc} \approx I_{ph}$$

$$I_{sc}(T_1) = \left(\frac{G}{G_{nom}}\right) I_{sc}(T_{1,nom})$$

where

$I_{sc(T1)}$: current at temperature T_1

$T_{1,nom}$ the temperature of cell from datasheet at STC

G_{nom}: irradiance from datasheet at STC

After calculation,[3] gives the equation of the PV

$$I = I_{ph} - I_0 \left[e^{q\left(\frac{V+I.R_S}{akT}\right)}\right] - \left(\frac{V + I.R_s}{R_p}\right)$$

where

a: diode quality factor between 1 and 2 and must be estimated. The value of "a" is equal to 1 for ideal diode.

V is the cell voltage. For a PV module, the cell voltage is multiplied by the total amount of the cells found within the series.

The reverse saturation current I_0 depends on the temperature T. It is calculated by the following equation [3]:

$$I_0 = I_0(T_1) \left(\frac{T}{T_1}\right)^{\frac{3}{n}} . e^{\frac{qV_q(T_1)}{ak\left(\frac{1}{T}-\frac{1}{T_1}\right)}}$$

The value of resistance series R_s is quantified from the slope dV/dI of the I-V curve at the point open circuit voltage [39]. The equation R_s is given by

$$R_s = -\frac{dV}{dI} - \frac{akT/q}{I_0 . e^{(\frac{qV_{oc}}{akT})}}$$

The model is completed by using the following recursive equations to find the currents [39]. The recursive equation is used to calculate the current for a PV cell. It is more convenient to solve numerically. The equation introduces a simplified method to calculate resistance series and neglect the resistance parallel.

$$I_{n+1} = I_n - \frac{I_{ph} - I_n - I_0\left[e^{q\left(\frac{V+I_n.R_S}{akT}\right)} - 1\right]}{-1 - I_0\left(\frac{q.R_s}{akT}\right)e^{q\left(\frac{V+I_n.R_S}{akT}\right)}}$$

3.2.3Model of the Photovoltaic module

The following model uses different method to calculate the resistance series and resistance parallel. For example, the BP MSX 120 is made of 72 solar cells (silicon nitride multicrystalline) in series and provides 120W of nominal maximum power. The maximum power point's voltage is 33.7 V and current delivered at maximum power point is 3.56 A. The parameters of the BP MSX120 are given in table 3.1, which is essential to model the PV array.

Short circuit current I_{sc}	*3.87 A*
Open circuit voltage V_{oc}	*42.1 V*
Current at maximum power point I_{MPP}	*3.56 A*
Voltage at maximum power point V_{MPP}	*33.7 V*
Number of cells in series N_s	*72*
Temperature coefficient of Isc	*(0.065±0.015)% ºC*
Temperature coefficient of Voc	*-(80±10)mV/ºC*
Pmax	*120W*

Table 3.1 PV module BP MSX120 datasheet at STC [Appendix B]

Different models of the photovoltaic are developed in literature [31, 33, 34, 35]. The following equation developed in [3] will be used mainly in this report. The model consists of finding the curve characteristic of the PV module from the datasheet. The equation used to calculate the I-V curve is:

$$I = I_{ph} - I_0 \left[e^{q\left(\frac{V+I.R_s}{N_s kTa}\right)} - 1 \right] - \left(\frac{V + I.R_s}{R_p} \right)$$

where

N_s: number of cells in series

The thermal voltage of the module with Ns cells connected in series is defined by

$$V_t = N_s kT/q$$

The current produced $I_{ph}$is linearly dependent of the solar radiation and the temperature

$$I_{ph} = I_{ph,nom} + K_i \Delta_T (\frac{G}{G_{nom}})$$

where

Ki: temperature coefficient current

ΔT: variation temperature

The diode saturation current I_0 and the reliance on the temperature can be seen through

$$I_0 = I_{0,n} \left(\frac{T}{T_{nom}}\right)^3 exp\left[\frac{qE_g}{ak}\left(\frac{1}{T_{nom}} - \frac{1}{T}\right)\right]$$

$$I_{0,n} = \frac{I_{sc,n}}{exp\left(\frac{V_{oc,n}}{aV_{t,n}}\right) - 1}$$

The series resistance R_s is calculated by determining the slope dV/dI of the I-V curve at the V_{oc}. By differentiating the equation, R_s become [39]

$$R_s = \frac{dI}{dV} - \frac{nkT/q}{I_0 . e^{q\left(\frac{V+I.R_a}{akT}\right)}}$$

At the open circuit voltage, voltage V is equal to the open circuit voltage V_{oc} with I equal to zero. The resistance series is:

$$R_s = -\frac{dV}{dI} - \frac{nkT/q}{I_0 . e^{(\frac{qV_{oc}}{akT})}}$$

Where

dV/dI: slope of the I-V curve at the V_{oc}. In some situations, R_p is neglected.

In [38], R_s and R_p are calculated iteratively. The goal is to find the values of R_s and R_p that makes the mathematical P-V curve coincide with the experimental peak power at the (V_{mp}, I_{mp}) point. The value of R_s and R_p are reached when the iteration stopped for P_{max}calculated is equal to P_{max} estimated.

The circuit model of the PV module is shown in figure 3.9. It is a controlled current source with the equivalent resistors and the equation of the model above. The variation of the power being taken by the load varies the PV voltage.

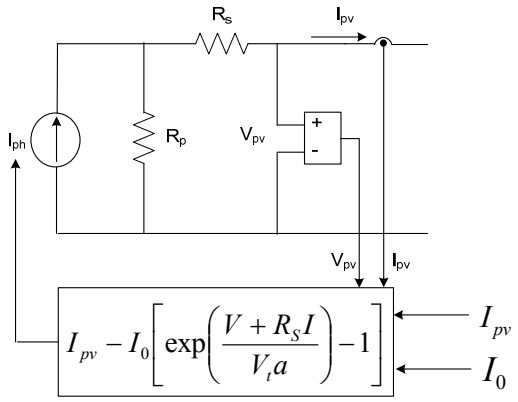

Figure 3.9: Circuit model of the photovoltaic module [3]

3.2.4 Photovoltaic array

The PV array is composed of several interconnected photovoltaic modules. The modeling process is the same as the PV module from the PV cells. The same parameters from the datasheet are used. To obtain the required power, voltage and current, the PV modules are associated in series and parallel. The number of modules connected in series and connected in parallel must be calculated. Figure 3.10 shows a photovoltaic array, which consists of multiple modules, linked in parallel and series. N_{ser} is the total quantity of modules within the series and N_{par} is amount of modules in parallel. The number of modules modifies the value of resistance in parallel and resistance in series. The value of equivalent resistance series and resistance parallel of the PV array are:

$$R_{s,array} = \frac{R_{s,module} . N_{ser}}{N_{par}}$$

$$R_{p,array} = \frac{R_{p,module} . N_{ser}}{N_{par}}$$

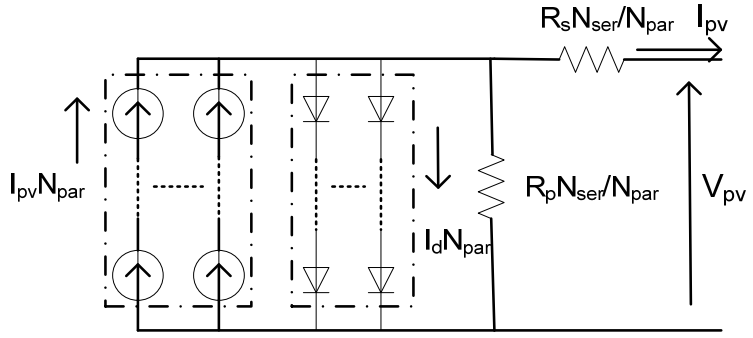

Figure 3.10PV Array composed of N_{ser}xN_{par} modules [3]

After extending the relation current voltage of the PV modules to a PV array, the new relation of current voltage of the PV array is calculated in [3] by

$$I = I_{pv}N_{par} - I_0 N_{par}\left[exp\left(\frac{V + R_s\left(\frac{N_{ser}}{N_{par}}\right)I}{V_t a N_{ser}}\right) - 1\right] - \frac{V + R_s\left(\frac{N_{ser}}{N_{par}}\right)I}{R_p\left(\frac{N_{ser}}{N_{par}}\right)}$$

Where I_0, I_{pv}, V_t are the same parameters used for a PV modules.

This equation is valid for any given array formed with identical modules.

The photovoltaic array will be simulated with this equation. The simulation circuit must include the number modules series and parallel. Figure 3.11 shows the circuitmodel of the PV array.

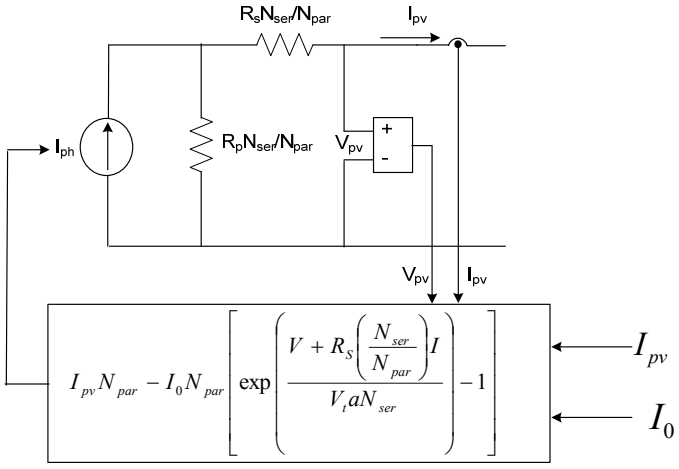

Figure 3.11: Model structure of the photovoltaic array [3]

3.3 DC/DC converter

3.3.1 Operation of the boost converter

The main purpose of the DC/DC is to convert the DC input from the PV into a higher DC output. The maximum power point tracker uses the DC/DC converter to adjust the PV voltage at the maximum power point.The boost topology is used for stepping up the low voltage input from the PV. A boost type converter steps up the PV voltage to high voltage necessary for the inverter.

Figure 3.12 shows the Boost converter. The DC input voltage is in series with an inductor L that acts as a current source. A switch T is in parallel with the current source that turns on and off periodically, providing energy from the inductor and the source to increase the average output voltage.

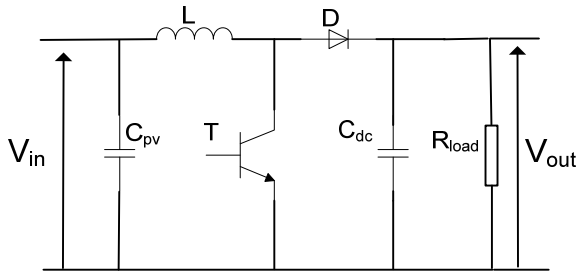

Figure 3.12:Topology of Boost converter

The voltage ratio for a boost converter is derived based on the time integral of the inductor voltage equal to zero over switching period. The voltage ratio is equivalent to the ratio of the switching period to the off time of the switch [50]

$$\frac{V_o}{V_{in}} = \frac{T}{t_{off}} = \frac{1}{1-D}$$

Thecapacitor $C_{dc}$is large enough to keep a constant output voltage, and the inductor provides energy when the switch is open, boosting the voltage across the load.

The duty cycle from the MPPT controller is to control the switch of the boost converter. It is a gate signal to turn on and off the switches by pulse width modulation. Figure 3.13 shows the DC/DC boost converter with the ideal switches open.

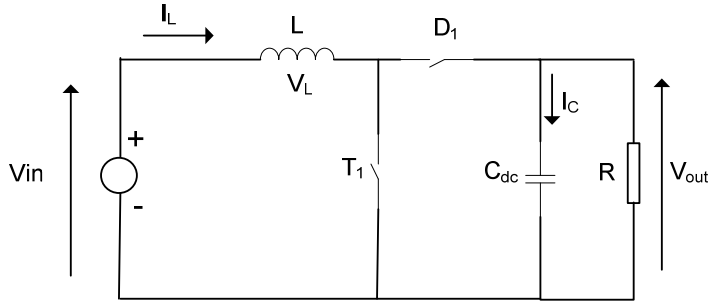

Figure 3.13:Schematic diagram of Boost converter

In In figure 3.14, the switch T_1 is on and D_1 is off, the circuit is split into two different parts: the source chargers the inductor on the left while the right has the capacitor, which is responsible for sustaining outgoing voltage via energy, stored previously. The current of inductor L is increased gradually.

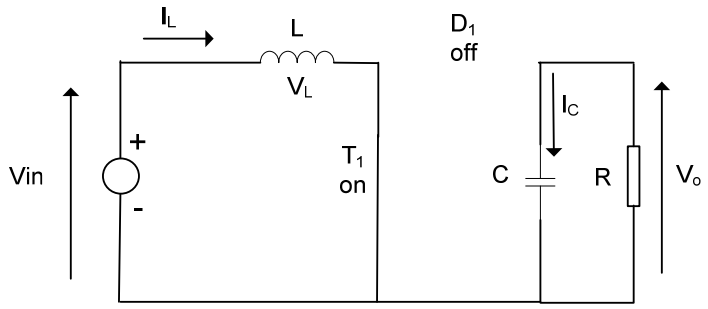

Figure 3.14:Diagram when switch T_1 is on and D_1 is off

In figure 3.15, the switch T_1 is off and D_1 is on, the energy along with the DC source that is stored within the inductor will help supplement power for the circuit that is on the right thereby resulting in a boost for the output voltage. Then, the inductor current discharges and reduces gradually. The output voltage could be sustained at a particular wanted level if the switching sequence is controlled.

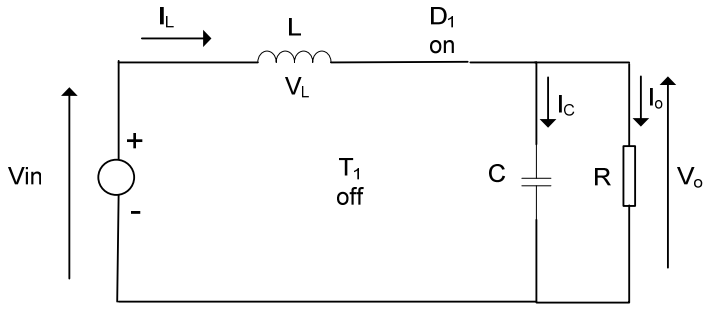

Figure 3.15:Diagram when switch T_1 is off and D_1 is on

When switch $T_1$is turn on,V_L can be expressed as described in [50]:

$$v_L = V_{in}$$

$$i_c = \frac{-v_{out}}{R}$$

While switch T_1 off, D_1 on

$$v_L = V_{in} - v_{out}$$

$$i_c = i_L - \frac{v_{out}}{R}$$

Assuming a small ripple approximation $v_o \approx V_o$ and $i_L \approx I$

In a stabilized condition, the time integral of the integral voltage around the course of a particular time has to be zero

$$\int_0^{T_s} V_L(t)dt = (V_{in})DT_s + (V_{in} - V_o)D'T_s$$

After equating to zero, the voltage output will be:

$$V_{out} = \frac{V_{in}}{D'} = \frac{V_{in}}{1 - D}$$

Assuming a lossless circuit $P_{in}=P_{out}$

$$\frac{I_{out}}{I_{in}} = (1 - D)$$

It can be seen that the output voltage increases as D increases. The ideal boost converter is capable of producing any output voltage greater than the input voltage.

Continuous conduction mode

In continuous conduction mode (CCM), the switch is ON for period t to t_{on} as shown figure 3.16. The inductor current is positive and ramp up linearly. The inductor voltage is V_{in}. Once the switch is turned OFF (figure 3.16), the current from the inductor reduces until the switch is once again turned on. The inductor voltage is the difference between V_{in} and V_{out}. In order to attain constant conduction, the voltage for the output becomes the function of the duty cycle D along with the voltage for the input V_{in}.

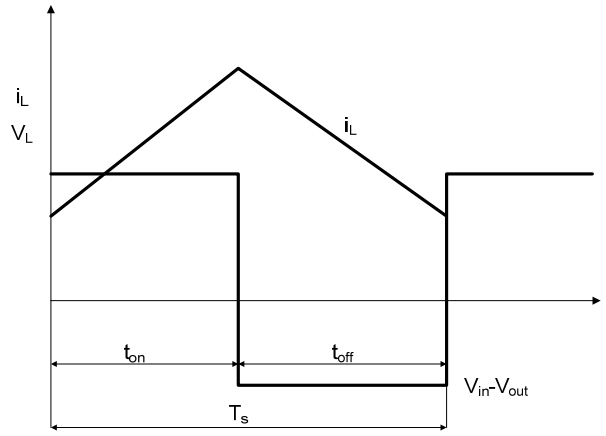

Figure 3.16: Continuous conduction mode [51]

Discontinuous mode

The boost converter functions in a discontinuous mode (DCM) if the current inductor drops to zero prior to the next turn-on of the switch. The inductor current falls

to zero at every period. Figure 3.17 shows the discontinuous conduction mode. The relation between input and output voltage become

$$\frac{V_{out}}{V_{in}} = \frac{D_1 + D}{D_1}$$

The average input current is calculated in [51]

$$I_{in} = \frac{V_{in}}{2L} DT_s(D + D_1)$$

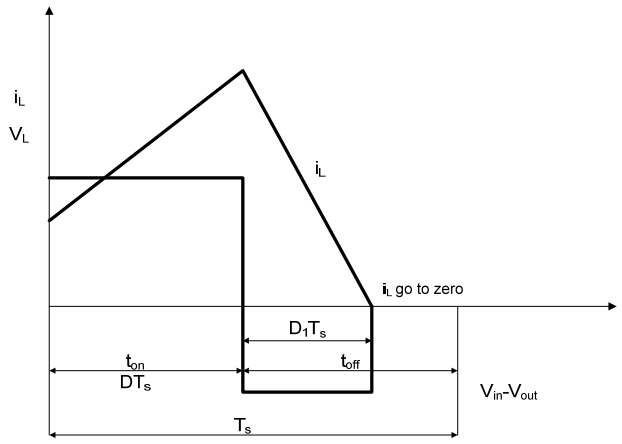

Figure 3.17: Discontinuous conduction mode [51]

Figure 3.18 summarizes the currents and voltages for output in terms of the boost converter. The control switch for the voltage of control is shown. The switch turns ON and OFF for a period t_{on} and $t_{off.}$ When the switch is on, the voltage across the switch is zero and once the switch is turned off, the voltage is V_{out}. The voltage across the inductor L is equal to the photovoltaic voltage during the on time of the transistor.

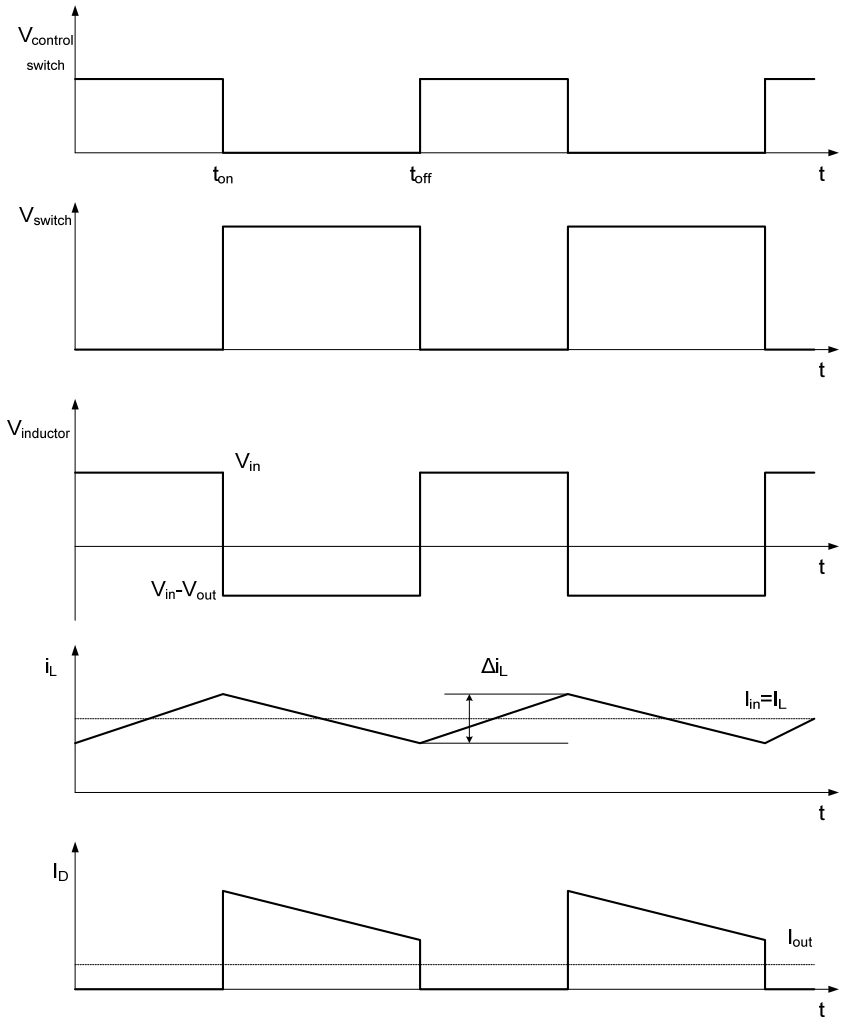

Figure 3.18:.Output waveform of DC/DC converter [14]

3.3.2 Selection of the inductor

The input inductor values can be calculated based on the energy discharged during t_{on} and t_{off} times and the current ripples. In photovoltaic system, the boost converter functions in the discontinuous and continuous modes of conduction. The conduction mode of the converter could change depending on the atmospheric

conditions. The inductor is then calculated based on the maximum inductor current and at maximum input power. In [50] and [53], the inductor of the boost converter is given by

$$L \geq \frac{V_{om}.D_m.(1-D_m)}{f_s|\Delta I_{Lripple}|}$$

where

D_m: duty cycle of the switch at maximum converter input power

f_s: switching frequency

V_{om}: maximum of the dc component of the output voltage

$\Delta I_{Lripple}$: ripple current of the inductor

3.3.3 Power decoupling capacitor

The power decoupling capacitor $C_{pv}$is the capacitor linked in parallel with the PV array. It is the capacitor at the input of the boost converter. The decoupling capacitor is calculated in [53] with

$$C_{PV} \geq \frac{I_{om}.{D_m}^2}{0.02\ (1-D_m)f_s V_{pv\_mpp}}$$

where

I_{om}: output current at maximum output power

V_{pv_nmpp}: PV output voltage at maximum power point

The capacitor in parallel with the load is the DC link capacitor.The value of the capacitor depends on the minimum ripple voltage. It is given in [18] with:

$$C_{DC} \geq \frac{V_{load}.D}{f_s \Delta V_{load} R_{load}}$$

where

V_{load}: output voltage of the boost converter

ΔV_{load}: output ripple voltage

The output voltage of the PV array depends on the variation of temperature and insolation. To compensate the variation of the output voltage of the PV, a dc link capacitor is installed between the PV and the inverter. It helps to reduce the voltage ripple and provides energy storage for a short period and for a rapid change of the PV voltage.

3.4 DC/AC inverter analysis

In this paragraph, inverter architectures and waveforms will be introduced as an overview. Detailed description of single-phase inverter and six-stepthree-phase will be analyzed for photovoltaic system. Detailed modulation strategies of the space vector modulation will be described for the three-phase inverter.

3.4.1 Single phase full bridge DC/AC inverter

In photovoltaic system, the DC/AC inverter is used to converts the power of the source by switching the DC input voltage (or current) in a pre-determined sequence to generate AC voltage (or current) output. Figure 3.19 shows the equivalent circuit of single-phase inverter. This has four switches that turn on and off to obtain a sinusoidal output.

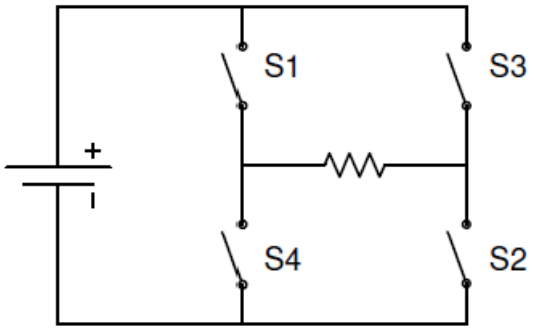

Figure 3.19: Equivalent circuit of the full bridge single-phase inverter [57]

The load of the inverter is a single-phase AC load or connected to single-phase grid power. The topology of the single-phase inverter is represented in figure 3.20. The single-phase inverter has four switches and four anti-parallel protective diodes. It provide path for the inductive current to flow when the switches are open and protect the switches from the large voltage by interrupting the inductive current.

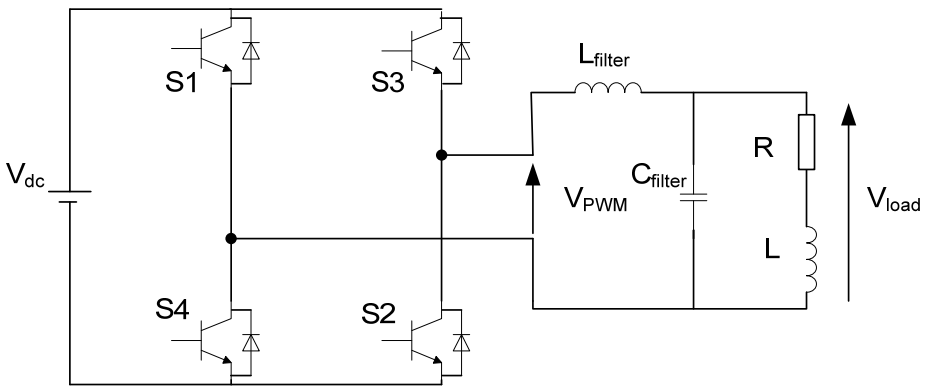

Figure 3.20 Topology of a single-phaseinverter with filter and load

To generate an AC waveform in single-phase inverter, the switches S1, S2 ON and S3, S4 off for period t1 and t2 as shown in figure 3.21. For that period, the output is a positive voltage.

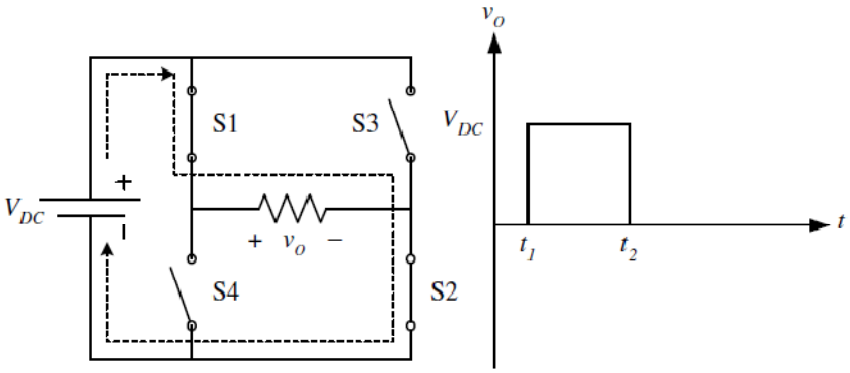

Figure 3.21: Output current for S1, S2 ON; S3, S4 OFF for t1 < t < t2 [57]

For period t2 to t3 in figure 3.22, the switches S3, S4 are on and S1 and S2 are off to obtain negative voltage.

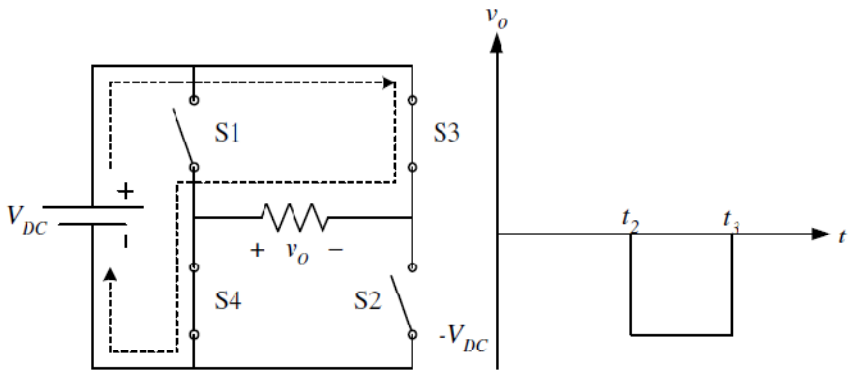

Figure 3.22: Output current for S3, S4ON; S1, S2 OFF for t2 < t < t3 [57]

Switches S1 and S4 should not be closed simultaneously, the same for switches S3 and S2. Otherwise short circuit of the DC bus will occur.

By following the switching scheme, the inverter output voltage will alternate between positive and negative (figure 3.23), and the sinusoidal fundamental component is obtained as shown in figure 3.24.

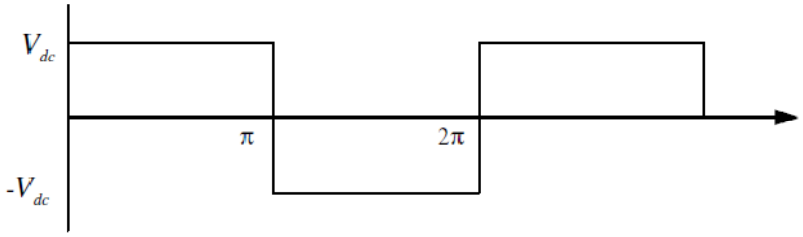

Figure 3.23: Single-phaseoutput voltage [57]

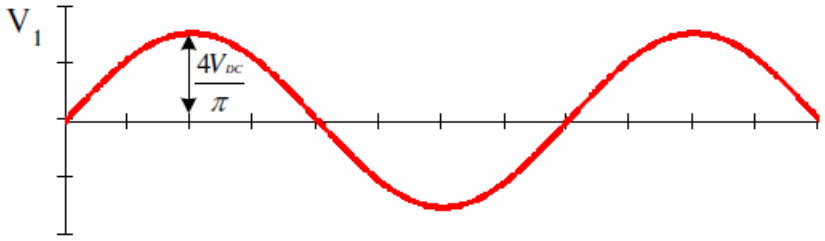

Figure 3.24: fundamental component [57]

The load voltage is calculated by

$$V_o = V_{DC}\ for\ period\ 0 < \varphi < \pi$$

$$V_o = -V_{DC}\ for\ period\ 0 < \varphi < \pi$$

The resulting output voltage has a fundamental alternating component and its time average is zero. The sharp transition in voltage indicates the presence of high frequency harmonics. The harmonics can be filtered with inductance and capacitor filters or controlled by implementing appropriate PWM techniques.

The instantaneous inductive load current is given in [58]

$$i_{Load}(\varphi) = \begin{Bmatrix} \frac{V_{DC}}{R} - \frac{V_{DC}}{R}\left(1 + \tanh\left(\frac{\pi R}{2\omega L}\right)\right) e^{\frac{-\varphi R}{\omega L}}, for\ 0 < \varphi < \pi \\ \frac{-V_{DC}}{R} + \frac{V_{DC}}{R}\left(1 + \tanh\left(\frac{\pi R}{2\omega L}\right)\right) e^{\frac{-(\varphi-\pi)R}{\omega L}}, for\ 0 < \varphi < 2\pi \end{Bmatrix}$$

where R is the resistive load and L is the inductance. A blanking time is introduced in the switching cycle in order to evade a short circuit across the DC bus. The short circuit happens if S1 and S4 are on simultaneously closed due to the time delay associated with process of turning the switch OFF. The blanking time is realized by

switching S1 and S3 or S4 and S2 OFF and hence the output voltage will be zero. The blanking time introduces low order harmonics to the voltage of the output, which is hard to filter out. Using the switching scheme with the blanking time, the output load voltage and current waveform is as shown in figure 3.25.

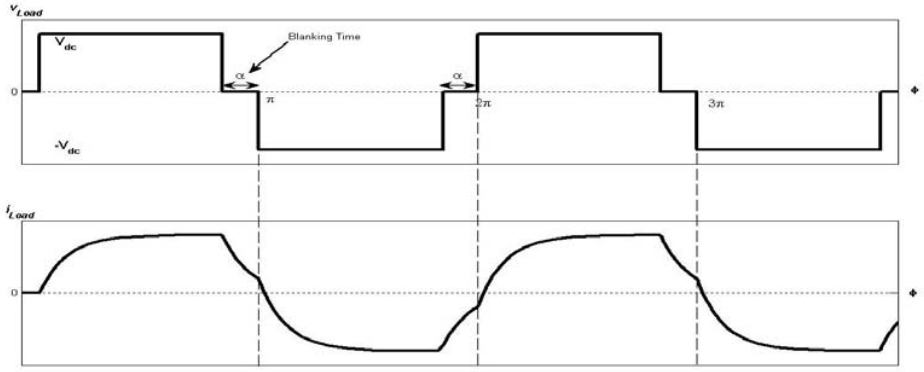

Figure 3.25: Output voltage and current with blanking time [59]

The magnitude of the n-th harmonic of the output voltage is given by Fourier analysis with [58]

$$V_n = 4V_{DC}\frac{\cos(n\alpha)}{n\pi}; n = 1, 2, 3 \ldots$$

Where α is the blanking time along with the scale of each harmonic rests on it. The blanking time is

$$\alpha = \frac{\pi}{2n}$$

The magnitude of the harmonic depends of the angle α. Figure 3.26 shows an example of voltage output harmonic spectrum when α is 10.

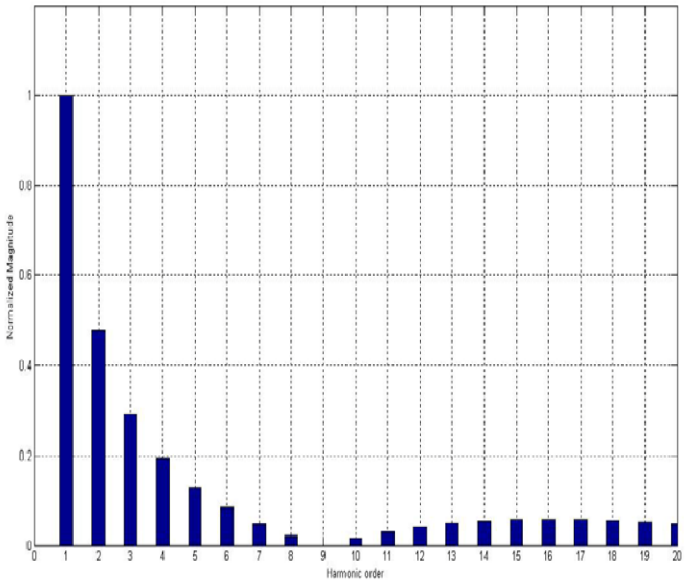

Figure 3.26: Harmonic of output voltage when α is 10. [59]

The PWM techniques provide control scheme to reduce harmonics. The technics can reduce the number of filter in high frequencies.

3.4.2 Six step inverter

The six-step inverter is used to obtain a three-phase voltage output from DC source. Three-phase voltage source inverter is a combination of three single-phase bridge circuits. A simplified diagram of a basic three-phase inverter bridge is shown in figure 3.27. There are diodes in antiparallel in addition to the main power devices. These diodes are called the return current or feedback diodes. It provides an alternate path for the inductive current.

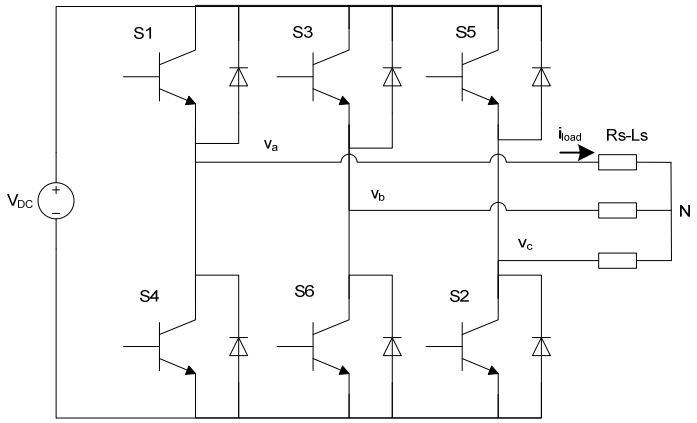

Figure 3.27: Three-phase six-step inverter

To obtain the three-phase AC current in six-step inverter, six gating signals need to be applied to the six switches of the inverter. The waveforms of gating signals H1, H3 and H5 are shown in figure 3.28. H1, H3, H5 are 3 phase symmetrical switching function with phase shift 120°. To produce the symmetrical three phase voltages across a three phase load the devices are switched ON for 180°. The switching signals of each inverter leg are displaced by 120° with respect to the adjacent legs. The switching signals S1 and S4 are complimentary, the same for S3 and S6, S5 and S2.

The switching sequence will be S1S2S3, S2S3S4, S3S4S5, S4S5S6, S5S6S1, S6S1S2, S1S2S3, … for a positive sequence. The sequence will be reversed to get the negative phase sequence.

The line to neutral voltages V_{an} represented the six step of the inverter. V_{bn} and V_{cn} have the same waveform with phase shift 120°.

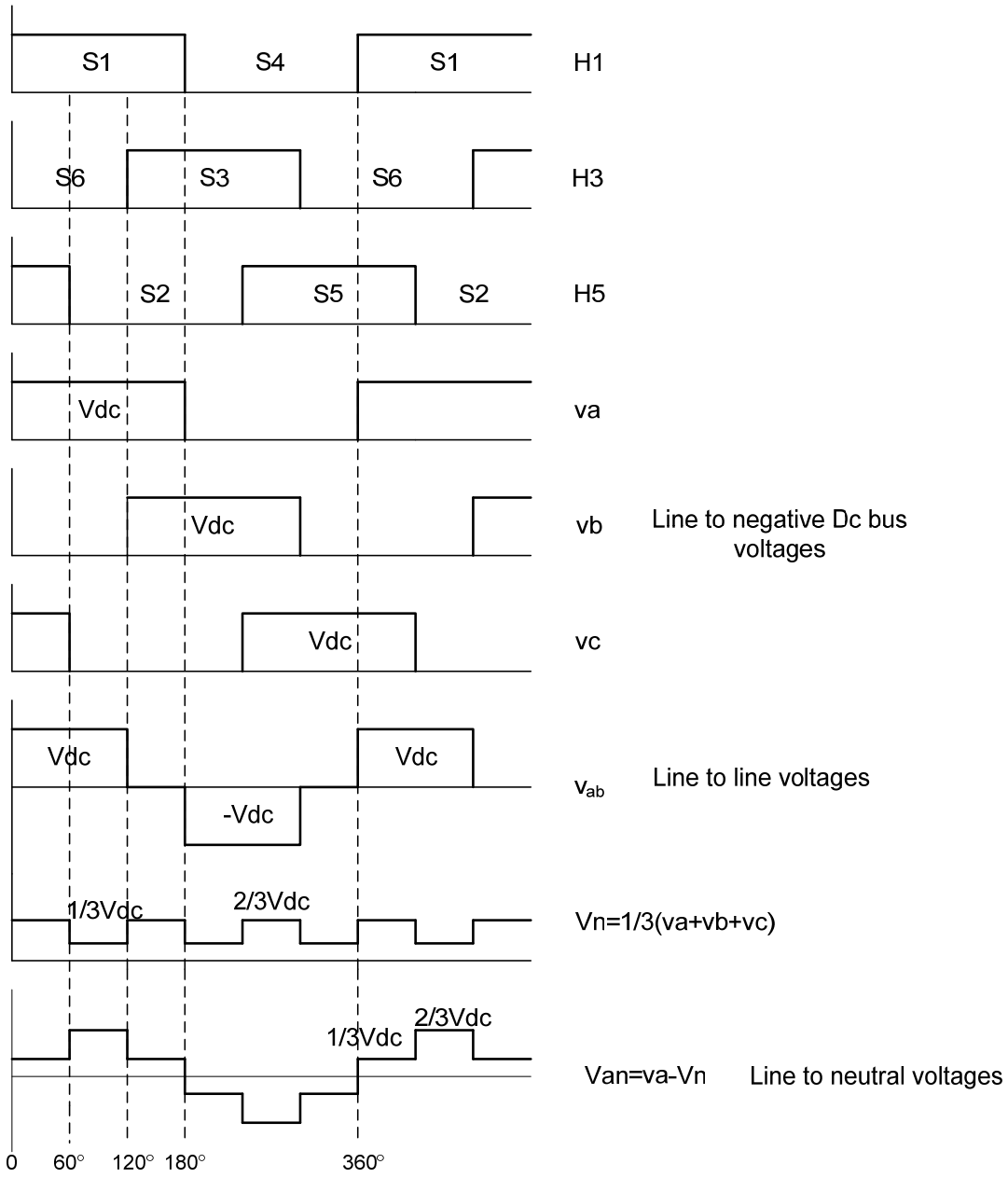

Figure 3.28: Waveforms of the switching functions.

Each switch is turned ON for 180°. The switches S1 and S4, which belong to the leftmost inverter leg, produce the output voltage for phase A. The switching signals for the switches in the middle leg, S3 and S6 for phase B, and are delayed by 120° from those for S1 and S4 respectively for a positive sequence. Similarly, for the same phase sequence, the switching signals for switches S5 and S2 are delayed from the switching signals for S3 and S6 by 120°.

It is called “six-step inverter” since there are six “steps” in the line to neutral (phase) voltage waveform as shown in figure 3.28.

For a six steps inverter, the output currents do not have harmonics of order three and multiples of three. Figure 3.29 represents the harmonics currents of the six steps inverter.

Control over output heft in a three-phase inverter could be attained by altering the voltage of the DC-link (V_{dc})

$$(V_{an})_{1,peak} = 1.278V_{DC}/2$$

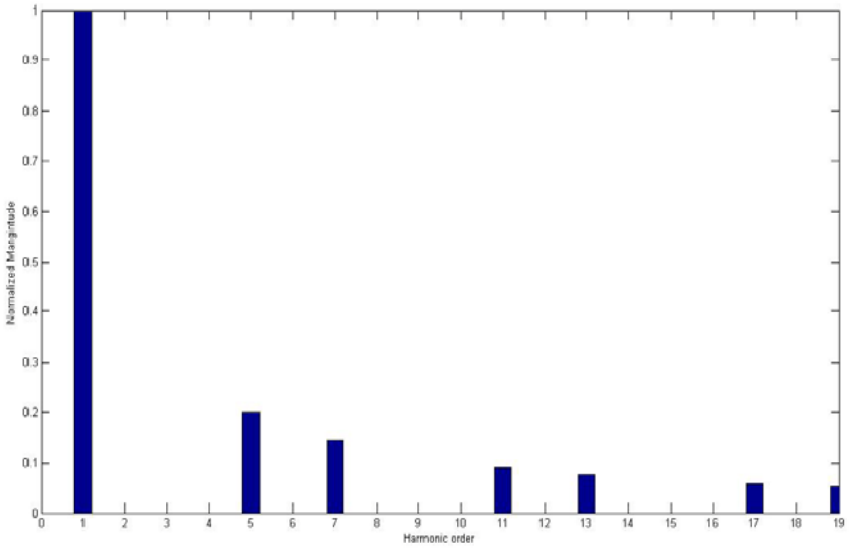

Figure 3.29: Phase voltage normalized spectrum [59]

In grid connected PV, the current output of the voltage source inverter will be injected to the grid. The output of the inverter should be in phase and have an identical frequency to the voltage of the grid.

3.5 Modulation strategies

3.5.1 SVPWM techniques

The three-phase power inverter is the same represented in figure 3.27.There are six power switchesS1 to S6. Each of them are controlled by individual switching variables which are obtained from the principles of space vector PWM.[62]The three-phase voltage in abc reference frame should be represented in dq reference frame for the Space vector PWM. The output voltages can be represented in the space as set of

vectors. These vectors correspond to switching combinations for the inverter switches. There are eight combinations for the voltage output as is made evident in figure 3.30.

The three phase output voltages in the full bridge inverter at any instant of time can be represented by a set of eight base space vectors as per the eight positions of switching in terms of the inverter. The principle of Space vector PWM is one cycle of the output voltage that can be represented by six sectors (60˚ each). A rotating reference voltage V_{ref} that is calculated through an estimate based on 3 adjacent vectors represent the desired output voltage.

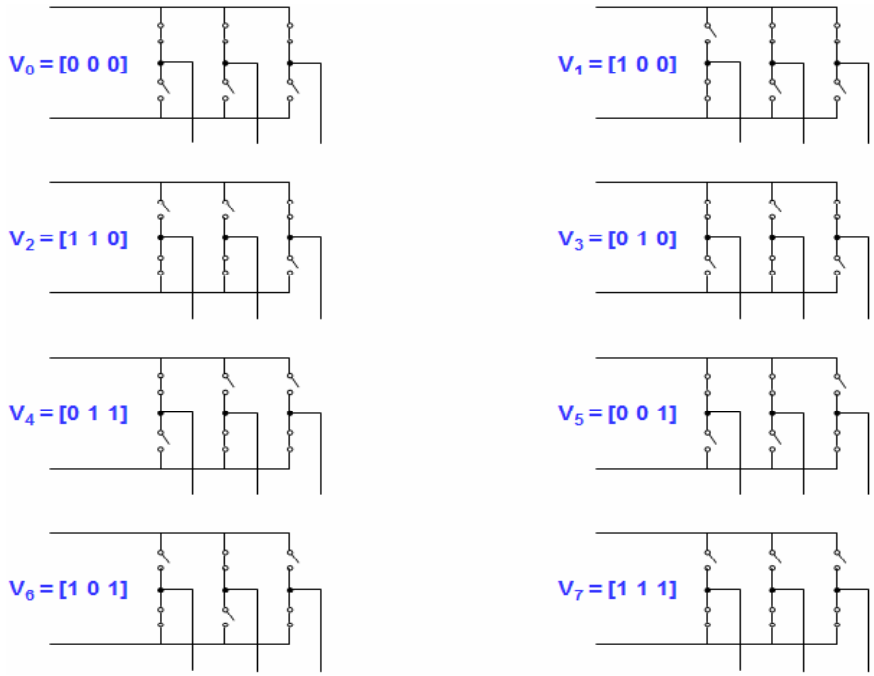

Figure 3.30 Eight switching states [23]

Figure 3.31 shows these base vectors V_1 through V_6 and the two zero vectors V_0 and V_7 which correspond to switching positions resulting in zero output voltage.

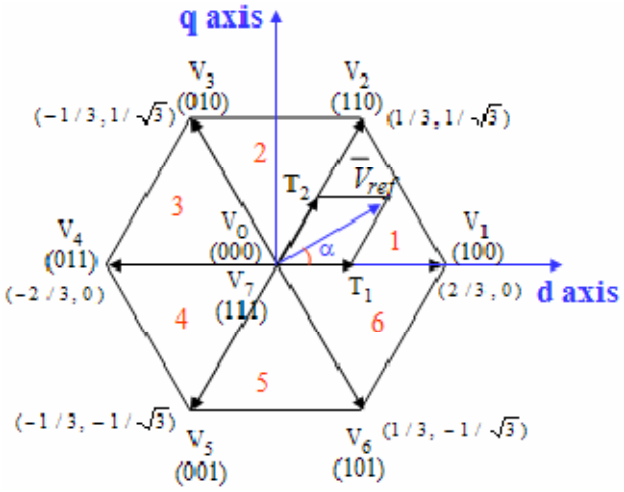

Figure 3.31: Switching vectors and the 6 sectors [60]

Figure 3.31 shows the approximate reference voltage vector V_{ref}, which uses the eight switching patterns (V_0 to V_7) [61]. In space vector modulation, the voltage vectors V_0 to V_7 for certain instances are applied in a manner that the "mean vector" of the PWM period T_z is equal to the desired voltage vector.

The principle of space vector PWM technique is that the voltage vector command is calculated by estimation via three adjacent vectors base. It is necessary to decompose the space voltage vector $\boldsymbol{V_{ref[\alpha,\beta]}}$ into directions of the sector base vectors. [46]. For instance, if V_{ref} is located in sector 1(figure 3.31), the base vectors are V_1, V_2 and V_0 (V_7 can also be used because it gives the same output voltage), if V_{ref} is located in sectors 2, the base vector surrounding V_{ref} are V_2, V_3 and V_0.

The timespan of every vector for the voltage is taken by calculations in sector 1 where

$T_z V_{ref} = T_1 V_1 + T_2 V_2 + T_0 V_0$

$T_z = T_1 + T_2 + T_0$

where V_1, V_2 and V_0 basically outline the triangular area in which V_{ref} are found. T_1, T_2 and T_0 are the matching vector periods and T_z is the sampling time

V_1 (100) is applied for a period of T_1

V_2 (110) is applied for period T_2

V_0 (000) or V_7 (111) is applied for period of T_0 for this sector.

Table 3.2 summarizes the switching pattern to be applied for each legs to obtain the voltage vectors. It shows the amplitude of the output line to neutral voltage and the line-to-line voltage.

Voltage Vectors	**Switching Vectors**			**Line to neutral voltage** $\times Vdc$			**Line to line voltage** $\times Vdc$		
	a	**b**	**c**	V_{an}	V_{bn}	V_{cn}	V_{ab}	V_{bc}	V_{ca}
V_0	0	0	0	0	0	0	0	0	0
V_1	1	0	0	$2/3$	$-1/3$	$-1/3$	1	0	-1
V_2	1	1	0	$1/3$	$1/3$	$-2/3$	0	1	-1
V_3	0	1	0	$-1/3$	$2/3$	$-1/3$	-1	1	0
V_4	0	1	1	$-2/3$	$1/3$	$1/3$	-1	0	1
V_5	0	0	1	$-1/3$	$-1/3$	$2/3$	0	-1	1
V_6	1	0	1	$1/3$	$-2/3$	$1/3$	1	-1	0
V_7	1	1	1	0	0	0	0	0	0

Table 3.2: Switching states of the inverter switches [60]

Determination of time duration T_1, T_2, T_0

$$T_z \cdot V_{ref} \cdot \begin{bmatrix}\cos\alpha \\ \sin\alpha\end{bmatrix} = T_1 \cdot \frac{2}{3} V_{dc} \begin{bmatrix}1 \\ 0\end{bmatrix} + T_2 \cdot \frac{2}{3} V_{dc} \begin{bmatrix}\cos\pi/3 \\ \sin\pi/3\end{bmatrix}$$

$0 \leq \alpha \leq \pi/3$ and define $a = \frac{\left|V_{ref[\alpha,\beta]}\right|}{\frac{2}{3}V_{dc}}$

$$T_1 = T_z \cdot a \cdot \frac{(\sin\pi/3 - \alpha)}{\sin\pi/3}$$

$$T_2 = T_z \cdot a \cdot \frac{\sin\alpha}{\sin\pi/3}$$

$$T_0 = T_z - T_2 - T_1$$

Switching time duration at any sector [2]

The base vectors change for each sector. Let define n is the sector 1 to 6 and $0 \leq \alpha \leq 60^{\circ}$

$$T_1 = \frac{\sqrt{3}.T_z.\left|V_{ref}\right|}{V_{dc}}\left(sin\left(\frac{\pi}{3} - \alpha + \frac{n-1}{3}\pi\right)\right)$$

$$T_1 = \frac{\sqrt{3}.T_z.\left|V_{ref}\right|}{V_{dc}}\left(\sin\frac{n}{3}\pi\cos\alpha - \cos\frac{n}{3}\pi\sin\alpha\right)$$

$$T_2 = \frac{\sqrt{3}.T_z.\left|V_{ref}\right|}{V_{dc}}\left(sin\left(\alpha - \frac{n-1}{3}\pi\right)\right)$$

$$T_2 = \frac{\sqrt{3}.T_z.\left|V_{ref}\right|}{V_{dc}}\left(\sin\alpha.\cos\frac{n-1}{3}\pi - \cos\alpha\,.\sin\frac{n-1}{3}\pi\right)$$

$$T_0 = T_z - T_1 - T_2$$

The duration T_1, T_2 and T_0 are applied for each sector to caculate the output voltage. The switching pattern is determine to have less switching of the devices. For instance in sector 1, T_z can be decomposed as

$$T_z = \frac{T_0}{4}.V_0 + \frac{T_1}{2}.V_1 + \frac{T_2}{2}.V_2 + \frac{T_0}{4}.V_7 + \frac{T_0}{4}.V_7 + \frac{T_2}{2}.V_2 + \frac{T_1}{2}.V_1 + \frac{T_0}{4}.V_0$$

Thisarrangement allows to prevent un-necessary switching and lower switching losses in practice and always maintains the total duration period T_z. Such arrangement is used for all the 6 sectors. It allows to have the voltage V_0 at the start and end of every cycleso when T_z repeats, there is no need to change the states of the switches.

In sector 2, the base voltages are V_2 and V_3 ; for sector 3, the base voltages are V_3 and V_4. Sometimes the order of T_1 and T_2 can be interchanged to avoid the changement of the state of the switches and to minimize the switching losses. If the switching frequency is 5400 hz then $1/T_z$=5400hz and the fundamental frequency is 60hz, then T_z repeats 15 times for each sector. For one period, the output voltage can be represented by 90 vectors. The switching time and switching sequence at each sector is summarized in figure 3.32.In this situation, the switching waveforms are symmetrical. The switching sequence is described below each switching pattern, for example for sector 1, switching sequence is 0,1,2,7,7,2,1,0, for sector 2, switching sequence is 0,3,2,7,7,2,3…and so on.

The DC input of the SVPWM is the output from the boost converter.

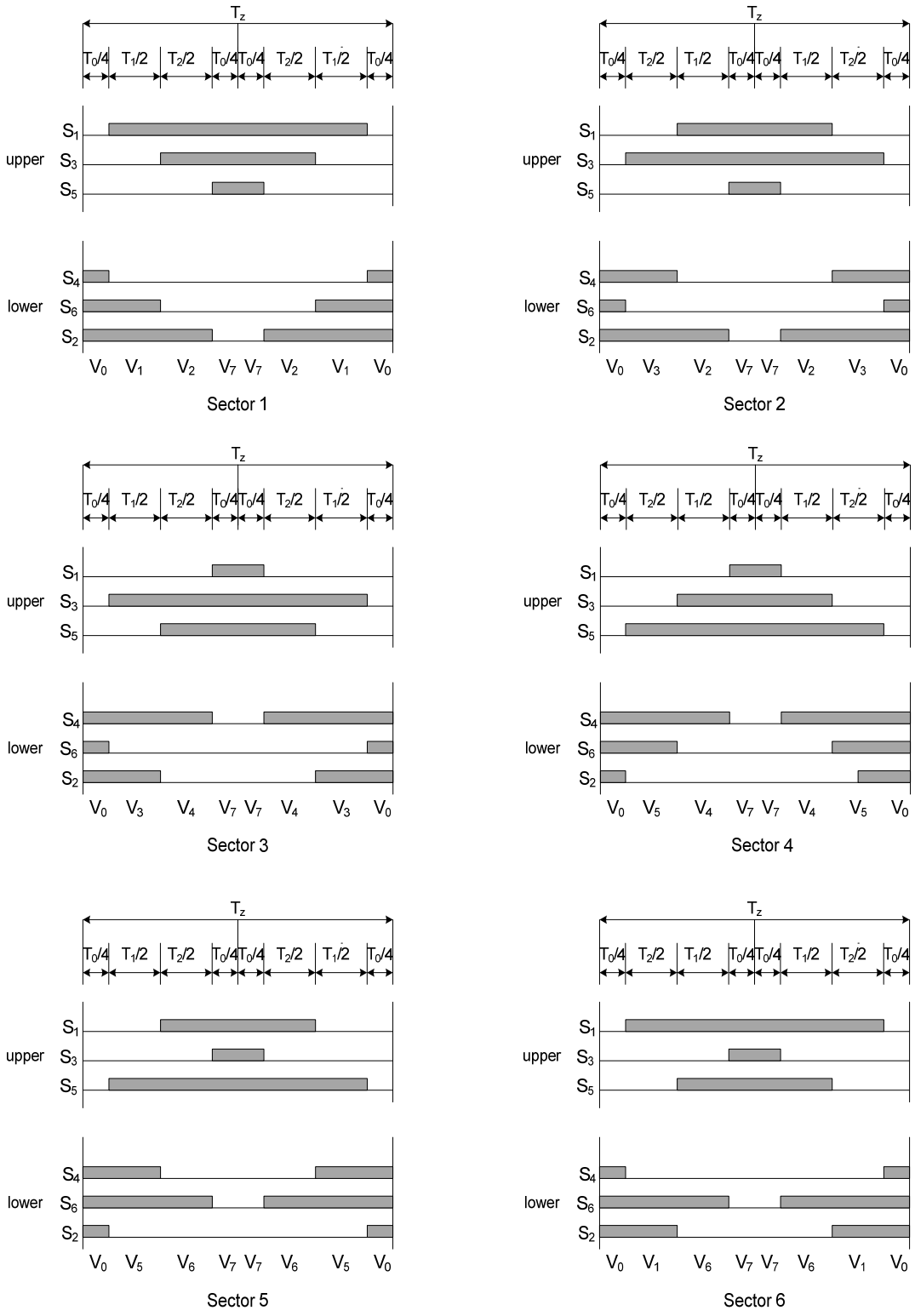

Figure 3.32: Space vector PWM switching patterns and sector duration

3.5.2 Sine PWM

In sine-triangle three-phase PWM inverter, three sinusoidal reference voltage waveforms at each phase are compared to the same triangular carrier. The three-referencevoltages are 120° apart.

$$v_{a,ref} = V_{ref} \sin(2\pi f \times t)$$

$$v_{b,ref} = V_{ref} \sin(2\pi f \times t - 2\pi/3)$$

$$v_{b,ref} = V_{ref} \sin(2\pi f \times t + 2\pi/3)$$

With this method, switch S1 is ON when triangular carrier is less than $v_{a,ref}$ and S4 is OFF. The output voltage $v_{a0}$is equal to V_{dc}. The same principles apply for the other legs of the converter. To summarize the principles:

$$v_{a,ref} > V_{tria} \rightarrow S1\ is\ ON$$

$$v_{a,ref} < V_{tria} \rightarrow S4\ is\ ON$$

$$v_{b,ref} > V_{tria} \rightarrow S2\ is\ ON$$

$$v_{b,ref} < V_{tria} \rightarrow S5\ is\ ON$$

$$v_{c,ref} > V_{tria} \rightarrow S3\ is\ ON$$

$$v_{c,ref} < V_{tria} \rightarrow S6\ is\ ON$$

Figure 3.33 shows the waveform of the sine triangle and the voltage reference comparison.

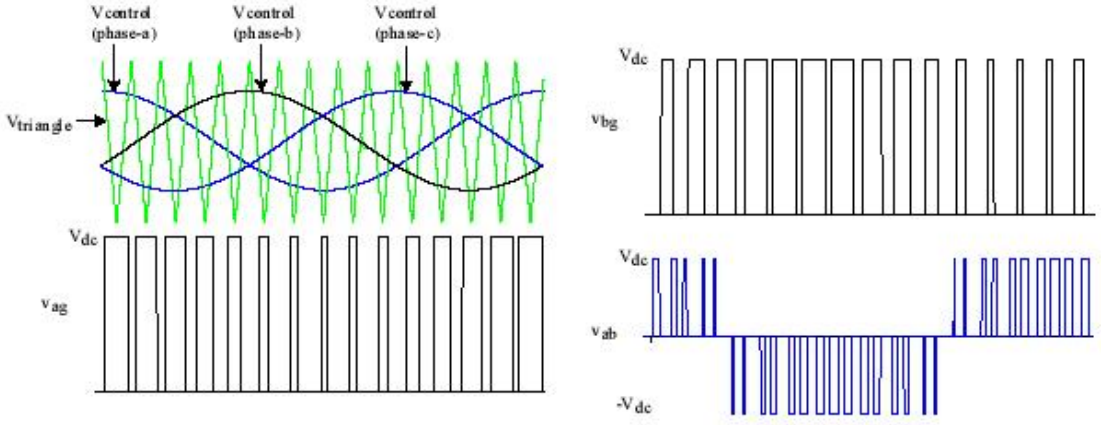

Figure 3.33: Sine triangle, voltage reference and phase voltage [52]

In sine triangle PWM, the amplitude modulation ratio (or index) m_a is defined by

$$m_a = \frac{peak\ amplitude\ of\ V_{tria}}{amplitude\ of\ V_{ref}}$$

where

V_{tria}:the peak amplitude of the triangular carrier

V_{ref} :peak amplitude of the sinusoidal reference signal

The frequencyof the triangular waveformf_{pwm} is the frequency of the inverter. The frequency of the reference is thefundamental output frequency. For a grid connected PV, it is the frequency of the grid 60 Hz. The ratio of those two frequencies gives the frequency modulation index

$$m_f = \frac{PWM\ frequency\ f_{pwm}}{fundamental\ frequency\ f_1}$$

The line to neutral fundamental frequency output voltage of the inverter is defined by [59]

$$v_{an,1} = \frac{m_a V_{DC}}{2} \sin(2\pi f_0 . t)$$

$$v_{bn,1} = \frac{m_a V_{DC}}{2} \sin(2\pi f_0 . t - \frac{2\pi}{3})$$

$$v_{an,1} = \frac{m_a V_{DC}}{2} \sin(2\pi f_0 . t + \frac{2\pi}{3})$$

The line-to-line voltage rms value at the fundamental frequency is obtained by multiplying the fundamental line to neutral fundamental frequency with$\sqrt{3}/\sqrt{2}$.

The switching frequency should be higher to reduce the harmonics at the output. Thus, less filter harmonics will be used.However, switching losses increase in proportion to the switching frequency.

In PV system, the DC voltage that is the output from the boost converter is the input for the inverter. A controller should be implemented in order to maintain the DC voltage in a constant manner. In addition, the voltage reference determines the output frequency and amplitude desired.

The function of inverter DC/AC is to generate AC output current i_{ac}in phase with the AC grid voltage v_{ac}. Switching frequency f_{pwm} is much greater than the AC line

frequency (60Hz or 50Hz).By controlling the switch duty ratio D of the inverter, it is possible to generate a sinusoidal current i_{ac} in phase with the AC line voltage. The input DC voltage V_{dc} must be greater than the peak AC line voltage.

3.6 Control of the boost converter with MPPT controller

3.6.1 Maximum power point techniques for PV

Fromthe characteristic I-V and P-V curves of photovoltaic modules, it is shown that there was a unique point for the maximum power (P_{MPP}). This point is defined as the maximum power point (MPP) with the optimal voltage V_{mpp} and the optimal current I_{mpp}.At this point, the entire PV system should operate with the maximum efficiency and produce its maximum output power.

The solar cell I-V characteristic is nonlinear and changes with irradiation and temperature. The location of the MPP is not known but need to be located. Differents MPPT methods have been realized. They vary in “complexity, sensors required for the voltage or current, convergence speed, cost, range of effectiveness and implementation hardware”[8].

The three main categories of MPPT algorithms are model-based algorithms, training based algorithms and searching algorithms.

Model-based MPPT algorithm

MPPT with Fractional short-circuit current method

This method is based on the measurement periodically of the PV short circuit current, which is approximately linear to the current maximum power point as shown in [45]

$$I_{MPP} \approx k_2 I_{SC}$$

Experimentally, $k_2$is a constant between 0.78 and 0.92. Once the constant k_2 is known, I_{MPP} is computed. The PV array needs to be shorted periodically to measure I_{sc}.

Fractional open circuit voltage

Similarly, the Fractional open-circuit voltage is based on the linear dependence between array voltages at maximum power V_{MPP} with its open circuit voltage V_{oc}[45].

$$V_{MPP} \approx k_1 V_{OC} \quad (13)$$

k_1 is a constant between 0.71 and 0.78. V_{oc} is measured by shortly shutting down the power converter.

The implementation of those methods are simple and cheap but here is excessive power loss and the efficiency of the PV is very low due to the inaccurate determination of the constant k_1 andk_2. The power loss is caused by the necessity to open and close the circuit for measurement. [45]

Searching MPPT algorithm

These algorithms are based on the measurementof the PV module output voltage and current. Then, it calculates the PV power and determines if the control parameter needs to be increased or decreased. The control parameter could be a reference signal (voltage or current) for a controller or it can be the duty ratio for the switching signal DC/DC converter.

The advantage of MPPT with searching algorithm is easy to implement, it does not require previous knowledge of the PV module characteristics. However, it is necessary to choose the dc link capacitor correctly, the switching frequency and the step size used in changing the control variable. The performance of MPPT algorithm can be affected from those parameters.

Among MPPT algorithms methods are Perturbation and observation (P&O), Hill climbing and Incremental conductance.

3.6.2 Perturb & Observe P&O/ Hill Climbing

P&O and Hill climbing use the same fundamental strategy. The duty ratio is the perturbation in hill climbing, while the voltage of the PV module is the perturbation for the P&O. Changing the value of the duty cycle causes a change to the current and as consequence, perturbs the voltage array. In Figure 3.34, the voltage and current are measured and the MPPT controller determines the voltage reference. The input for the

regulator PI is the difference of the $V_{ref}$and V_{pv}. The voltage regulated generates the PWM for the converter.

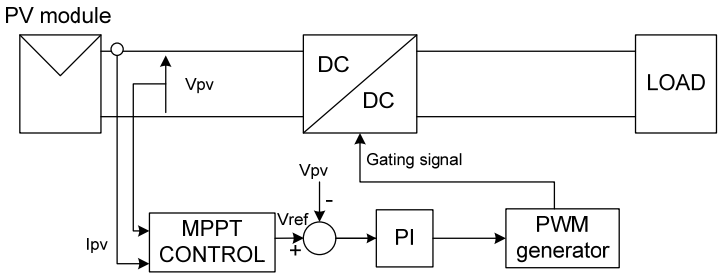

Figure 3.34: Block diagrams of MPPT with P&O [41]

For Hill climbing, there is no regulator, only the duty ratio controls the converter directly as shown in figure 3.35.

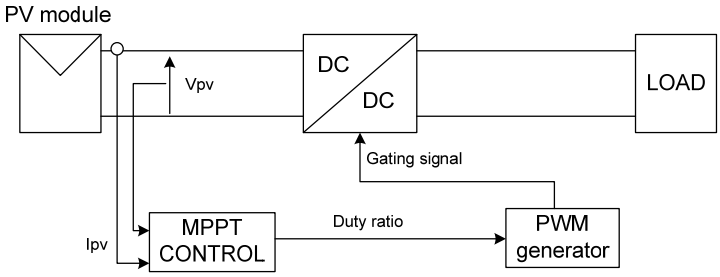

Figure 3.35: Block diagrams of MPPT with Hill Climbing [41]

In Figure 3.36, it can be observed that incrementing the PV voltage increases the power of the PV and decrementing the PV voltage decreases the power of the PV when operating on the left of the MPP. On the right of MPP, incrementing the voltage decreases the power and decrementing the voltage increases the power. This process

will be implemented in the MPPT controller to extract the maximum power from the PV module.

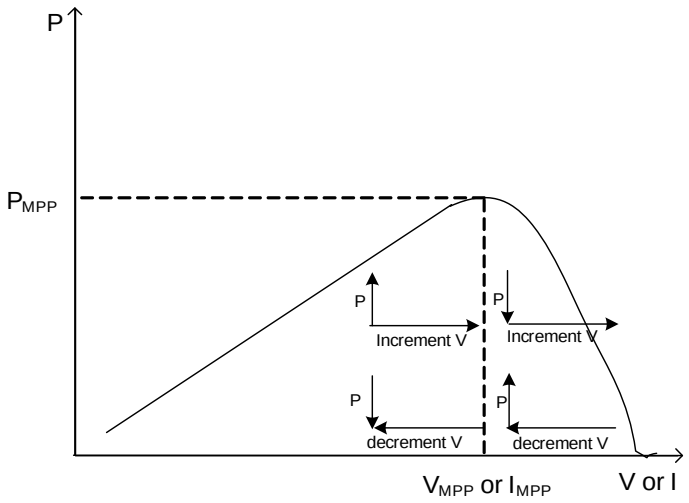

Figure 3.36: Principle of P&O

The system oscillates around the MPP with this method. The process of incrementing and decrementing can fail under rapid change in irradiation [45]. The system diverges away from MPP if the irradiance increases suddenly.

To remedy those problems, improved methods of perturb and observe are used: reduced perturbation step size, variable step size, three points weights comparison methods and optimized sampling rate[45].

Figure 3.37 described the flow chart of the perturb and observe method. At the input, there are the photovoltaic voltage and photovoltaic current. The power is then calculated from those two parameters. The sign of the power determines the duty cycle

output of the MPP controller. In simulation, the duty ratio of the boost converter is the control variable. Perturbing the duty ratio of the converter perturbs the PV array current I_{pv} and consequently perturbs the PV array voltage. The initial value of the duty cycle and PV power are given. The voltage and current of the PV array are measured first and then the power P is calculated. The power is then compared with the previous value. If the difference is positive, the duty cycle is incremented. The switch used is ideal and the boost output voltage is supposed to be constant. The range of the duty cycle is limited between zero and one to ensure that the boost will step up the input voltage within limit.

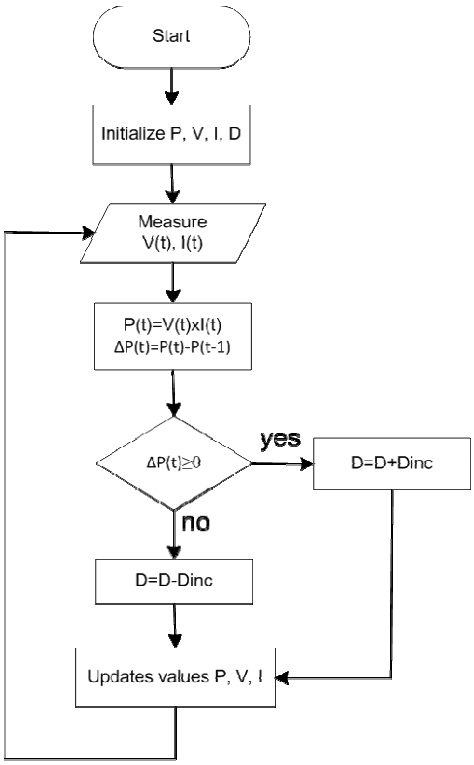

Figure 3.37: Flow chart for P&O [41]

3.6.3 Incremental conductance INC

The INC method is based on the principle that the derivative of the PV array power curve is zero at maximum power point (MPP), i.e. the slope of the power curve is zero($dp/dV=0$) [45]. The slope of power curve is positive on the left of the MPP and negative on the right.

In this method, the PV model operates at maximum power when the Voltage reference $V_{ref}$is reached. When there is a variation of the irradiation or the temperature, the current ΔI changes and then the MPP.

The algorithm decrements or increments the duty cycle and tracks the new MPP again. A fast calculation of the slope is required and the sampling rates should be high in order to obtain a better result. This method requires an appropriate value of the increment size. The MPP may be tracked rapidly with bigger increments but the system might oscillate about the MPP.

Figure 3.38 represents the algorithm for the incremental conductance. The input data is similar to the Perturb and Observe method. The algorithm starts by measuring the voltage and current of the PV. Then, it calculates the difference from the previous measurement and determines the power. The difference of voltage and current will need to be performed at each step.

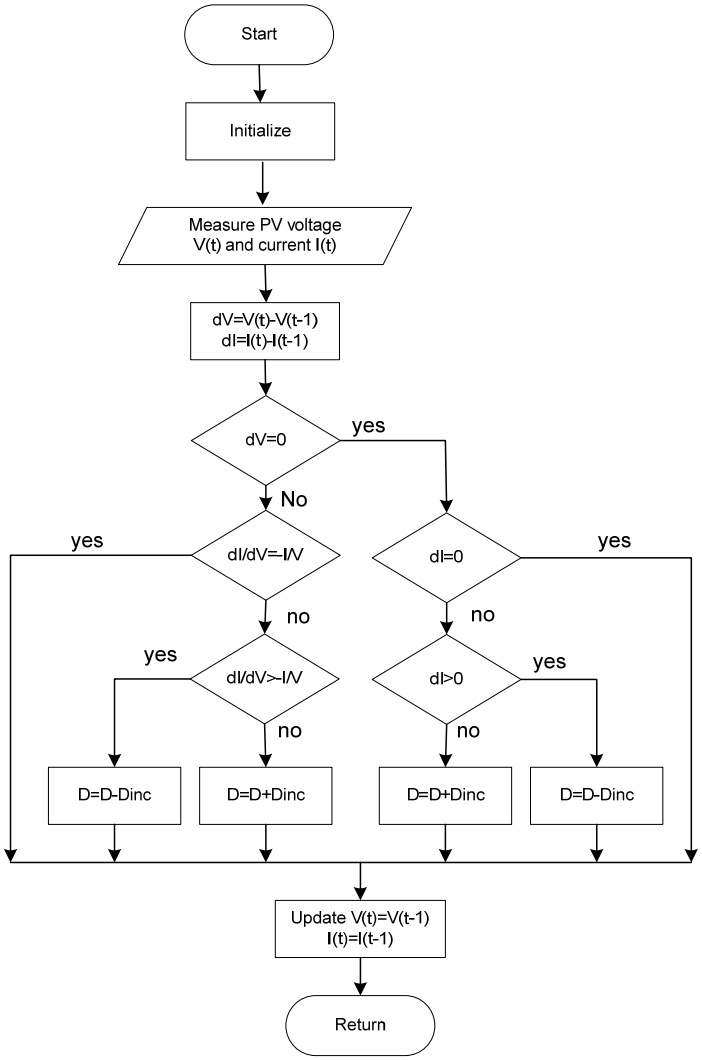

Figure 3.38: Flow chart of Incremental conductance [45]

The duty cycle is incremented or decremented. The output of the incremental algorithm is the duty cycle, which is the optimal value to command the boost converter. The PV array will operate at maximum power with duty cycle from the MPPT controller. The variation of the duty cycle varies the boost converter voltage. The algorithm keeps tracking until MPP is reached.

3.6.4 Duty cycle step optimization

The performance of the Perturb and Observe depends on the sampling interval and the duty-cycle perturbation of the algorithm [48]. Those parameters set "the dynamic response of the MPPT, such as speed, accuracy and stability" [49]. The duty cycle step must be chosen properly. Since the Perturb and Observe technique oscillates around the maximum power point, reducing the duty cycle step can minimize the oscillation and the steady state losses. However, the controller is less efficient when the atmospheric conditions change rapidly [48].

The other parameter to consider is the sampling interval of the algorithm. Higher sampling interval can cause instability. The maximum power can be missed between sampling interval if the perturb and observe algorithm samples the PV voltage and current too quickly. In [48] suggested that the sampling interval of the algorithm should be set as small as possible without causing oscillation of the system and the divergence away from the MPP. Otherwise, the instability will reduce the efficiency of the PV.

3.7 Proposed control strategy for the two stage PV system

Figure 3.39 shows an example of voltage and current control block of two stages PV system. A voltage control is required to maintain the DC link voltage constant. The boost DC/DC converter is driven by the duty cycle from the MPPT. Then, the

voltage from the boost is compared to the reference voltage V_{ref}. It uses the same principle as described in [6]. A PID controller can be used for the voltage controller.

For the current control, the three-phase current in abc reference frame is decoupled in dq reference frame. The current i_q* reference is set to zero to obtain a power factor unity in grid-connected PV. The current i_d* reference is the current from the voltage controller. The difference of current Δi_d and Δi_q are the input for the PID controller. The outputs from the current controller are the voltage reference for the SVPWM. The voltage reference in dq reference frame are v_d*, v_q*.The input command for the SVPWM are v_d*, v_q* and the phase angle θ. The three-phase inverter uses SVPWM modulation techniques.

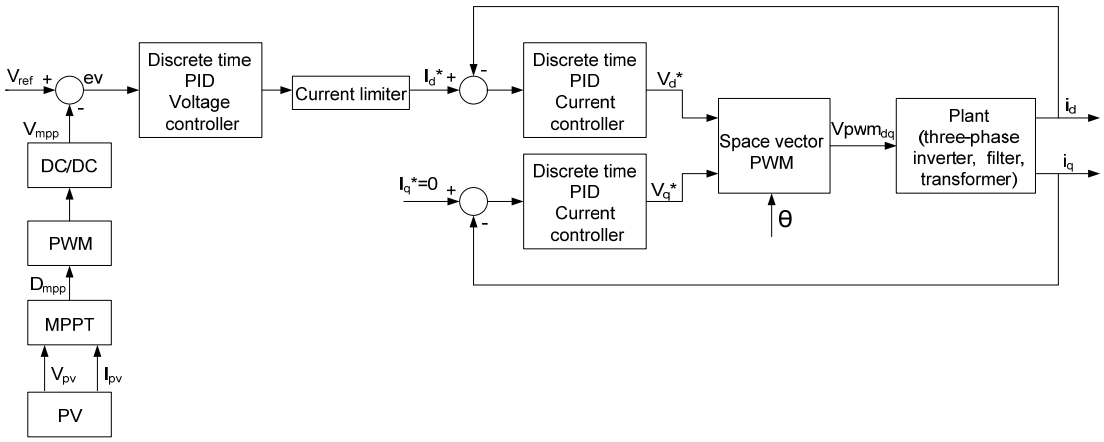

Figure 3.39: Voltage and current control block for PV system

Figure 3.40 represents the entire PV system. It shows the boost converter with the three-phase inverter. Filters with inductor and capacitor are used for the current. The power electronic system is based from [27]. The AC current produced from the

DC/AC inverter is filtered, then delta-wye transformer steps up the voltage. A delta-wye transformer is required to isolate the PV from the grid. A phase lock system is necessary to determine the phase of the grid voltage. The control system is the same as described above. This typical two stage PV system can be used for grid connected PV with unity power factor.

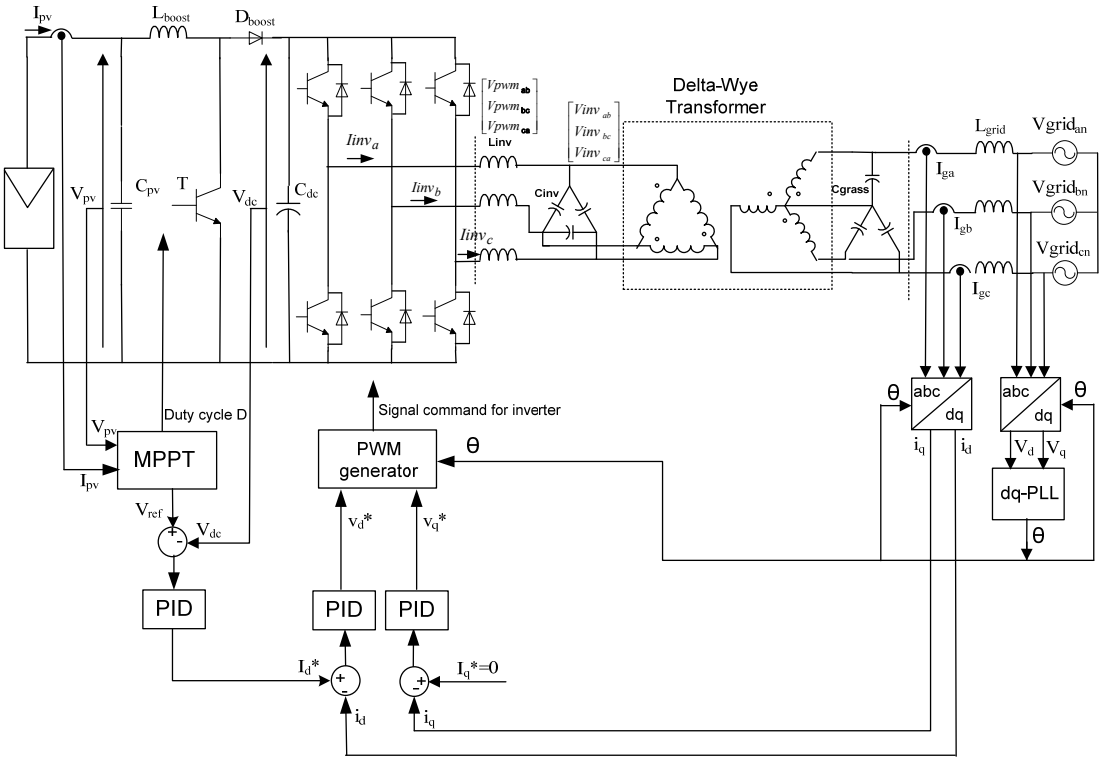

Figure 3.40: A two stages PV system with voltage control and current control

Chapter 4: Simulation ofthe Photovoltaic System Using Matlab / Simulink

4.1 Simulation of the photovoltaic array

The simulation of the photovoltaic array is realized with Simulink block. The matlab model of the photovoltaic array isbased from [3]. Certain variables are modified for the application with maximum power point tracking. The input parameters required for the model are:

N_s: number of cells in series

N_{pp}: number modules in parallel

N_{ss}: number of modules in series

A: 1.3977, diode constant

k: 1.38e-23, boltzmann constant

I_{scn}: nominal short-circuit voltage

K_p: voltage temperature constant

K_i: current temperature coefficient

V_{mp}: voltage maximum power at STC

I_{mp}: current at maximum power at STC

The PV characteristics from datasheet is usedto generate the file necessary for R_s, R_p.and other parameters for the maximum power point. The initial setupis used to obtain the I-V curve characteristics of the PV array andshow the maximum power point of the PV. The model of the PV is used with the boost converter to determine the performance of the maximum power point tracker.

The model of the photovoltaic array has been implemented in Simulink as shown in figure 4.1. The temperature and the irradiance are specified. The simulation allows having the curve I-V and P-V characteristics. The Simulink model uses a current source, voltage source and the value of the resistance in series and parallel of the PV.

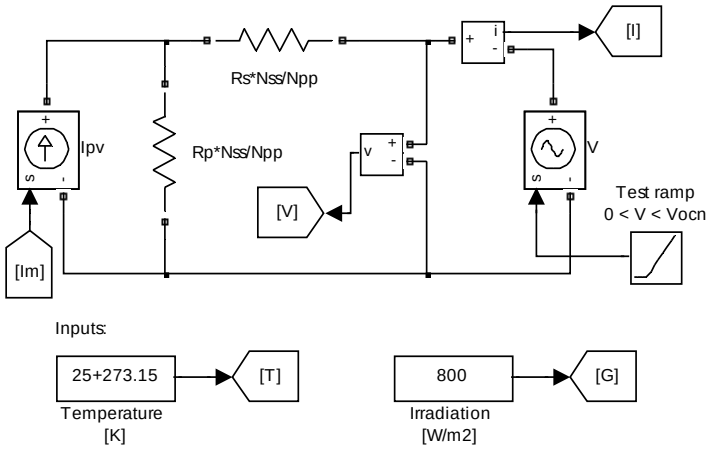

Figure 4.1: Simulation of the PV module [3]

The number of modules in series and parallel are set with N_{ss} and N_{pp}. The I_m result is used for the Simulink block as a current source to obtain the voltage and current delivered from the PV.

Figure 4.2 is the representation block of the PV that can be used with different power circuits in Simulink. It can be noted that the inputs of the PV are the irradiation and temperature, the outputs are the voltage and the current.

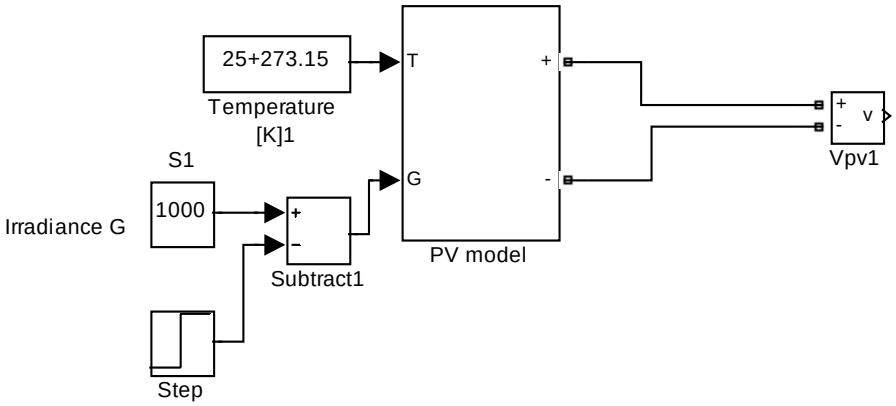

Figure 4.2 Simulink block of the photovoltaic array

The figure 4.3 shows the mask interface of this PV model. The input parameter for this model is the photovoltaic current. The variation ofthe current from the photovoltaic varies the photovoltaic output voltage. The Simulink model is derived from the model described in [3].

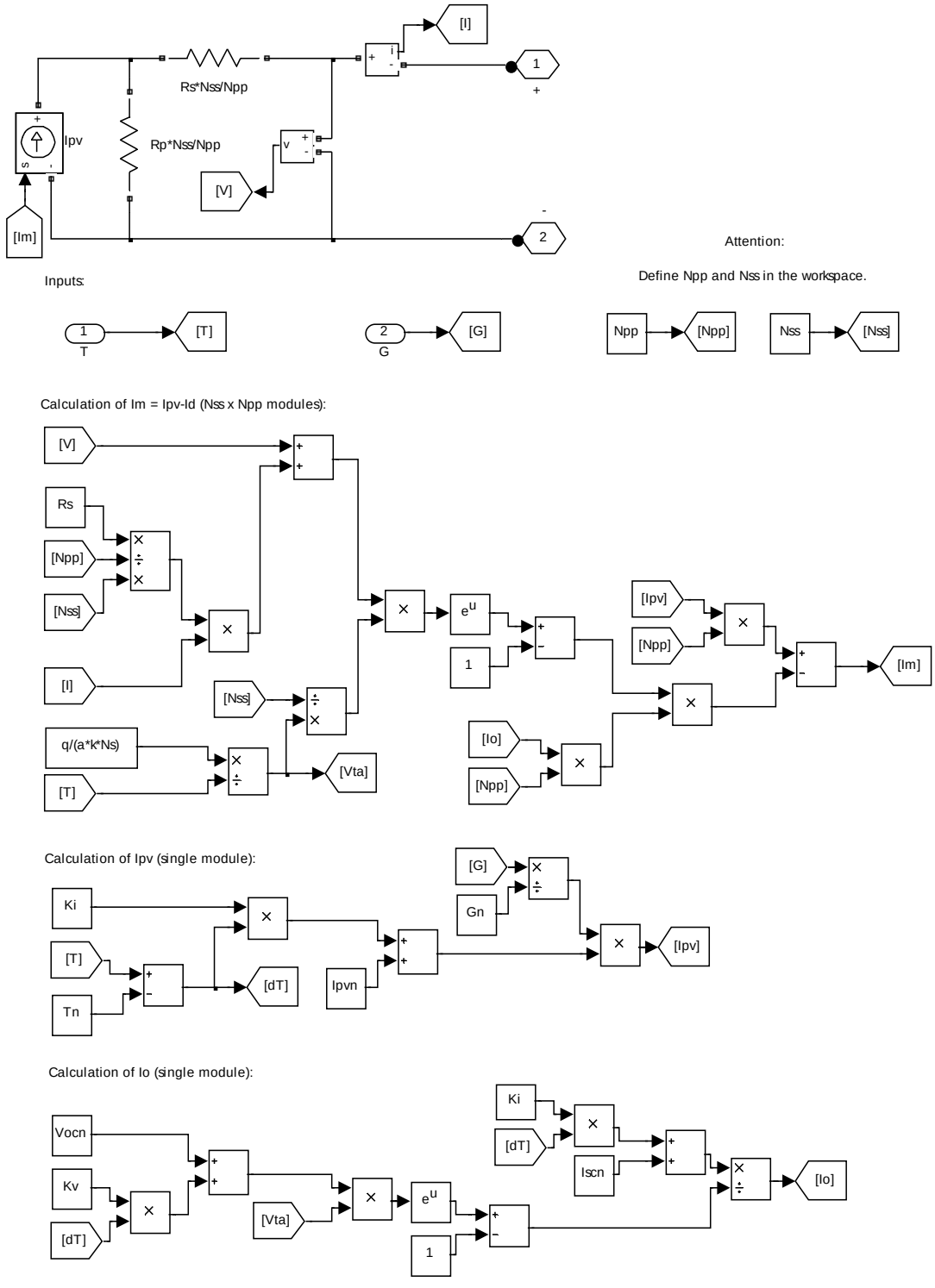

Figure 4.3: Simulink subsystem model of the photovoltaic array [3]

4.2 Simulink model of boost converter with MPPT controller

Figure 4.4 shows the Simulation of the boost converter. The input of the boost converter is the photovoltaic output voltage. The inductance and the capacitor need to be specified. The switching command of the transistor is obtained from the MPPT controller.

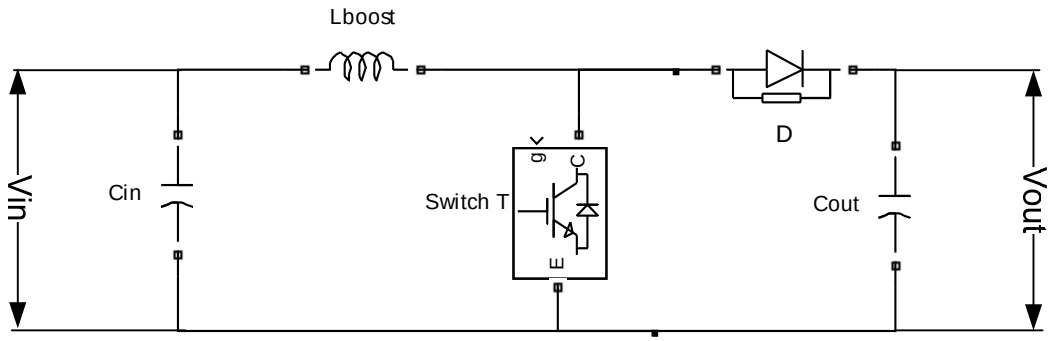

Figure 4.4: Boost converter in Simulink

The maximum power point controller block is shown in figure 4.5. The voltage and the current of the photovoltaic array are the input, and the duty cycle is the output. The duty cycle is compared to a triangle wave signal to generate the PWM. The frequency of the triangle wave is the pulsation frequency of the boost converter.

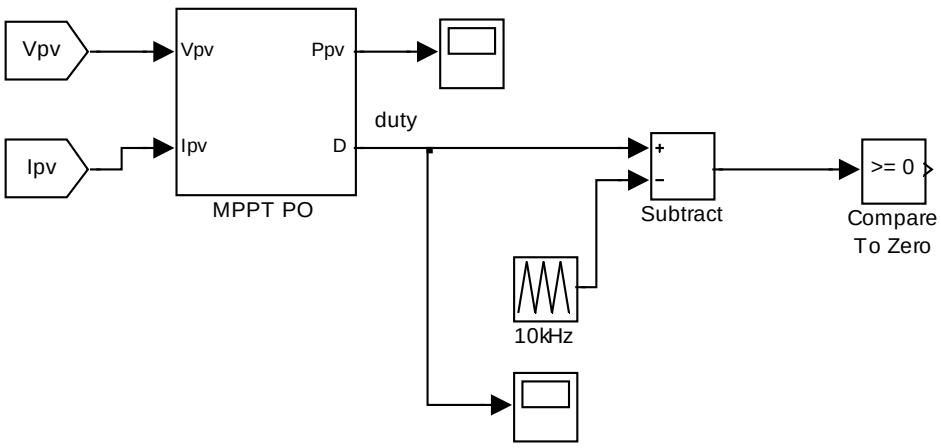

Figure 4.5: Simulink block for MPPT

The perturb and observe algorithm is implemented and shown in figure 4.6. The duty cycle is increased or decreased until the maximum power point of the photovoltaic is reached. The step of the duty cycle is constant, and it determines the efficiency and accuracy of the MPPT controller.

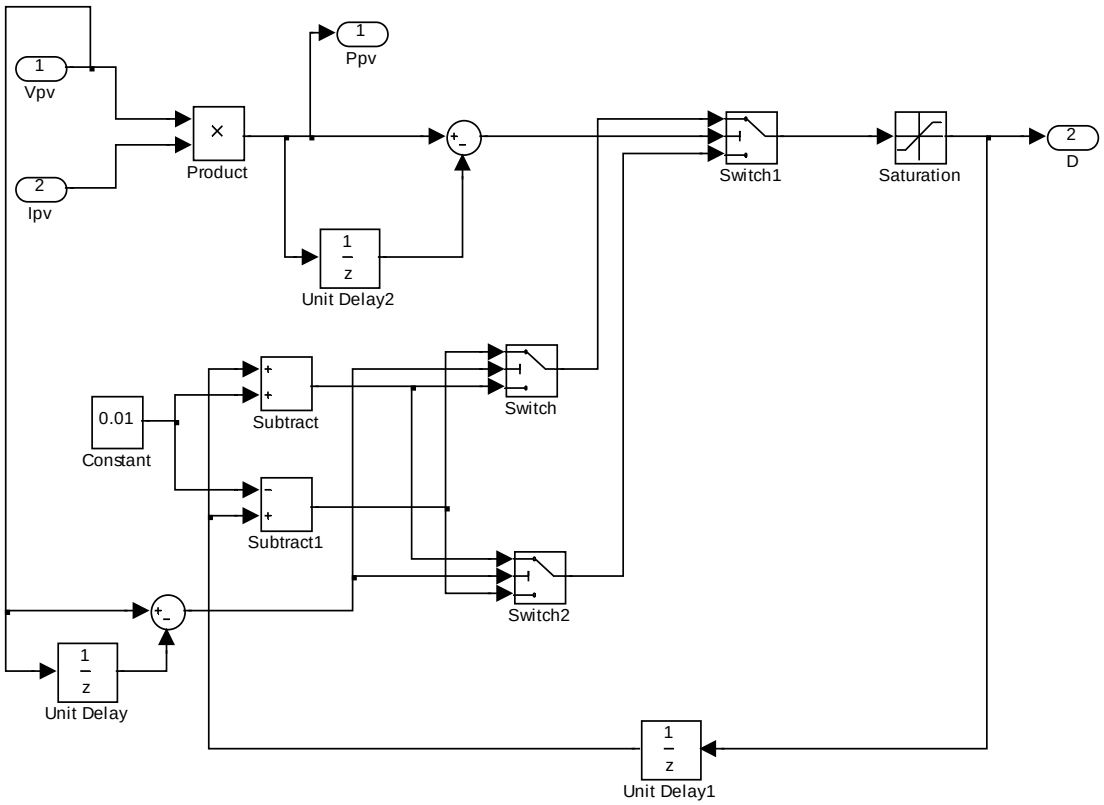

Figure 4.6: Simulink model of the MPPT with perturb and observe

Figure 4.7 is the simulation of the Boost converter, the photovoltaic array and maximum power point controller in Simulink. The system has a resistive load to test the simulation.

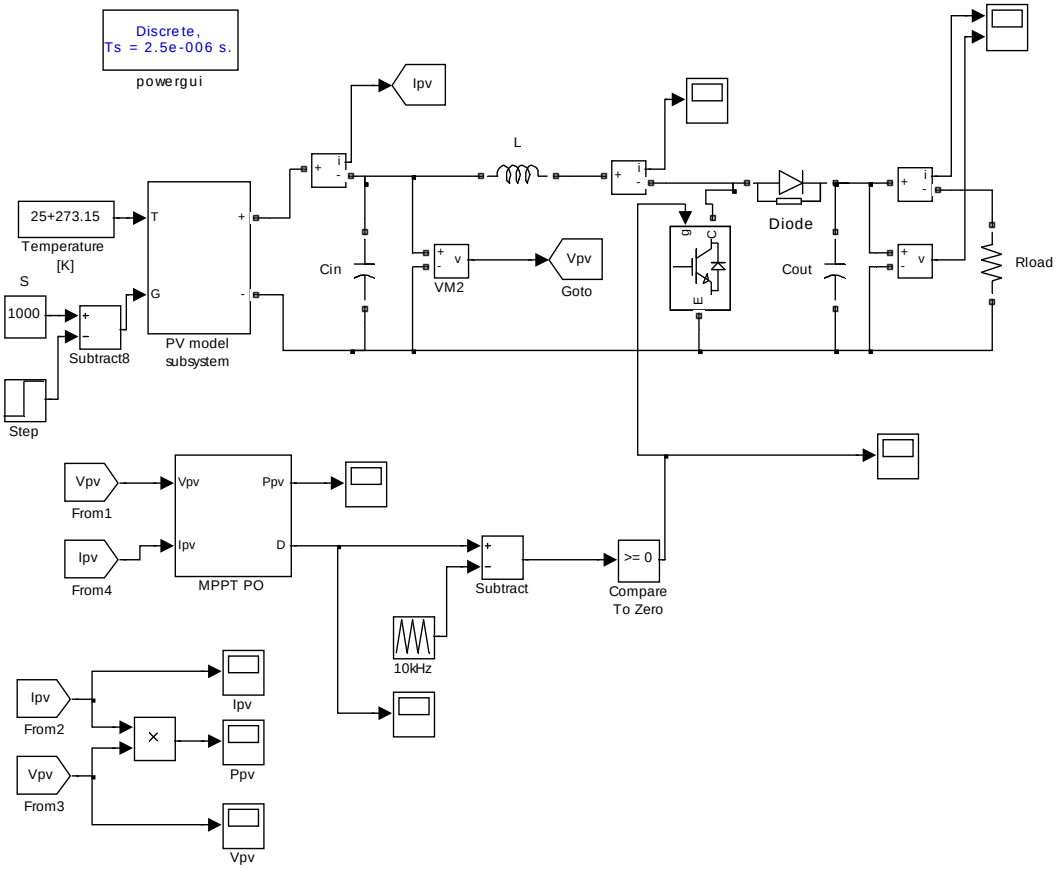

Figure 4.7: Simulink model of the photovoltaic system with MPPT controller

4.3 Simulation full bridge inverter with SVPWM

This simulation explains the method to simulate the SVPWM in Simulink. Figure 4.8 shows the Simulink model of the SVPWM. “Sector determination” gives the sector number according to the angle input. Then sector number, angle and the sampling time are used to calculate T_1, T2and T_0. The region determination block obtains the region in which the vector falls into according to the fundamental frequency. ”SVPWM” block calculates the switching time according to section 3.5.1

and generates SVPWM signals for the power switches. Appendix B gives detailed of the matlab program for SVPWM.

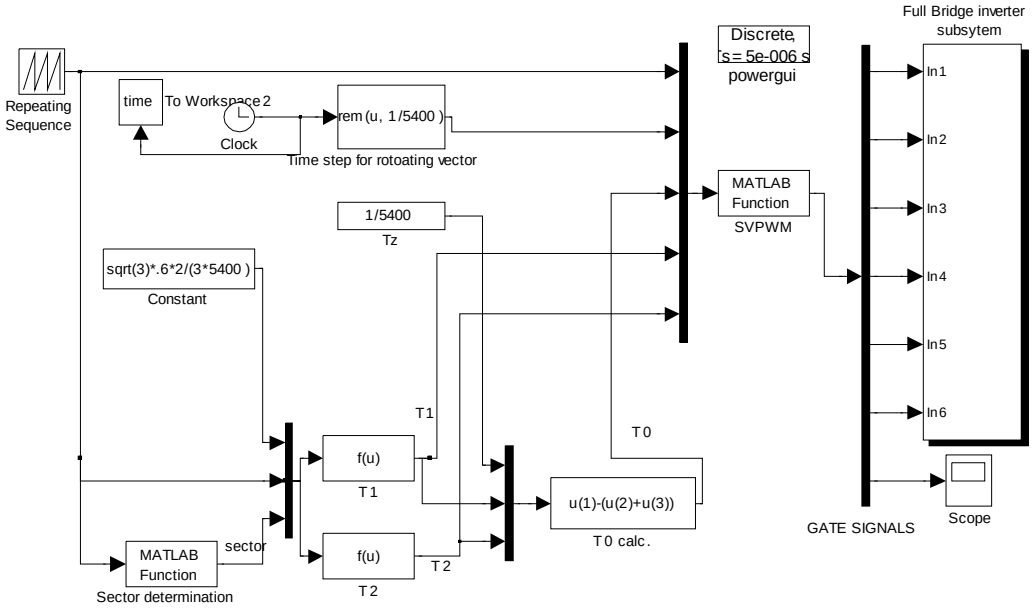

Figure 4.8: Simulink block generating the gate signal

Figure 4.9 shows the Simulink model of the inverter.Six ideal switches represent the three-phase inverter. It can be simulated independent of the PV source to test the SVPWM program. To summarize, the simulation steps are:

- Generate the fundamental frequency with the repeating sequence block
- Determine sector,
- Determine time duration T_1, T_2, T_0,

- Determine the switching time (T_a, T_b and T_c and their complimentary Ta', Tb' and Tc') of each transistor (S1 to S6).
- Generate the inverter output voltages

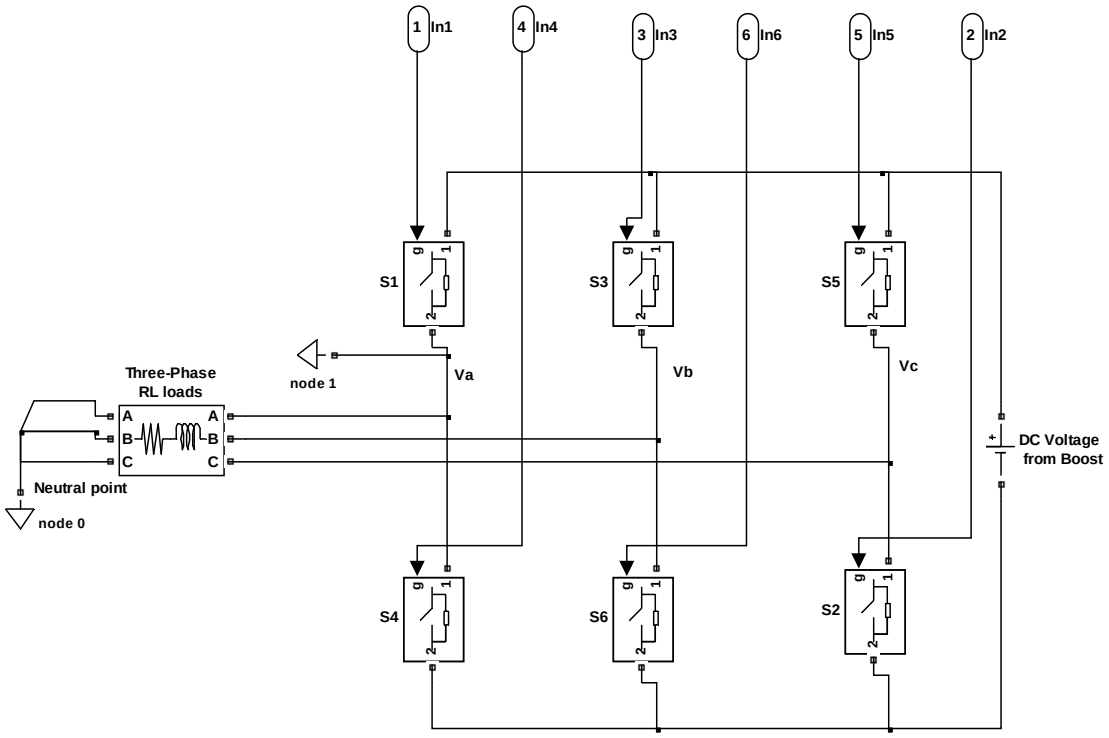

Figure 4.9: Simulink block three-phase inverter

In PV system, the output voltage of the boost converter replaces the DC source. The gates signal of the six switches are the same as described in section 3.7. It depends on voltage from PID current controller vd*, vq* and the phase angle θ. In this technical report, a general simulation of the SVPWM is presented without the current controller.

4.4 Simulation of the PV with three-phase inverter

The simulation of the three-phase photovoltaic system is realized by adding a three-phasefull bridge inverter from the Simulink block toolbox. A pulse generator block is used to generate the PWM signal of the inverter. Figure 4.10 shows the settings of the pulse generator. The carrier frequency, sampling time and modulation index, can be set up with the pulse generator block.

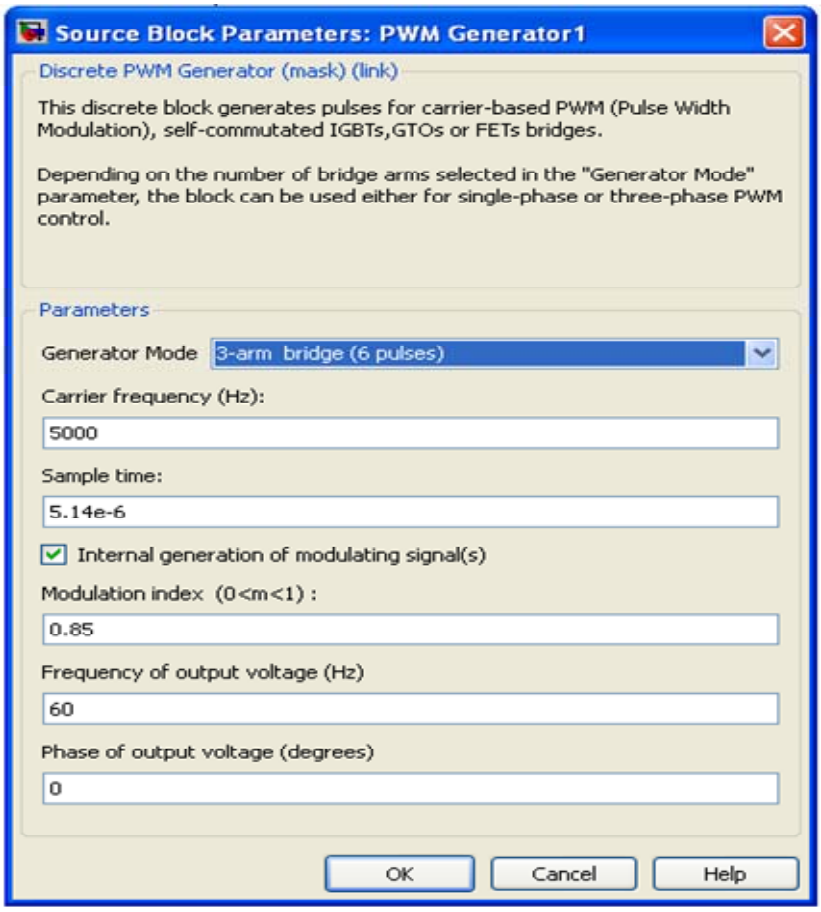

Figure 4.10: Pulse generator

The PV system with three-phase inverter shown in figure 4.11 is used. The three-phase inverter has three-phase inductance filter and resistance load. An inverter block from Simulink is the three-phase inverter. The PV, boost and MPPT, remain the same. The pulse generator produces the gating signal for the inverter block. The output voltage from the boost converter is the DC voltage for the three-phase inverter.

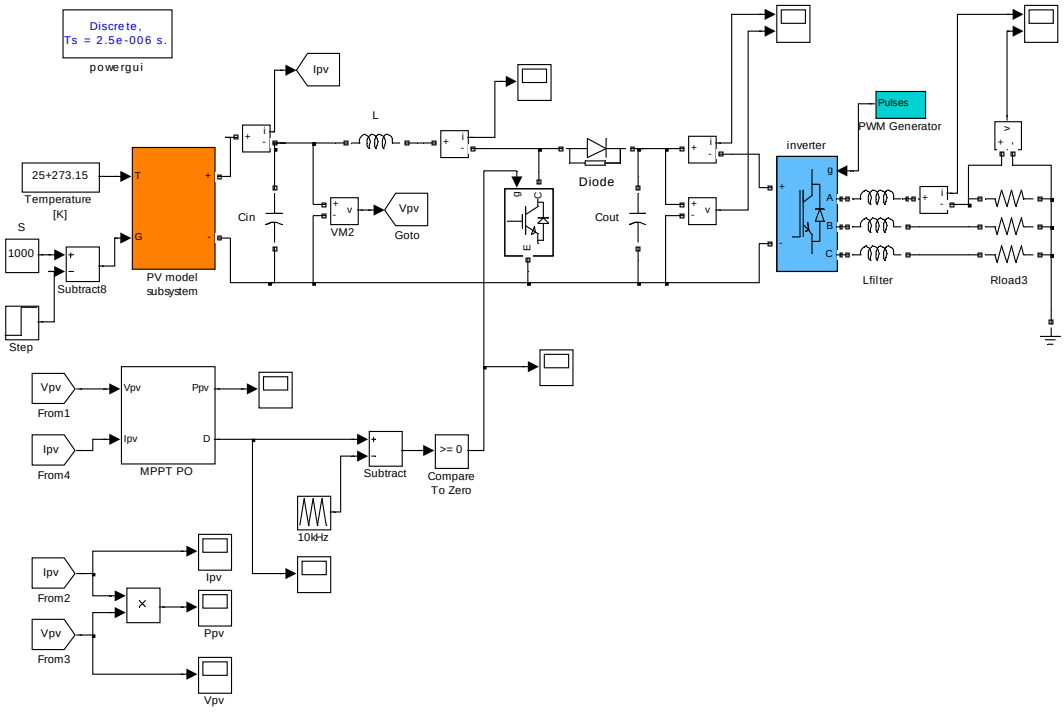

Figure 4.11: Simulation of the PV with boost and three-phase inverter

Chapter 5: Simulation Results

The model of the photovoltaic system in the previous chapter is used to determine the performance of the MPPT controller with boost converter. This simulation presents an analysis of the photovoltaic array with boost converter and resistive load. The temperature, irradiance and load, are varied to determine the performance of the MPPT and track the maximum power of the PV.

5.1 Photovoltaic array characteristics

5.1.1 The I-V and P-V characteristics

The photovoltaic model used is the BP MSX 120. It has a maximum power output 120 W. The datasheet of the PV is given in appendix 2. The table 5.1 givesthe characteristic of the module BP MSX 120 at STC 25C.

Short circuit current Isc	3.56 A
Current at maximum power point Impp	3.87 A
Voltage at maximum power point Vmpp	33.7 V
Open circuit voltage Voc	42.1 V
Number cells in series ns	72

Table 5.1: PV module BP MSX 120 datasheet values at STC

The module BP MSX 120 is connected in series and parallelto achieve a maximum power output of 12 kW and output voltage 337 V. Table 5.2.givesthe characteristic of the PV for maximum power 12 kW. A PV of 12 KW is made from the BP MSX 120 with 10 modules in series and 10 modules in parallel.

Number of modules in a string seriesNss	10
Number of modules in a string parallel Npp	10
Output voltage rating	337 V
Output current rating	35.6 A
Maximum power output	12 000 W

Table 5.2: Characteristics of 12 kW photovoltaic

The specifications of the resistance R_s and R_p of the PV array are given in table 5.3, which was obtained from the simulation of the photovoltaic array.

Parameters	1 module	12 kW array
Iph	3.8713 A	38.71 A
I0	0.323 μA	3.23 μA
A	1.3977	1.3977
Rs	0.473 Ω	0.18 Ω
Rsh	1367 Ω	520 Ω

Table 5.3 Photovoltaic module 12 kW parameters values at STC

In figure 5.1, the characteristics current-voltage of the PV module BP MSX 120 is shown. It can be noted that the maximum current output is 3.87 A and the maximum voltage is 33.7 V. They are the same as the values given from the manufacturerin table 5.1.

Figure 5.1 is the power versus voltage curve of the BP MSX 120. It can be noted that the maximum power of the single module is 120 W.

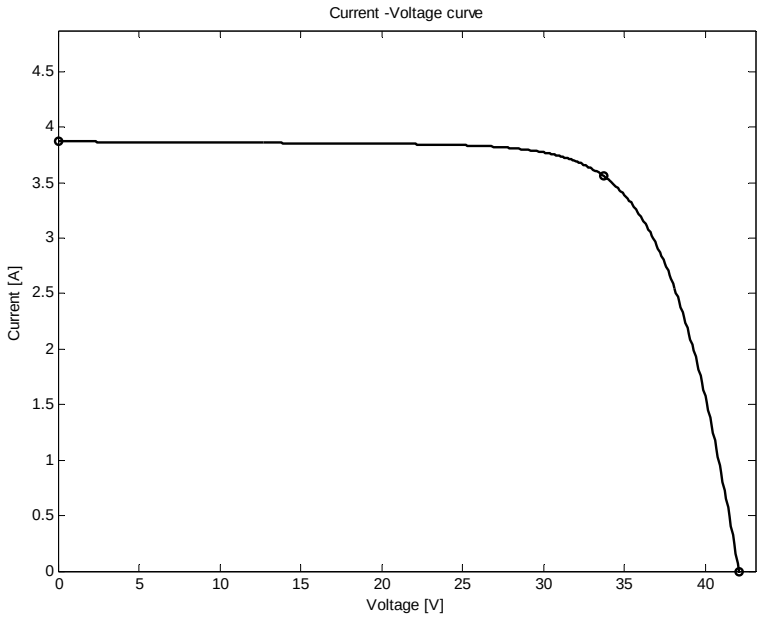

Figure 5.1: I-V curve of the BP MSX 120 module at T=25C and G=1

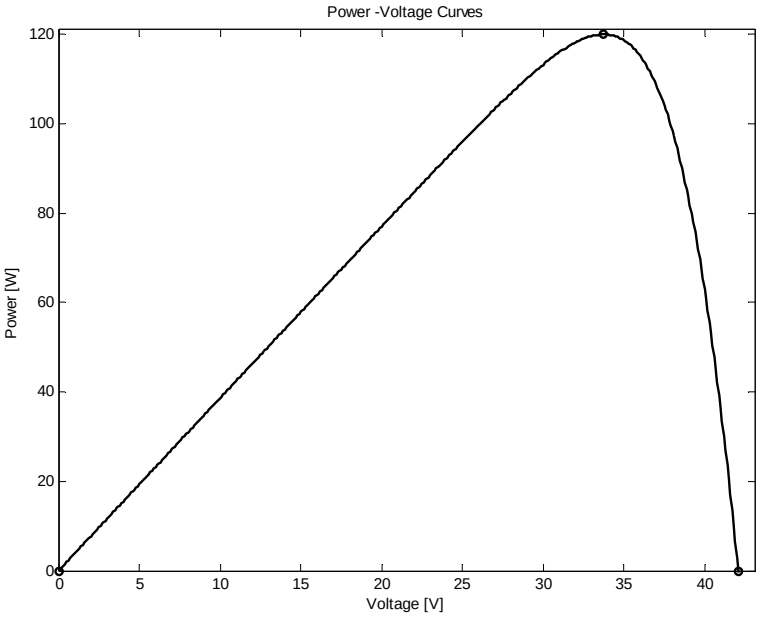

Figure 5.2: P-V curve of the BP MSX 120 module at T=25C and G=1

Figure 5.3 and 5.4 are the characteristics of the PV array 12000 W. The current and voltage at maximum power are respectively 35.6 A and 337 V. The maximum power with the PV array 12 kW is ten times the PV module BP MS120.

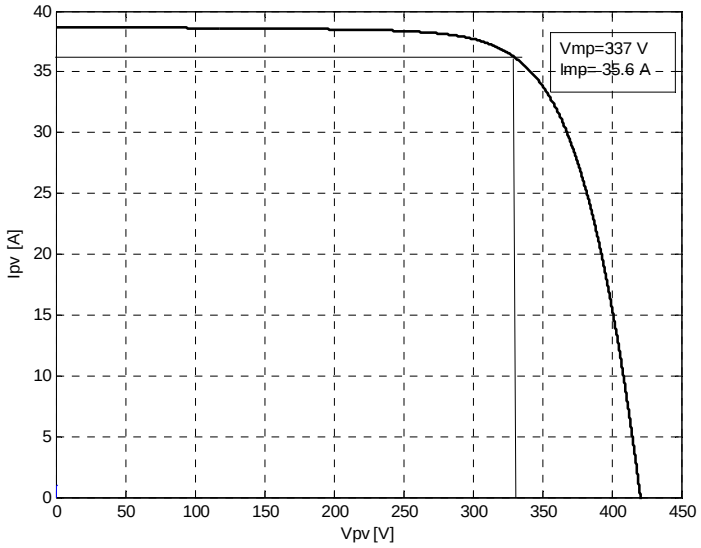

Figure 5.3: I-V curve of the PV array 12000 W

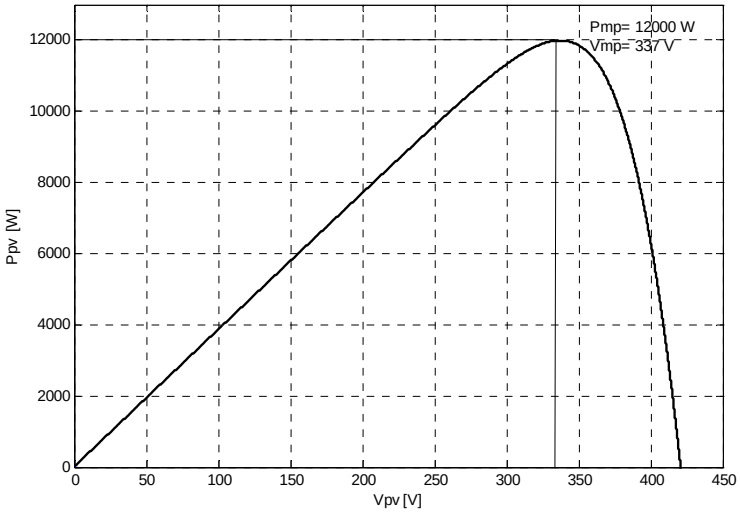

Figure 5.4: P-V curve of the PV array 12000 W

5.1.2 Simulation PV with variation temperature

In figure 5.5, the temperature varies from 25ºC, 50ºC and 75ºC. The variation of the temperature has an impact to the output voltage of the PV. The variation of the temperature affectsthe output current less.

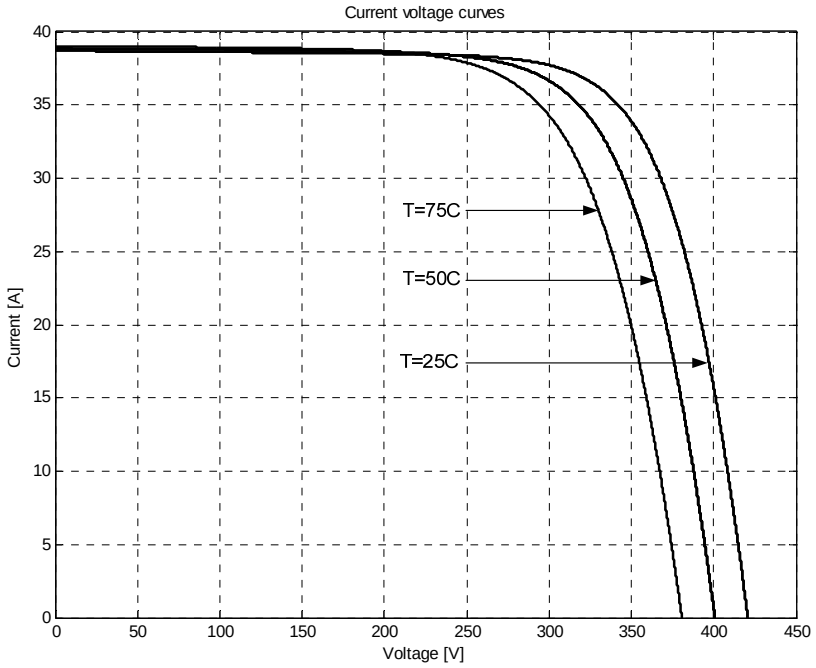

Figure 5.5:I-V characteristics with variation of temperature

5.1.3 Simulation of the PV with variation irradiation

In this case, the irradiance varies from 600, 800 and 1000 and the temperature is constant. The Simulink model in figure 4.1 was used. The result in figure 5.6 is the power-voltage curve which shows that the maximum power of the PV decrease when the irradiance decreases. The figure 5.7 is the current-voltage curve, which shows that the current decreases significantly when the irradiance decreases.

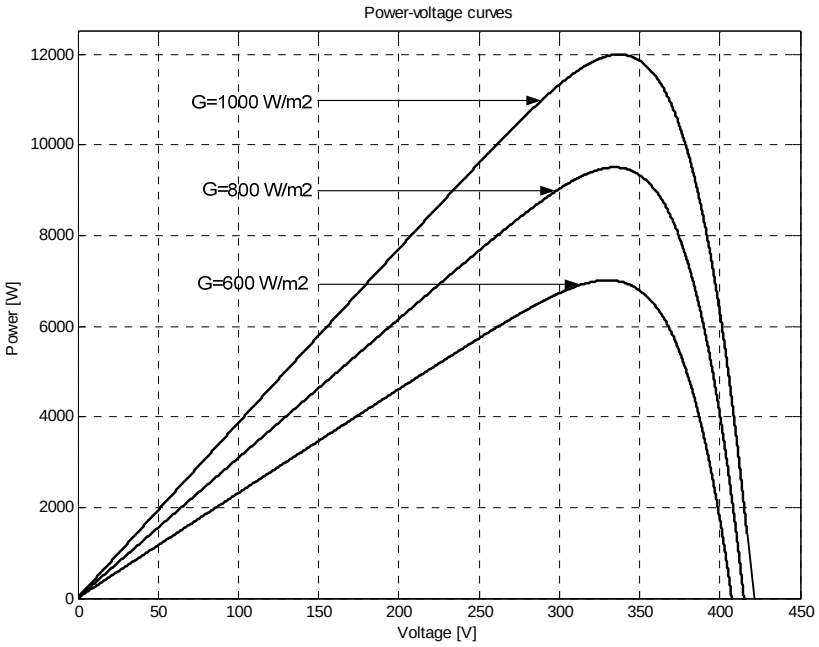

Figure 5.6: P-V characteristics of the PV at various irradiance

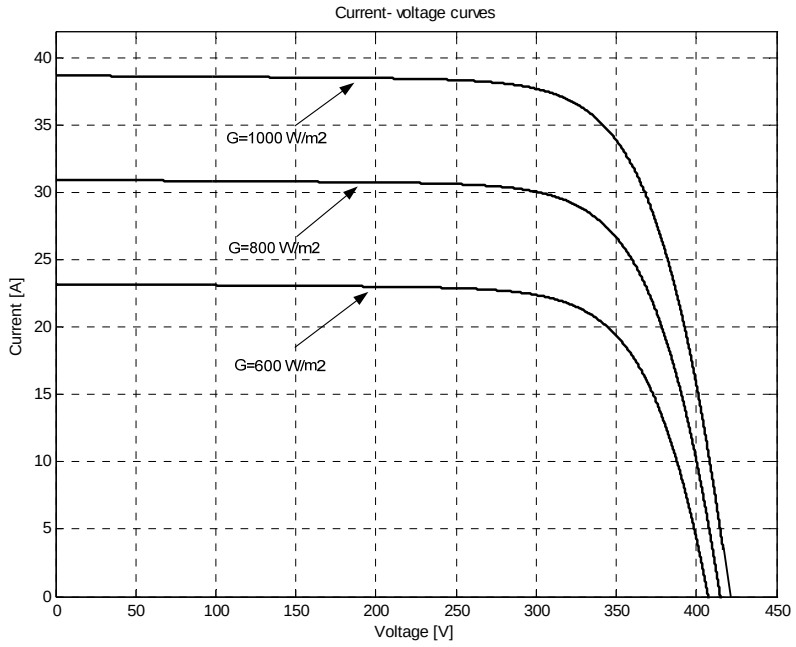

Figure 5.7: I-V characteristics of the PV at various irradiance

5.2 Photovoltaic system with a Boost converter and MPPT controller

The simulation presents an analysis of the photovoltaic array 12000W with the boost converter to track the maximum power point. The PV system parameters are:

- DC bus voltage Vdc: 540 V (nominal), 200 V (min)
- AC output voltage of the inverter: 208 V (LL), 120 V (L-N), 60 Hz

The boost parameters are calculated from [50] and, the inductance and capacitance values are given in table 5.4. The boost input voltage nominal is 337 V and, the output voltage is 540 V.

Vin (nom)	337 V
Vout (nom)	540 V
Cin	78.6 μF
Lboost	444 μH
Cout	154.69 μF
Rload	24.3 Ω
Switching frequency	10 kHz

Table 5.4 PV system specifications

Maximum power point controller is used to control the boost converter. Perturb and Observe algorithm is implemented to track the maximum power of the PV module.

Photovoltaic output power, voltage and current

The simulation is run at t=0s to 1.5 s. At the beginning, the irradiation is set at G=1000 [W/m2] and at t=0.8 s a step change of irradiation to 600 [W/m2] is performed. Figure 5.8 represented the output power of the PV array. The output power of the PV varies from 12000 W to 7000 W. The PV array operates at maximum power when there is a variation of the irradiance.

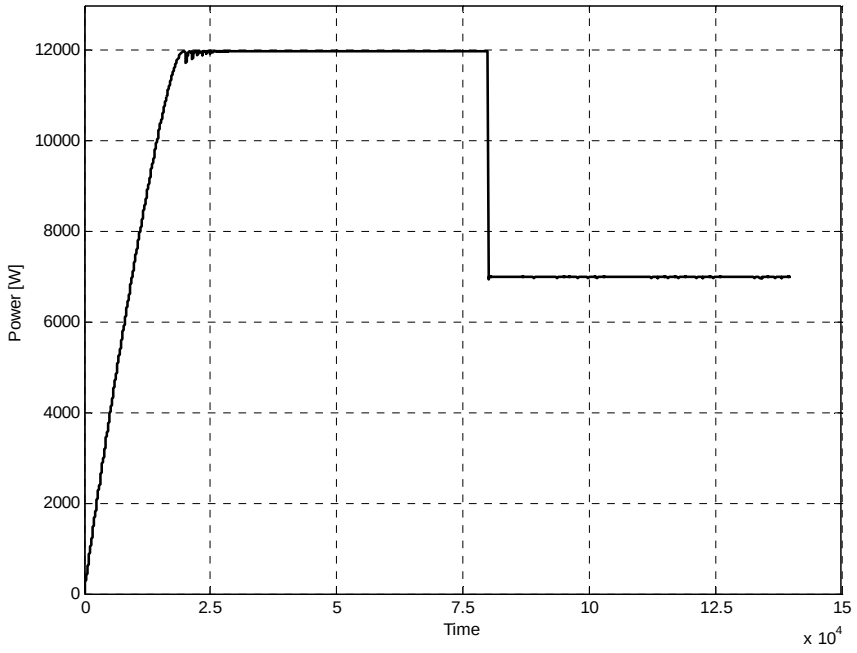

Figure 5.8: Step change of the Photovoltaic power output

Figure 5.9 is the output voltage of the PV with the step change of the irradiance. The output voltage oscillates around the maximum power with the perturb and observe algorithm.

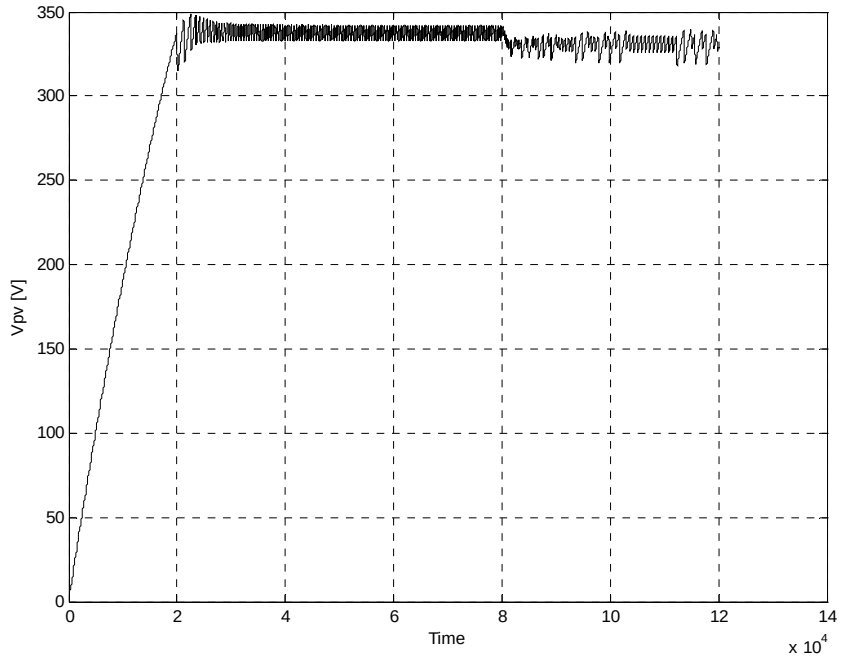

Figure 5.9: Photovoltaic output voltage for varied irradiation at =0.8 s

In figure 5.10, the current of the PV changes when the irradiance changes.The PV current I_{pv} reaches steady state after 0.0002 s. Moreover, the current oscillates around the MPP. When the irradiance drops, the current drops from35 A to 22 A. The current at 22 A is the maximum current of the PV under 600 W/m2 irradiance. The MPPT can track the maximum power almost instantly.

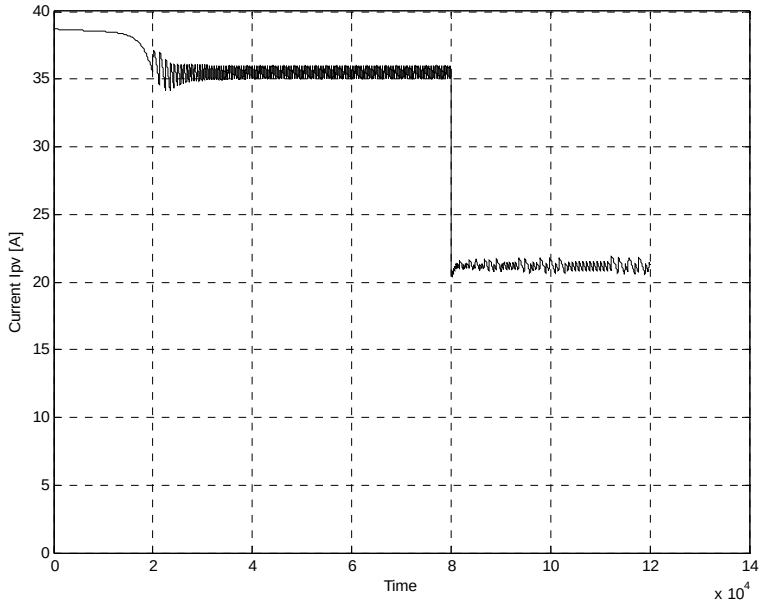

Figure 5.10:Photovoltaic output currentfor variant irradiation at =0.8 s

Boost converter output power, voltage and current.

The same simulation is performed to test the performance of the boost converter. Figure 5.11, 5.12 and 5.13 are respectively the output power, voltage and current of the boost converter. The output power of the boost converter is still 12000 W when the irradiance is at 1000. The boost converter boosts the input voltage from 337 V to 540 V then drops to 420 V when the irradiance changes.

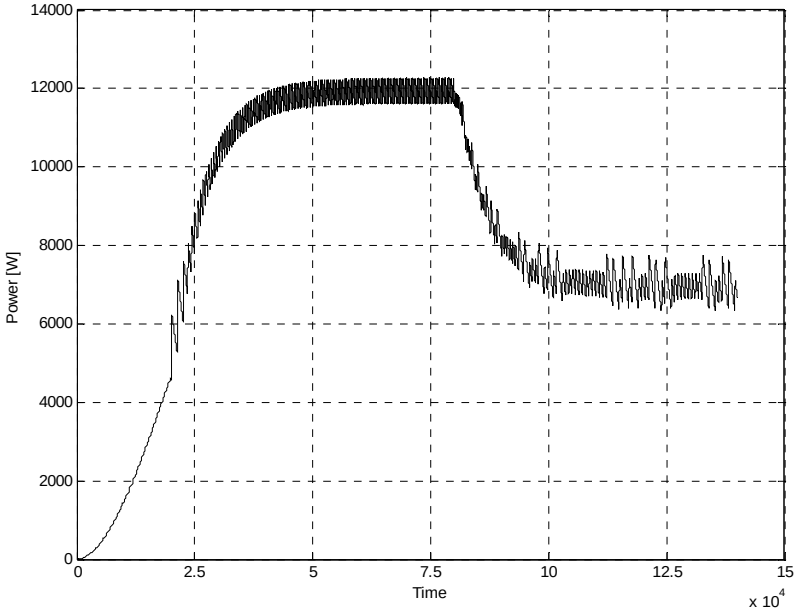

Figure 5.11: Output power of the boost converter

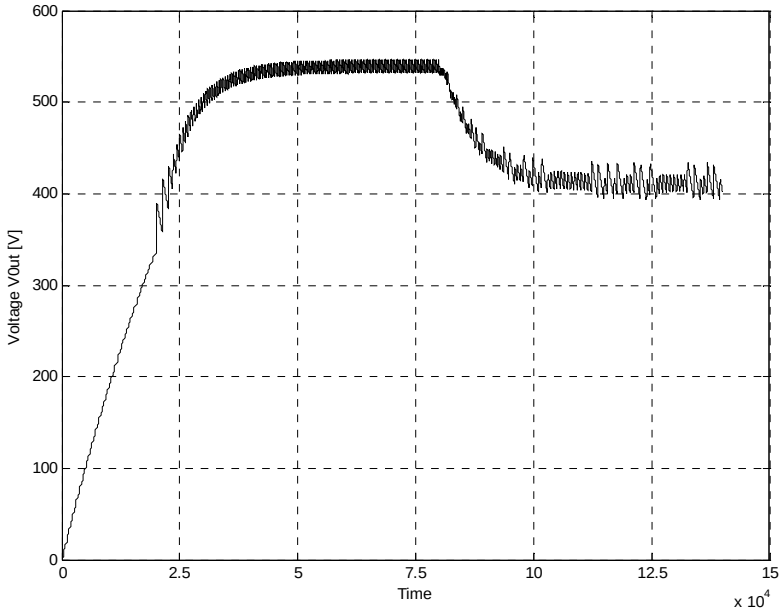

Figure 5.12: Output voltage of the boost converter.

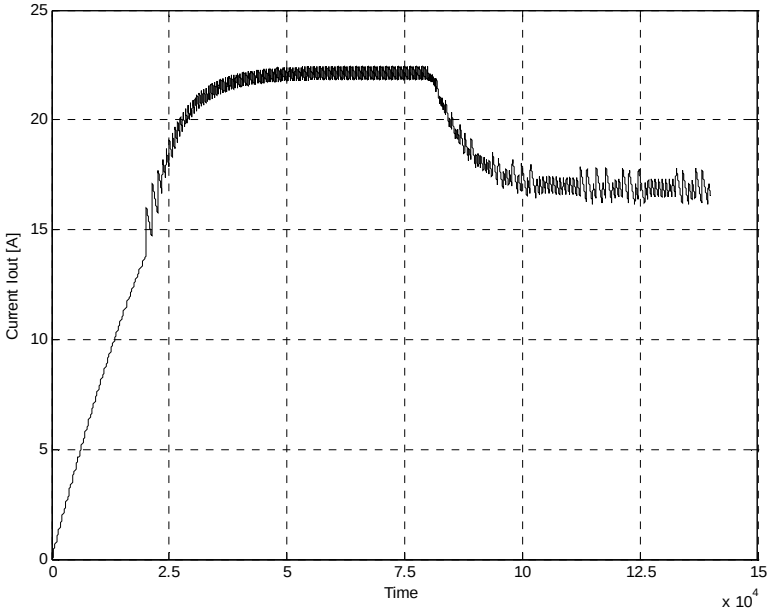

Figure 5.13: Output current boost converter

Performance of the photovoltaic system for a step change of the load

Two simulations were performed to test the performance of the photovoltaic array and the maximum power point controller. First, the simulation is run with resistive load of 24.3 ohm at the terminal of the boost converter. The PV is set at irradiance equal to one and temperature to 25ºC. The result of the simulation is in figure 5.14. The left side is the photovoltaic voltage, current and power. In addition, the right side is the load voltage, current and power, which is the boost converter output. It can be noted that, with the 24.3-ohm load, the PV delivers 337 V and 12000W, which is the maximum power of the PV. Moreover, the boost converter increases the voltage up to 540 V. The output power is equal to the input power, which gives the output current

22.22 A. The boost converter was able to track the maximum power of the PV by variation of its duty cycle.

Then, the load is increased at 36.43 ohm, which is one and half times the initial load. The irradiance and the temperature of the PV remain the same. The results are shown in figure 5.14. The PV voltages, current and power are expected to remain the same, even if the load is increased. The PV output depends with the irradiance and temperature. For that reason, the PV should still deliver 12000W. At the load side, since there is no voltage control, the output voltage was at 667 V and the current at 18A in order to keep the power delivered to the load at 12000 W. The duty cycle of the boost converter is varied to track the maximum power and transfer the power to the load. The photovoltaic array should always give the maximum power, voltage and current independent of the load. The boost converter and the MPP regulate the duty cycle accordingly. In this situation the design of the boost, determine the output voltage.

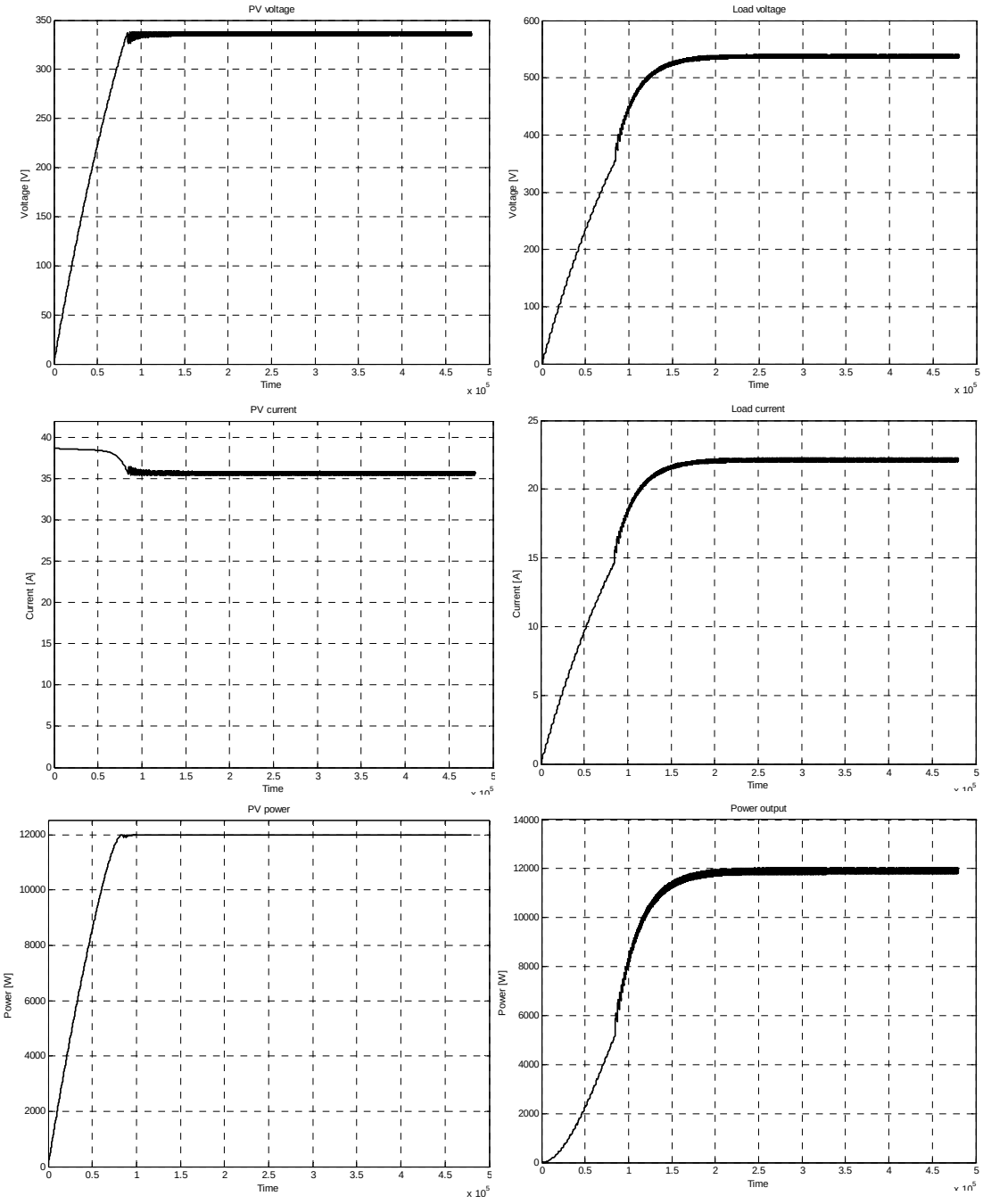

Figure 5.14: Left side is voltage, current and power of the PV; right side is load voltage, current and power with resistive load 24.3 Ω

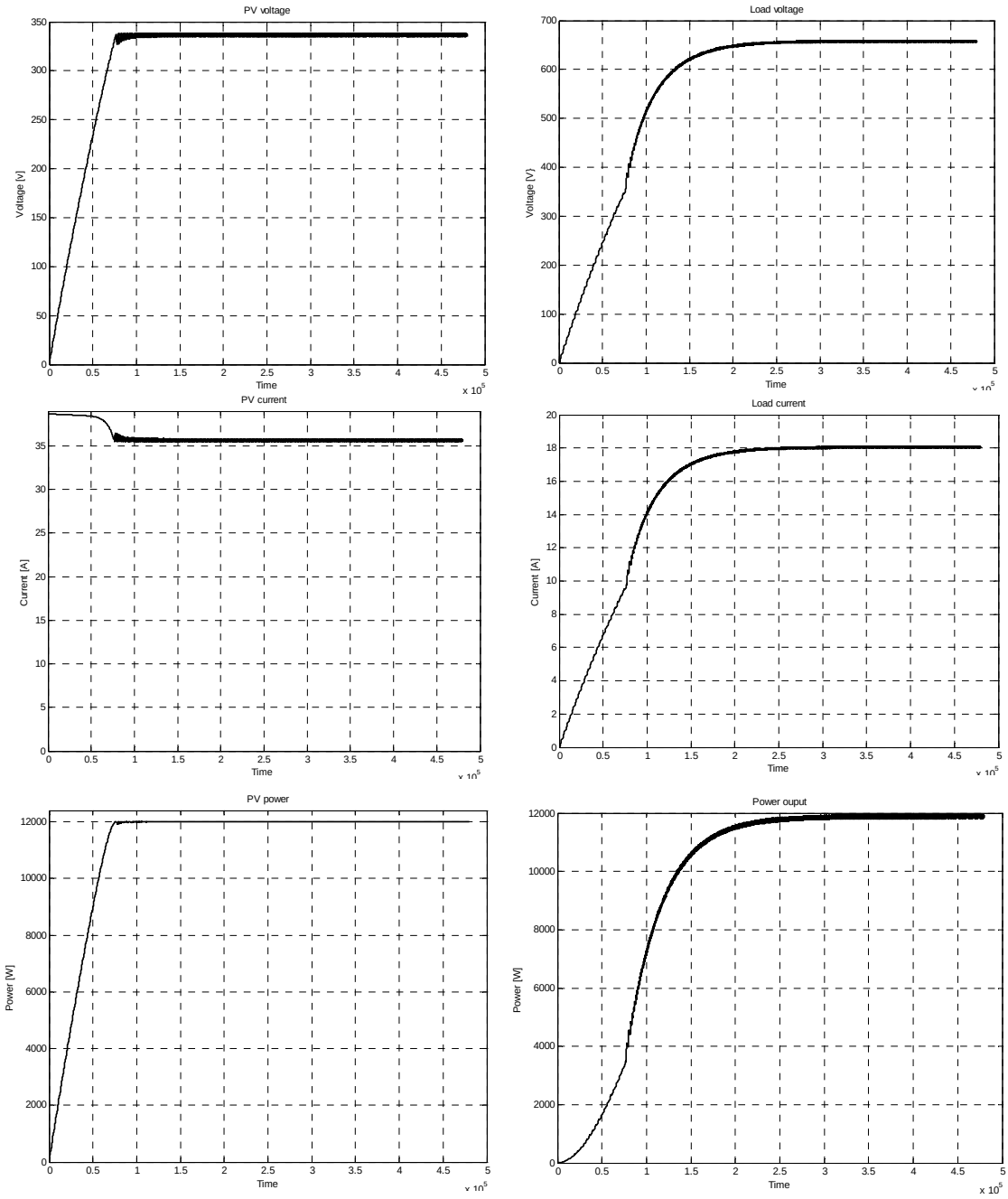

Figure 5.15: Left side is voltage, current and power of the PV; right side is load voltage, current and power with resistive load 36.45 Ω

5.3 Photovoltaic connected to a three-phase inverter

In this simulation, the output of the boost converter is connected to the three-phase inverter and the three-phase resistive load. The MPPT controller still tracks the maximum power of the photovoltaic array. The simulation model in figure 4.11 is used to simulate the three-phase photovoltaic system with 10 Ω resistive loads on each phase. The carrier frequency is set at 5 kHz and the sampling time is 5.4e-6 s. The three-phase inverter delivers a three-phase current to the load. Figure 5.16 shows a sinusoidal load current for phase a.The DC voltage produced by the photovoltaic system is converted into AC current to the load

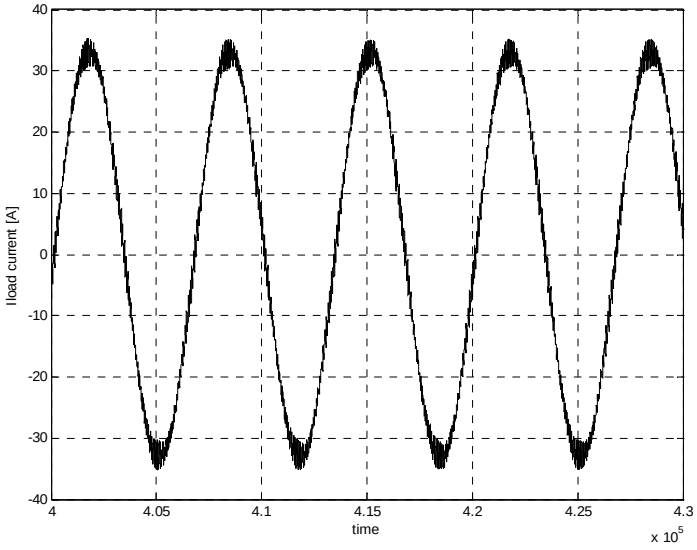

Figure 5.16: Three phase inverter output current

The simulated phase to phase and phase to ground voltages are presented in figure 5.17 and 5.18.

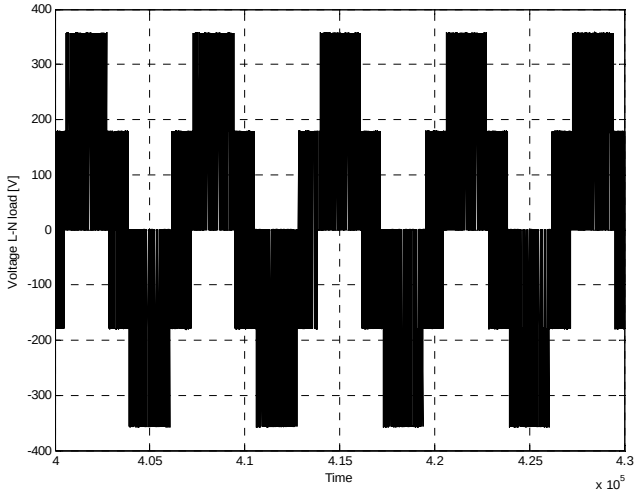

Figure 5.17Three phase inverter Output phase to ground voltage

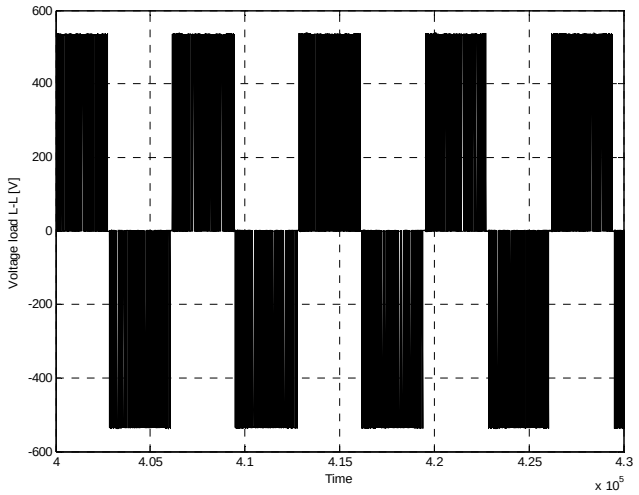

Figure 5.18: Three phase inverter Output phase to phase voltage

Figure 5.19 is the photovoltaic voltage and figure 5.20 is the photovoltaic current. The PV system still operates at maximum power with the MPPT; the power produced by the PV is independent of the load. Without the current control and the voltage

control,the DC link voltage is not constant.The voltage of the DC link is dependent of the load. Figure 5.21 is the power generated by the PV. It has a maximum power of 12000 W. The figures display on the right below are a zoom in portion of the plots on the left.It shows the oscillation of the voltage and current around the MPP.

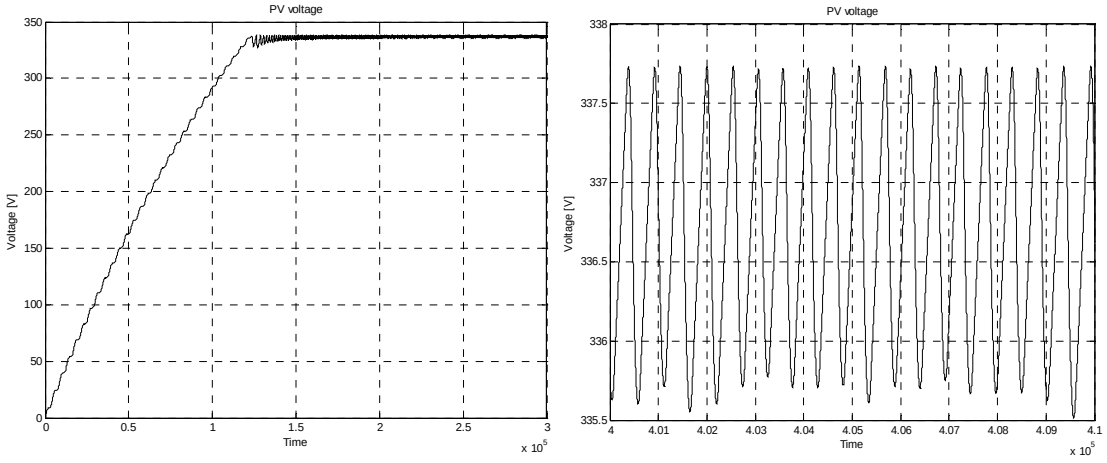

Figure 5.19: PV voltage and zoom of the PV voltage

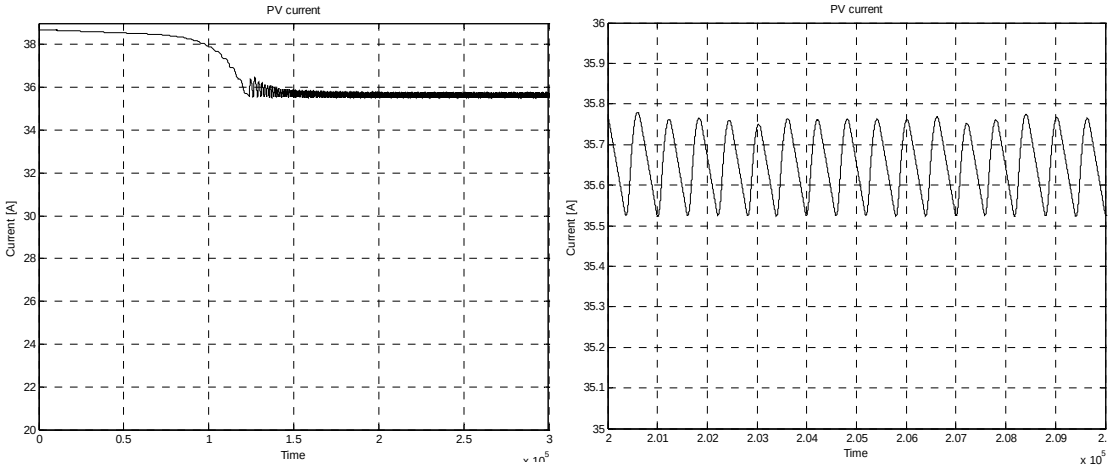

Figure 5.20: PV current and zoom of the PV current

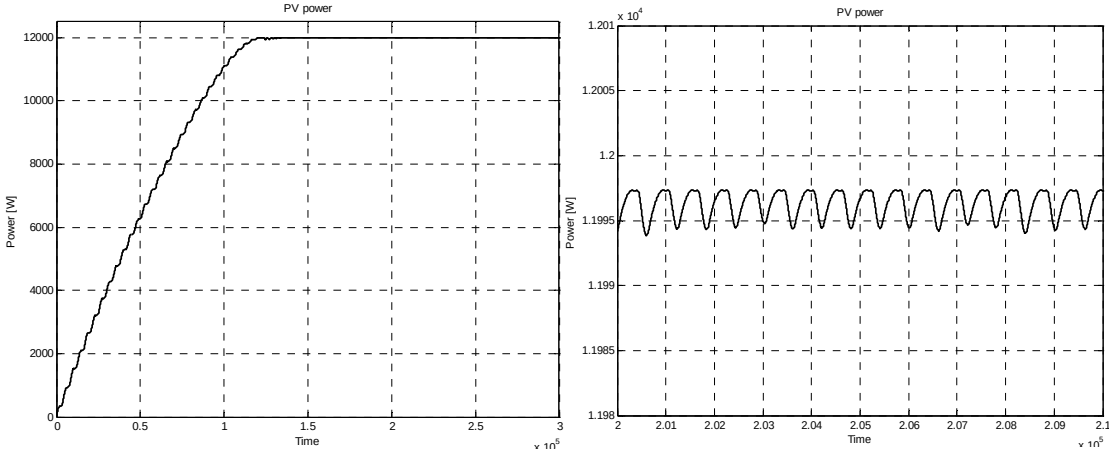

Figure 5.21: PV power and zoom of the PV power

Figure 5.22 is the output voltage of the boost converter. The input voltage 337 V is boosted to 540 V.

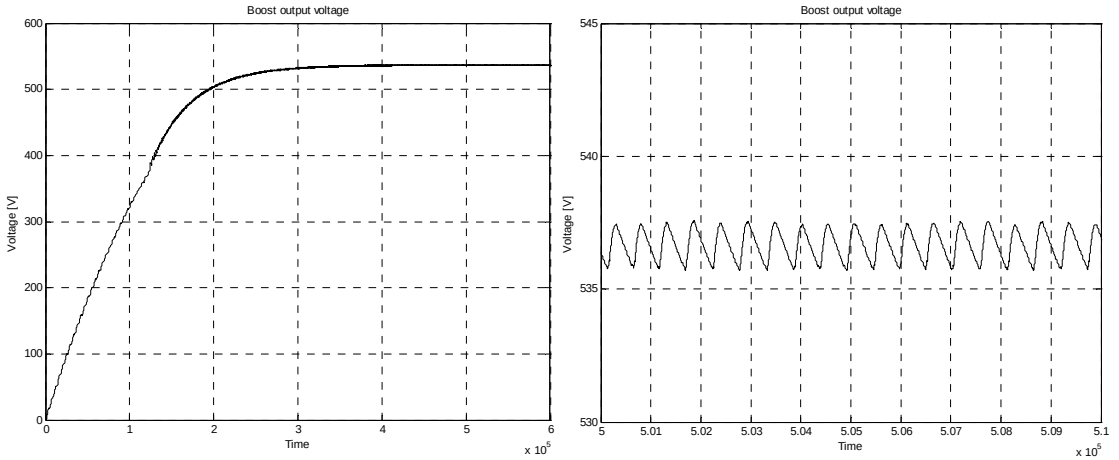

Figure 5.22: Output boost voltage

Chapter 6: Conclusion and Further Work

6.1 Conclusion

In this technical report, the study of the photovoltaic system with maximum power point controller has been developed. From the theory of the photovoltaic, a mathematic model of the PV has been presented.Then, the photovoltaic system with DC-DC boost converter, maximum power point controller and resistive load have been designed. Finally, the system has been simulated with Simulink MATLAB.

First, the simulations of the PV panels showed that the simulated models were accurate to determine the characteristics voltage current because the current voltage characteristics are the same as the characteristics given from the datasheet. In addition, when the irradiance or temperature varies, the PV models output voltage current change. Then, the simulation showed that Perturb and observe algorithm can track the maximum power point of the PV, it always runs at maximum power no matter what the operation condition is. The results showed that the Perturb and observe algorithm delivered an efficiency close to 100% in steady state.

.

The simulations of the PV with maximum power point, boost converter and resistive load were performed by varying the load, the irradiance and the temperature.

Finally, the PV performance and the maximum power point was analyzed, and the three phase full bridge DC-AC inverter was simulated on a resistive load. The results showed that the DC voltage generated by the PV array could produce an AC current sinusoidal at the output of the inverter. The amplitude of the current depends on the PV power.

6.2 Further work

Extensive simulation of the PV system should be done. A voltage control can be implemented to keep the boost converter output voltage constant. The simulation of the PV with three-phase inverter and current control can be performed. The current control will regulate the current that will be injected to the load. In case of grid connected PV system, synchronization to the grid can be added. Adding a phase locked loop to the system is an intriguing study to determine the performance of the grid connected PV.

Finally, a laboratory setup should be made to verify the simulation results with the experimental tests. Further studiescan still be done with PV system for research purposesand thedetailed PV simulator can be used for educational purposes.

References

[1] Jiyong Li and Honghua Wang, "A Novel Stand-alone PV generation System based on Variable Step Size INC MPPT and SVPWM control,"*Power Electronics and Motion Control Conference, 2009. IPEMC '09. IEEE 6th International*, July 2009*,* pp.2155-2160.

[2] Zeng, Q., Chang L. and Song, P., "SVPWM-based Current controller with Grid Harmonic Compensation for three-phase grid connected VSI," *Power Electronics Specialists Conference, 2004. PESC 04. 2004 IEEE 35th Annual,* vol. 4, April 2005pp. 2494-2500.

[3] Villalva, M.G., Gazoli, J.R. and Filho, E.R.;"Modeling and circuit-based simulation of photovoltaic arrays,"*Power Electronics Conference, IEEE 2009. COBEP '09. Brazilian*, December 2009, pp. 1244-1254.

[4] Zhou Dejia, Zhao Zhengming, Eltawil, M. and Yuan Liqiang; "Design and control of a Three-phase Grid connected Photovoltaic system with developed Maximum power point tracking,"*Applied Power Electronics Conference and Exposition, 2008. APEC 2008. Twenty-Third Annual IEEE,* May 2008, pp. 973-979.

[5] Zhou Xuesong,Song Daichun, Ma Youjie and Cheng Deshu, "Grid-connected control and simulation of single-phase two-level photovoltaic power generation system based on repetitive control,"*Measuring Technology and Mechatronics Automation (ICMTMA), 2010 International Conference,* vol. 2,May 2010,pp. 366-369.

[6] Liang Ma, Wang Ran and Zheng, T.Q., "Modeling and Control of 100 kW Three-phase grid-connected Photovoltaic inverter,"*Industrial Electronics and Applications (ICIEA), 2010 the 5th IEEE Conference*, July 2010, pp. 825-830.

[7] Rujia Men and Xiaoqing Han, "Optimum control and simulation for a grid-connected photovoltaic system," *Probabilistic Methods Applied to Power Systems (PMAPS), 2010 IEEE 11th International Conference*, July 2010, pp. 431-435.

[8] Azevedo, G.M.S., Cavalcanti, M.C., Oliveira, K.C., Neves, F.A.S. and Lins, Z.D., "Evaluation of maximum power point tracking methods for grid connected photovoltaic systems,"Conference on *Power Electronics Specialists, 2008. PESC 2008. IEEE*, August 2008, pp. 1456-1462.

[9] Kjaer, S.B., Pedersen, J.K. and Blaabjerg, F., "A Review of single-phase grid connected inverters for photovoltaic modules*,"Industry Applications, IEEE Transactions* , vol. 41, September 2005, pp.1292-1306.

[10] Jain, S. and Agarwal, V., “A single-stage grid connected inverter topology for solar PV systems with maximum power point tracking,”*IEEE Transactions onPower Electronics,* vol. 22, September 2007, pp. 1928-1940.

[11] Weiping Luo and Gujing Han, “Tracking and controlling of maximum power point application in grid-connected photovoltaic generation system,” *Second International Symposium on Knowledge Acquisition and Modeling 2009, KAM ’09,*vol. 3, December 2009, pp. 237-240.

[12] Hui Zhang, Hongwei Zhou, Jing Ren, Weizeng Liu, Shaohua Ruan and Yongjun Gao, “Three-phase grid-connected photovoltaic system with SVPWM current controller,”*Power Electronics and Motion Control Conference, 2009*. IPEMC '09. IEEE 6th International, July 2009, pp. 2161-2164.

[13] Meza, C., Negroni, J.J., Guinjoan, F. and Biel, D., “Inverter Configuration Comparative for Residential PV-grid connected systems,”*32nd Annual Conference onIEEE Industrial Electronics, IECON 2006*, April 2007, pp. 4361-4366.

[14] Calais, M., Myrzik, J., Spooner, T. and Agelidis, V.G., “Inverters for single-phase grid connected photovoltaic systems – an overview,”*Power Electronics Specialists Conference, 2002. pesc 02. 2002 IEEE 33rd Annual*, vol. 4, November 2002,pp. 1995-2000.

[15] Sera, Dezso, Teodorescu, Remus and Rodriguez, Pedro, "PV panel model based on datasheet values,"*International Symposium on Industrial Electronics, 2007. ISIE 2007. IEEE*, November 2007, pp. 2393-2396.

[16] Altas, I.H. and Sharaf, A.M., "A photovoltaic array simulation model for matlab Simulink GUI environment," *International Conference onClean Electrical Power, 2007. ICCEP '07,* July 2007,pp. 341-345.

[17] Dhople, S.V., Davoudi, A. and Chapman, P.L., "Dual stage Converter to improve transfer efficiency and maximum power point tracking feasibility in photovoltaic energy-conversion systems," *Applied Power Electronics Conference and Exposition (APEC), 2010 Twenty-Fifth Annual IEEE*, March 2010, pp. 2138-2142.

[18] Hasaneen, B.M. and Elbaset Mohammed, A.A., "Design and simulation of DC/DC converter,"*Power System Conference, 2008. MEPCON 2008. 12th International Middle-East*, July 2008,pp. 335-340.

[19]Koutroulis, E., Kalaitzakis, K., Voulgaris, N.C., "Development of a microcontroller-based photovoltaic maximum power point tracking control system," *Transactions on Power Electronics, IEEE*, vol. 16, August 2002, pp. 46-54.

[20] Calais, M. and Agelidis, V.G., "Multilevel Converters fo Single-phase grid connected photovoltaic Systems – An overview," *IEEE International*

Symposium on Industrial Electronics, 1998. Proceedings. ISIE '98, vol. 1, August 2002, pp. 224-229.

[21] Gonzalez, R. Lopez, J. Sanchis, P. Marroyo, L,**"**Transformerless Inverter for Single-Phase Photovoltaic Systems", *,IEEE Transaction in Power electronics 2007 volume 22 issue 2,* page 693-697.

[22] Svein Erik Evju,"Fundamentals of Grid Connected Photo-Voltaic Power Electronic Converter Design",*Norwegian University of Science and Technology*., june 2007, avalaible at NTNU Innovation and creativity.

[23] Ali Keyhani, "Department electrical engineering, OSU class notes Electromechanical devices*", lecture 25*, 2009

[24]H.W. van der Broeck, H.-C. Skudelny, and G.V. Stanke, "Analysis and realization of a pulsewidth modulator based on voltage space vectors," *IEEE Transactions on Industry Applications*, vol.24, pp. 142-150, 1988

[25] Luis Castaner, Santiago Silvestre,"Modeling Photovoltaic Systems Using PSpice", Wiley, 2002

[26] Timothy L. Skvarenina, "The Power Electronics Handbook, Industrial electronics series", CRC Press, 2002.

[27] Ali Keyhani, Mohammad N. Marwalli, Min Dai, " Integration of Green and Renewable Energy in Electric Power Systems", Wiley, 2010

[28] IEEE Std 1547-2003.“IEEE Standard for Interconnecting Distributed Resources with Electric Power systems”, 2003

[29] IEEE Std. 929-2000,“IEEE Recommended Practice for Utility Interface of Photovoltaic (PV) Systems”, 2000

[30] IEC 61727 second edition 2004, “International standard, Photovoltaic (PV) systems- Characteristics of the utility interface”, 2004

[31] Chan, D.S.H. and Phang, J.C.H., “Analytical methods for the extraction of solar –cell single and double diode parameters from I-V characteristics,” *IEEE Transactions on Electron Devices*, vol. 34, August 2005, pp. 286-293.

[32] Hui Zhang; Hong Ji; Jing Ren; Lin Shan and Yongjun Gao, “Research on MPPT control and Implementation method for Photovoltaic generation system and its simulation,” *Power Electronics and Motion Control Conference, 2009. IPEMC '09. IEEE 6th International*, July 2009, pp. 2108-2112.

[33]Ortiz-Rivera, E.I., “Maximum power point tracking using the optimal duty ratio for DC-DC converters and Load matching in photovoltaic application,” *Applied Power Electronics Conference and Exposition, 2008. APEC 2008. Twenty-Third Annual IEEE*, May 2008, pp. 987-991.

[34] Sachin Puranik,“Control of fuel cell based green energy systems for distributed generation applications”,*Avalaible from Ohio State University library*, The Ohio state University 2009

[35] Hui Zhang Hong Ji Jing Ren Lin Shan Yongjun Gao, "Research on MPPT control implementation method for photovoltaic generation system and its simulation",*Power Electronics and Motion Control Conference, 2009. IPEMC '09. IEEE 6th International, 2009,* pp. 2108-2112

[36]Fangrui Liu, Shanxu Duan, Fei Liu, Bangyin Liu and Yong Kang, "A variable step size INC MPPT method for PV systems," *IEEE Transactions on Industrial Electronics,*vol. 55,June 2008, pp. 2622-2628.

[37]Fangrui Liu, Yong Kang, Yu Zhang and Shanxu Duan, "Comparison of P&O and hill Climbing MPPT methods for grid-connected PV converter,"*3rd IEEE Conference on Industrial Electronics and Applications, 2008. ICIEA 2008*, August 2008, pp. 804-807.

[38] Gow, J.A. and Manning, C.D., "Development of photovoltaic array model for use in power electronics simulation studies," *Electric Power Applications, IEE Proceedings*, vol. 146, August 2002, pp. 193-200.

[39] Akihiro Oi,"Design and simulation of photovoltaic water pumping system",*California Polytechnic State University*, San Luis Obispo. September 2005

[40] Huan-Liang Tsai, Ci Siang,"Development of generalized photovoltaic model using Matlab Simulink", *Proceedings of the World Congress on Engineering and Computer Science,* WCECS 2008, October 22 - 24, 2008, San Francisco, USA

[41] Fangrui Liu, Yong Kang, Yu Zhang and Shanxu Duan, "Comparison of P&O and hill Climbing MPPT methods for grid-connected PV converter," *3rd IEEE Conference on Industrial Electronics and Applications, 2008. ICIEA 2008,* August 2008, pp. 804-807.

[42] Elgendy, M.A., Zahawi, B., Atkinson, D.J., "Analysis of the performance of DC Photovoltaic Pumping systems with maximum power point tracking,"*4th IET Conference on Power Electronics, Machines and Drives, 2008. PEMD 2008.*, May 2008, pp. 426-430.

[43] Fangrui Liu, Shanxu Duan, Fei Liu, Bangyin Liu and Yong Kang, "A variable Step size INC MPPT Method for PV Systems," *IEEE Transactions on Industrial Electronics*, June 2008, vol. 55, pp. 26622-2628.

[44] Ortiz-Rivera, E.I., Eduardo I, Ortiz-Rivera,"Maximum power point tracking using the optimal duty ratio for DC-DC converters and Load matching in photovoltaic application," *Applied Power Electronics Conference and Exposition, 2008. APEC 2008. Twenty-Third Annual IEEE*, May 2008, pp. 987-991.

[45] Esram, T. and Chapman, P.L., "Comparison of Photovoltaic array maximum power point tracking techniques," *IEEE Transactions on Energy Conversion*, vol.22, May 2007, pp.439-449.

[46] Van der Broeck, H.W.,Skudelny, H.-C. and Stanke, G.V."Analysis and Realization of a Pulsewidth Modulator Based on Voltage Space Vectors", *IEEE*

Transactions on Industry Applications, vol. 24, No. 1, January/February 1988, pp. 142 – 149.

[47]Rathnakumar, D., LakshmanaPerumal, J. and Srinivasan, T., "A new software implementation of space vector PWM" in *Proceedings of IEEE Southeast Conference*, April 2005, pp.131 – 136.

[48] Femia, N., Petrone, G., Spagnuolo, G. and Vitelli, M. "Petrone Increasing efficiency of P&O MPPT by converter Dynamic matching",*2004 IEEE International Symposium onIndustrial Electronics*, vol. 2, January 2006, pp. 1017 – 1021.

[49] Bae, H.S.; Park, J.H.; Cho, B.H. and Yu, G.J.; , "New control strategy for 2 stage Utility connected photovoltaic power conditioning system with a low cost digital processor", *Power Electronics Specialists Conference, 2005. PESC '05. IEEE 36th* , January 2006, pp. 2925 - 2929.

[50] N. Mohan, W. P. Robbin, and T. Undeland, "Power Electronics: Converters,Applications, and Design*", 2nd Edition, New York*, Wiley,1995

[51] Hasaneen, B.M. and Elbaset Mohammed, A.A., "Design and Simulation of DC/DC boost converter*", Power System Conference, 2008. MEPCON 2008. 12th International Middle-East* , July 2008, pp. 335 - 340.

[52] Steven Pekarek, "ACSL/Graphic Modeller Component Models for ElectricPowerEducation",

Avalaibleathttp:///ewh.ieee.org/soc/es/Nov1998/08/PWMINV.HTM, Accessed 4/19/2011

[53] M. Sahlhi, R. El- Bachtiri, E Matagne,"The development of the new maximum power point tracker for a PV panel", *REPEER Group, LESSI laboratory, Faculty of sciences dhar el-Mehrez, USMBA University*, Received: 21 Sept 2007; accepted: 29 Oct 2007

[54] Solar Energy Industries Association, "US solar Market Insight 2010 year review",www.seia.org, accessed 1/10/11

[55] U.S Department of Energy, "Multi program plan 2008-2012",*www1.eere.energy.gov/solar/.../solar_program_mypp_2008-2012.pdf,* accessed 1/30/10.

[56] Nasiri, A. "Integrating energy storage with renewable energy systems",*Industrial Electronics, 2008. IECON 2008. 34th Annual Conference of IEEE*,10-13 Nov. 2008, pp. 18

[57] Dr. Zainal Salam, "Power Electronics and Drives" (Version 3-2003): *UTM-JB,encon.fke.utm.my/courses/see5433/Chopper-2003.PPT,* accessed 10/9/10

[58] R. Shaffer, "Fundamentals of Power Electronics with MATLAB,"C.R Media, Boston, 2007

[59] Abu-hamdeh, Muthanna S,"Modeling of Bi-directional Converter for Wind Power Generation', The Ohio State University 2009, available from Ohiolink.edu

[60] K. Vinoth Kumar, Prawin Angel Michael, Joseph P. John and Dr. S. Suresh Kumar,"Simulation and comparison of SVPWM and SVPWM control", *ARPN Journal of Engineering and Applied Sciences*, VOL. 5, NO. 7, JULY 2010

[61] Kocalmis, A. Sunter, S. "Simulation of space vector PWM controller for a three level", IEEE Industrial Electronics, *IECON 2006 - 32nd Annual Conference on*, pp. 1915-1920

[62] Jim Woo Jung, " Project #2 Space vector PWM inverter", *Department of electrical and computer engineering*, Ohio state university, February 2005

..

Appendix A: Boost parameters

Sizing the boost converters

The boost converter parameters are:

- Vin (nom): 337 V
- Vout (nom): 540 V
- PV maximum power: 12000 W
- Fs: 10 kHz
- Maximum inductor current ripple: 10 %

The inductor L is calculated with the following equation [50]:

$$L \geq \frac{V_{om}.D_m.(1-D_m)}{f_s\left|\Delta I_{Lripple}\right|}$$

Where Vom is 540 V the maximum output voltage of the boost converter. The duty cycle Dm is obtained from:

$$\frac{V_o}{V_{in}} = \frac{T}{t_{off}} = \frac{1}{1-D}$$

$$D = 1 - \frac{V_{in}}{V_{out}}$$

$$D = 0.3759$$

The output current is given by

$$I_{om} = \frac{P_{out}}{V_{out}}$$

The converter is supposed no loss. The PV input power is the output power.

$$I_{om} = \frac{12000}{540} = 22.21\ A$$

The reisistive load is

$$R_{load} = \frac{540}{22.21} = 24.3\ ohm$$

The inductor L is

$$L \geq \frac{540 \times 0.3759 \times (1 - 0.3759)}{10000 \times 2 \times 35.6 \times 0.1}$$

$$L \geq 444\ \mu H$$

For the input capacitor the relation in paragraph 3.3.3 is used.

$$C_{in} \geq \frac{I_{om}.{D_m}^2}{0.02\ (1 - D_m) f_s V_{pv\_mpp}}$$

$$C_{in} \geq \frac{22.21 \times 0.3759^2}{0.02 \times (1 - 0.3759) \times 10000 \times 337}$$

$$C_{in} \geq 78.6 \mu F$$

For the output capacitor C_{out}, the following relation is used

$$C_{out} \geq \frac{V_{load}.D}{f_s \Delta V_{load} R_{load}}$$

$$C_{out} \geq \frac{540 \times 0.3759}{10000 \times 5.4 \times 24.3}$$

$$C_{out} \geq 154.69 \mu F$$

Appendix B: Listings matlab programs

Matlab file for the photovoltaic

```
% Matlab script for modeling a photovoltaic array
%
% Tested with MATLAB Version 7.3.0.267 (R2006b)
%
% Author: Marcelo Gradella Villalva
% Email: mvillalva@gmail.com
% University of Campinas, Brazil - May/2009
% http://www.unicamp.br

%Modified by Falinirina Rakotomananandro december 2010
%
% You may freely modify and distribute this file.
% Please cite my work if you find it useful.
%
% For more information refer to:
%
% M. G. Villalva, J. R. Gazoli, E. Ruppert F.
% "Comprehensive approach to modeling and simulation of photovoltaic arrays"
% IEEE Transactions on Power Electronics, 2009
% vol. 25, no. 5, pp. 1198--1208, ISSN 0885-8993
%
% M. G. Villalva, J. R. Gazoli, E. Ruppert F.
% "Modeling and circuit-based simulation of photovoltaica arrays"
% Brazilian Journal of Power Electronics, 2009
% vol. 14, no. 1, pp. 35--45, ISSN 1414-8862
%
% Visit: http://sites.google.com/site/mvillalva/pvmodel

clear all

clc

%% Information from the BP MSX120 solar array datasheet
%% PV array 12000 W with 10 modules in series and 10 modules in parralel

%  You may change these parameters to fit the I-V model
%  to other kinds of solar arrays.

Iscn = 3.87;           %Nominal short-circuit voltage [A]
Vocn = 42.1;           %Nominal array open-circuit voltage [V]
Imp = 3.56;            %Array current @ maximum power point [A]
Vmp = 33.7;            %Array voltage @ maximum power point [V]
Pmax_e = Vmp*Imp;      %Array maximum output peak power [W]
Kv = -0.08;            %Voltage/temperature coefficient [V/K]
Ki = 0.00065;          %Current/temperature coefficient [A/K]
Ns = 72;               %Nunber of series cells

%% Array with Nss x Npp modules
Nss = 16;
Npp = 42;
```

```
%% Constants

k = 1.3806503e-23;   %Boltzmann [J/K]
q = 1.60217646e-19;  %Electron charge [C]
a = 1.3977;            %Diode constant

%% Nominal values

Gn = 1000;          % Nominal irradiance [W/m^2] @ 25oC
Tn = 25 + 273.15;    % Nominal operating temperature [K]


%% Adjusting algorithm

% The model is adjusted at the nominal condition
T = Tn;
G = Gn;

Vtn = k * Tn / q;                  %Thermal junction voltage (nominal)
Vt = k * T / q;                    %Thermal junction voltage (current temperature)

Ion = Iscn/(exp(Vocn/a/Ns/Vtn)-1);    % Nominal diode saturation current

Io = Ion;

% Reference values of Rs and Rp
Rs_max = (Vocn - Vmp)/ Imp;
Rp_min = Vmp/(Iscn-Imp) - Rs_max;

% Initial guesses of Rp and Rs
Rp = Rp_min;
Rs = 0;

tol = 0.001; % Power mismatch Tolerance

P=[0];

error = Inf; %dummy value

% Iterative process for Rs and Rp until Pmax,model = Pmax,experimental

while (error>tol)

%  Temperature and irradiation effect on the current
dT = T-Tn;
Ipvn = (Rs+Rp)/Rp * Iscn;         % Nominal light-generated current
Ipv = (Ipvn + Ki*dT) *G/Gn;       % Actual light-generated current
Isc = (Iscn + Ki*dT) *G/Gn;       % Actual short-circuit current

% Increments Rs
Rs = Rs + .01;
```

```
% Parallel resistance
Rp = Vmp*(Vmp+Imp*Rs)/(Vmp*Ipv-Vmp*Io*exp((Vmp+Imp*Rs)/Vt/Ns/a)+Vmp*Io-Pmax_e);

% Solving the I-V equation for several (V,I) pairs
clear V
clear I

V = 0:.1:45;              % Voltage vector
I = zeros(1,size(V,2));    % Current vector

for j = 1 : size(V,2) %Calculates for all voltage values

% Solves g = I - f(I,V) = 0 with Newntonn-Raphson

g(j) = Ipv-Io*(exp((V(j)+I(j)*Rs)/Vt/Ns/a)-1)-(V(j)+I(j)*Rs)/Rp-I(j);

while (abs(g(j)) > 0.001)

g(j) = Ipv-Io*(exp((V(j)+I(j)*Rs)/Vt/Ns/a)-1)-(V(j)+I(j)*Rs)/Rp-I(j);
glin(j) = -Io*Rs/Vt/Ns/a*exp((V(j)+I(j)*Rs)/Vt/Ns/a)-Rs/Rp-1;
I_(j) = I(j) - g(j)/glin(j);
I(j) = I_(j);

end

end % for j = 1 : size(V,2)

plott = 1; %Enables plotting during the algorithm execution

if (plott)

 %Plots the I-V and P-V curves

 %Current x Voltage
 figure(1)
 grid on
 hold on
 title('I-V curve - Adjusting Rs and Rp');
 xlabel('V [V]');
 ylabel('I [A]');
 xlim([0 Vocn+1]);
 ylim([0 Iscn+1]);

 %Plots I x V curve
 plot(V,I,'LineWidth',2,'Color','k')

 %Plots the "remarkable points" on the I x V curve
 plot([0 Vmp Vocn],[Iscn Imp 0],'o','LineWidth',2,'MarkerSize',5,'Color','k')

 %Power x Voltage
 figure(2)
 grid on
 hold on
```

```
  title('P-V curve - Adjusting peak power');
  xlabel('V [V]');
  ylabel('P [W]');
  xlim([0 Vocn+1])
  ylim([0 Vmp*Imp+1]);

end % if(plott)

  % Calculates power using the I-V equation
  P = (Ipv-Io*(exp((V+I.*Rs)/Vt/Ns/a)-1)-(V+I.*Rs)/Rp).*V;

  Pmax_m = max(P);

  error = (Pmax_m-Pmax_e);

if (plott)

  %Plots P x V curve
  plot(V,P,'LineWidth',2,'Color','k')

  %Plots the "remarkable points" on the power curve
  plot([0 Vmp Vocn],[0 Vmp*Imp 0],'o','LineWidth',2,'MarkerSize',5,'Color','k')

end % if (plott)

end % while (error>tol)


%% Outputs

 % I-V curve
 figure(3)
 grid on
 hold on
 title('Adjusted I-V curve');
 xlabel('V [V]');
 ylabel('I [A]');
 xlim([0 Vocn+1]);
 ylim([0 Iscn+1]);

 plot(V,I,'LineWidth',2,'Color','k') %

 plot([0 Vmp Vocn ],[Iscn Imp 0 ],'o','LineWidth',2,'MarkerSize',5,'Color','k')

 % P-V curve

 figure(4)
 grid on
 hold on
 title('Adjusted P-V curve');
 xlabel('V [V]');
 ylabel('P [W]');
 xlim([0 Vocn+1]);
```

```
ylim([0 Vmp*Imp+1]);

plot(V,P,'LineWidth',2,'Color','k') %

plot([0 Vmp Vocn ],[0 Pmax_e 0 ],'o','LineWidth',2,'MarkerSize',5,'Color','k')


disp(sprintf('Model info:\n'));
disp(sprintf(' Rp_min = %f',Rp_min));
disp(sprintf('     Rp = %f',Rp));
disp(sprintf(' Rs_max = %f',Rs_max));
disp(sprintf('     Rs = %f',Rs));
disp(sprintf('      a = %f',a));
disp(sprintf('      T = %f',T-273.15));
disp(sprintf('      G = %f',G));
disp(sprintf(' Pmax,m = %f  (model)',Pmax_m));
disp(sprintf(' Pmax,e = %f  (experimental)',Pmax_e));
disp(sprintf('    tol = %f',tol));
disp(sprintf('P_error = %f',error));
disp(sprintf('    Ipv = %f',Ipv));
disp(sprintf('    Isc = %f',Isc));
disp(sprintf('    Ion = %f',Ion));
disp(sprintf('\n\n'));
```

Matlab file for the plot

```
%program to plot IV for T=25 G=1
A=xlsread('IVplant.xls');
B=xlsread('IVplant1.xls');
plot(A,B,'black','linewidth',2)
hold on

%ipv800
load ipv800.mat
C=ipv;
C=ipv(:,2)
plot(A,C)
```

Matlab file for the space vector PWM

```
function y= sv(u)
%%
angle=u(1);
time=u(2);
T0=u(3);
T1=u(4);
T2=u(5);

%%Decide in which sector
```

```
if (0 < angle)&&(angle <= pi/3)
   S = 1;
elseif (pi/3 < angle)&&(angle <= 2*pi/3)
   S = 2;
elseif (2*pi/3 < angle) && (angle <= pi)
   S = 3;
elseif (pi < angle) && (angle <= 4*pi/3)
   S = 4;
elseif (4*pi/3 < angle) && (angle <= 5*pi/3)
   S = 5;
elseif (5*pi/3 < angle) && (angle <= 2*pi)
   S = 6;
else
   S = 1;
end

if (S == 1)  % first sector
   %Switching pattern  8, 1,2,7,7,2,1,8
   if (0 <= time) && (time <= T0/4)
      V = 8;   % switching pattern 8 for period of T0
   elseif (T0/4 < time) && (time <= (T0/2+T1)/2)
      V = 1; % switching pattern 1 for period of T1
   elseif ((T0/2+T1)/2 < time) && (time <= .5*(T2+T0/2+T1))
      V = 2;
   elseif (.5*(T2+T0/2+T1) < time) && (time <= .5*(T2+T0+T1))
      V = 7;
   elseif (.5*(T2+T0+T1) < time) && (time <= .5*(T2+3*T0/2+T1))
      V = 7;
   elseif (.5*(T2+3*T0/2+T1) < time) && (time <= .5*(2*T2+3*T0/2+T1))
      V = 2;
   elseif (.5*(2*T2+3*T0/2+T1) < time) && (time <= .5*(2*T2+3*T0/2+2*T1))
      V = 1;
   elseif (.5*(2*T2+3*T0/2+2*T1) < time) && (time <= (T2+T0+T1))
      V = 8;
   else
      V = 8;
   end

elseif (S == 2)  % second sector
  %Switching pattern  8, 3, 2, 7,7, 2, 3, 8
   if (0 <= time) && (time <= .5*(T0/2))
      V = 8;   % switching pattern 8 for period of T0
   elseif (.5*(T0/2) < time) && (time <= .5*(T0/2+T2))
      V = 3; % switching pattern 1 for period of T2
   elseif (.5*(T0/2+T2) < time) && (time <= .5*(T2+T0/2+T1))
      V = 2;
   elseif (.5*(T2+T0/2+T1) < time) && (time <= .5*(T2+T0+T1))
      V = 7;
   elseif (.5*(T2+T0+T1) < time) && (time <= .5*(T2+3*T0/2+T1))
      V = 7;
   elseif (.5*(T2+3*T0/2+T1) < time) && (time <= .5*(T2+3*T0/2+2*T1))
      V = 2;
   elseif (.5*(2*T2+3*T0/2+T1) < time) && (time <= .5*(2*T2+3*T0/2+2*T1))
```

```
        V = 3;
    elseif (.5*(2*T2+3*T0/2+2*T1) < time) && (time <= (T2+T0+T1))
        V = 8;
    else
        V = 8;
    end
elseif (S == 3)  % third sector
    %Switching pattern  8, 3, 4, 7, 4, 3, 8
    if (0 <= time) && (time <= .5*(T0/2))
        V = 8;   % switching pattern 8 for period of T0
    elseif (.5*(T0/2) < time) && (time <= .5*(T0/2+T1))
        V = 3; % switching pattern 1 for period of T1
    elseif (.5*(T0/2+T1) < time) && (time <= .5*(T2+T0/2+T1))
        V = 4;
    elseif (.5*(T2+T0/2+T1) < time) && (time <= .5*(T2+T0+T1))
        V = 7;
    elseif (.5*(T2+T0+T1) < time) && (time <= .5*(T2+3*T0/2+T1))
        V = 7;
    elseif (.5*(T2+3*T0/2+T1) < time) && (time <= .5*(2*T2+3*T0/2+T1))
        V = 4;
    elseif (.5*(2*T2+3*T0/2+T1) < time) && (time <= .5*(2*T2+3*T0/2+2*T1))
        V = 3;
    elseif (.5*(2*T2+3*T0/2+2*T1) < time) && (time <= (T2+T0+T1))
        V = 8;
    else
        V = 8;
    end

elseif (S == 4)  % forth sector
   %Switching pattern  8, 5, 4, 7, 4, 5, 8
    if (0 <= time) && (time <= .5*(T0/2))
        V = 8;   % switching pattern 8 for period of T0
    elseif (.5*(T0/2) < time) && (time <= .5*(T0/2+T2))
        V = 5; % switching pattern 1 for period of T2
    elseif (.5*(T0/2+T2) < time) && (time <= .5*(T2+T0/2+T1))
        V = 4;
    elseif (.5*(T2+T0/2+T1) < time) && (time <= .5*(T2+T0+T1))
        V = 7;
    elseif (.5*(T2+T0+T1) < time) && (time <= .5*(T2+3*T0/2+T1))
        V = 7;
    elseif (.5*(T2+3*T0/2+T1) < time) && (time <= .5*(T2+3*T0/2+2*T1))
        V = 4;
    elseif (.5*(2*T2+3*T0/2+T1) < time) && (time <= .5*(2*T2+3*T0/2+2*T1))
        V = 5;
    elseif (.5*(2*T2+3*T0/2+2*T1) < time) && (time <= (T2+T0+T1))
        V = 8;
    else
        V = 8;
    end
elseif (S == 5)  % fifth sector
    %Switching pattern  8, 5, 6, 7, 6, 5, 8
    if (0 <= time) && (time <= .5*(T0/2))
        V = 8;   % switching pattern 8 for period of T0
```

```
    elseif (.5*T0/2 < time) && (time <= .5*(T0/2+T1))
       V = 5; % switching pattern 1 for period of T1
    elseif (.5*(T0/2+T1) < time) && (time <= .5*(T2+T0/2+T1))
       V = 6;
    elseif (.5*(T2+T0/2+T1) < time) && (time <= .5*(T2+T0+T1))
       V = 7;
    elseif (.5*(T2+T0+T1) < time) && (time <= .5*(T2+3*T0/2+T1))
       V = 7;
    elseif (.5*(T2+3*T0/2+T1) < time) && (time <= .5*(2*T2+3*T0/2+T1))
       V = 6;
    elseif (.5*(2*T2+3*T0/2+T1) < time) && (time <= .5*(2*T2+3*T0/2+2*T1))
       V = 5;
    elseif (.5*(2*T2+3*T0/2+2*T1) < time) && (time <= (T2+T0+T1))
       V = 8;
    else
       V = 8;
    end
  elseif (S == 6)  % sixth sector
    %Switching pattern  8, 1, 6, 7, 6, 1, 8
    if (0 <= time) && (time <= .5*T0/2)
       V = 8;   % switching pattern 8 for period of T0
    elseif (.5*T0/2 < time) && (time <= .5*(T0/2+T2))
       V = 1; % switching pattern 1 for period of T2
    elseif (.5*(T0/2+T2) < time) && (time <= .5*(T2+T0/2+T1))
       V = 6;
    elseif (.5*(T2+T0/2+T1) < time) && (time <= .5*(T2+T0+T1))
       V = 7;
    elseif (.5*(T2+T0+T1) < time) && (time <= .5*(T2+3*T0/2+T1))
       V = 7;
    elseif (.5*(T2+3*T0/2+T1) < time) && (time <= .5*(T2+3*T0/2+2*T1))
       V = 6;
    elseif (.5*(2*T2+3*T0/2+T1) < time) && (time <= .5*(2*T2+3*T0/2+2*T1))
       V = 1;
    elseif (.5*(2*T2+3*T0/2+2*T1) < time) && (time <= (T2+T0+T1))
       V = 8;
    else
       V = 8;
    end
  end
  if (V == 1) % switching pattern corresponds to base vector V1 S1S3S5 = 100 (S2S4S6=011)
    y(1) = 1;
    y(3) = 0;
    y(5) = 0;
    y(4) = 0;
    y(6) = 1;
    y(2) = 1;
  elseif (V == 2)
    y(1) = 1;
    y(3) = 1;
    y(5) = 0;
    y(4) = 0;
    y(6) = 0;
    y(2) = 1;
```

```
elseif (V == 3)
    y(1) = 0;
    y(3) = 1;
    y(5) = 0;
    y(4) = 1;
    y(6) = 0;
    y(2) = 1;
elseif (V == 4)
    y(1) = 0;
    y(3) = 1;
    y(5) = 1;
    y(4) = 1;
    y(6) = 0;
    y(2) = 0;
elseif (V == 5)
    y(1) = 0;
    y(3) = 0;
    y(5) = 1;
    y(4) = 1;
    y(6) = 1;
    y(2) = 0;
elseif (V == 6)
    y(1) = 1;
    y(3) = 0;
    y(5) = 1;
    y(4) = 0;
    y(6) = 1;
    y(2) = 0;
elseif (V == 7)
    y(1) = 1;
    y(3) = 1;
    y(5) = 1;
    y(4) = 0;
    y(6) = 0;
    y(2) = 0;
elseif (V == 8)
    y(1) = 0;
    y(3) = 0;
    y(5) = 0;
    y(4) = 1;
    y(6) = 1;
    y(2) = 1;
else
    y(1) = 0;
    y(3) = 0;
    y(5) = 0;
    y(4) = 1;
    y(6) = 1;
    y(2) = 1;
end
 y(7)=S;
 end
```

Appendix C: Datasheet BP MSX120

bp solar

BP MSX 120

120-Watt Multicrystalline
Photovoltaic Module

BP Solar's MSX series is a premium line of PV modules with a 25-year performance warranty, tightly controlled electrical parameters, and labeling showing each module's tested electrical characteristics. Providing 120 watts of nominal maximum power, the MSX 120 is used primarily in large battery-equipped PV systems or—through an inverter—to provide AC power directly to a load. Typical applications include grid-supplemental residential and commercial systems, telecommunications, remote villages and clinics, pumping, and land-based navigation aids. Its attractive bronze-anodized frame also suits it well for architectural applications.

This product is available as a framed module or an unframed laminate, in 12V or 24V nominal configurations, with either:

- Dual high-volume junction boxes which allow on-site 12V/24V selection by rewiring (MSX 120);
- Installation-speeding DC-rated polarized connectors (MSX 120MC).

Proven Materials and Construction

BP Solar's quarter-century of field experience shows in every aspect of these module's construction and materials:

- 72 multicrystalline silicon solar cells configured as one series string or two 36-cell series strings (bypass diodes are included);
- Cells are laminated between sheets of ethylene vinyl acetate (EVA) and high-transmissivity low-iron 3mm tempered glass;
- Frame strength exceeds requirements of certifying agencies.

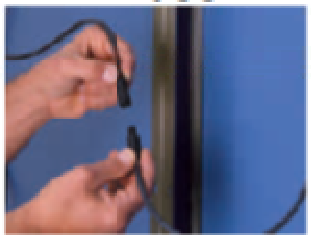

Weatherproof Connectors

MSX 120MC output is via heavy-duty (4mm²/AWG #12) output cables with polarized weatherproof DC-rated connectors which provide reliable low-resistance connections, eliminate wiring errors, and speed installation. Asymmetrical cables enable side-by-side or end-to-end module placement in arrays.

High-Capacity Versatile Junction Box

The junction boxes of the MSX 120 are raintight (IP54 rated) and accept PG13.5 or 1/2" nominal conduit or cable fittings. Their volume (411cc, 25 cubic inches) and 6-terminal

Bronze Anodized Universal Frame

connection blocks enable most system array connections (putting modules in series or parallel) to be made right in the boxes. Options include:

- an oversize terminal block which accepts conductors up to 25mm² (AWG #4); standard terminals accept up to 6mm² (AWG #10);
- a Solarstate™ charge regulator.

Products with junction boxes may be rewired to provide 12V or 24V output.

Limited Warranties

- Power output for 25 years;
- Freedom from defects in materials and workmanship for 5 years.

See our website or your local representative for full terms of these warranties.

Individually Tested and Labeled

Each module tested and labeled with its actual output—voltage, current, and power at maximum power point (P_{max})—at Standard Test Conditions and Standard Operating Conditions.

BP MSX 120

MSX 120 laminates also qualify for the above listings and certifications; MSX 120MC laminates are UL-recognized. MSX 120 modules and laminates with junction boxes are also certified by PowerMark Corporation and approved by Factory Mutual Research for application in NEC Class 1, Division 2, Groups C & D hazardous locations.

TUV

01-4003-2 2/02

Quality and Safety

MSX 120 and MSX 120MC modules are manufactured in our ISO 9001-certified factories, listed by Underwriter's Laboratories for electrical and fire safety (Class C fire rating), certified by TÜV Rheinland as Class II equipment, and comply with the requirements of IEC 61215 including:

- repetitive cycling between -40°C and 85°C at 85% relative humidity;
- simulated impact of 25mm (one-inch) hail at terminal velocity;
- a "damp heat" test, consisting of 1000 hours of exposure to 85°C and 85% relative humidity;
- a "hot-spot" test, which determines a module's ability to tolerate localized shadowing (which can cause reverse-biased operation and localized heating);
- static loading, front and back, of 2400 pascals (50 psf); front loading (e.g. snow) of 5400 pascals (113 psf).

Electrical Characteristics[1]

	MSX 120	MSX 110[4]
Maximum power (P_{max})[2]	120W	110W
Voltage at P_{max} (V_{mp})	33.7V	33.6V
Current at P_{max} (I_{mp})	3.56A	3.3A
Minimum P_{max}	114W	105W
Short-circuit current (I_{sc})	3.87A	3.6A
Open-circuit voltage (V_{oc})	42.1V	41.6V
Temperature coefficient of I_{sc}	(0.065±0.015)%/°C	
Temperature coefficient of V_{oc}	-(80±10)mV/°C	
Temperature coefficient of power	-(0.5±0.05)%/°C	
NOCT[3]	47±2°C	
Maximum system voltage	600V (U.S. NEC rating) 1000V (TÜV Rheinland rating)	
Maximum series fuse rating	20A	

Notes

1. These data represent the performance of typical MSX 110 and MSX 120 products in 24V configuration. The data are based on measurements made in accordance with ASTM E1036 corrected to SRC (Standard Reporting Conditions, also known as STC or Standard Test Conditions), which are:
   - illumination of 1 kW/m² (1 sun) at spectral distribution of AM 1.5 (ASTM E892 global spectral irradiance);
   - cell temperature of 25°C.
2. During the stabilization process which occurs during the first few months of deployment, module power may decrease approximately 3% from typical P_{max}.
3. The cells in an illuminated module operate hotter than the ambient temperature. NOCT (Nominal Operating Cell Temperature) is an indicator of this temperature differential, and is the cell temperature under Standard Operating Conditions: ambient temperature of 20°C, solar irradiation of 0.8 kW/m², and wind speed of 1 m/s.
4. The power of solar cells varies in the normal course of production; the MSX 110 is assembled using cells of slightly lower power than the MSX 120.

MSX 120 I-V Curves